Report No. CG-D-04-98

Objective Analysis of Oceanic Data for Coast Guard Trajectory Models Phase II

Applied Mathematics, Inc.
1622 Route 12, P.O. Box 637
Gales Ferry, CT 06335

Final Report
December 1997

DISTRIBUTION STATEMENT A
Approved for public release;
Distribution Unlimited

Prepared for:

U.S. Department of Transportation
United States Coast Guard
Operations, (G-O)
Washington, DC 20593-0001

and

United States Coast Guard
Research and Development Center
1082 Shennecossett Road
Groton, CT 06340-6096

NOTICE

Marc B. Mandler
Technical Director
United States Coast Guard
Research & Development Center
1082 Shennecossett Road
Groton, CT 06340-6096

Technical Report Documentation Page

1. Report No. CG-D-04-98	2. Government Accession No.	3. Recipient's Catalog No.
4. Title and Subtitle Objective Analysis of Oceanic Data for Coast Guard Trajectory Models, Phase II		5. Report Date December 1997 6. Performing Organization Code Project No: 1012.3.8
7. Author(s)		8. Performing Organization Report No. R&DC 14/97
9. Performing Organization Name and Address Applied Mathematics, Inc. 1622 Route 12, P.O. Box 637 Gales Ferry, CT 06335		10. Work Unit No. (TRAIS) 11. Contract or Grant No. DTRS-57-95-C-00013
12. Sponsoring Agency Name and Address U.S. Department of Transportation United States Coast Guard Operations, (G-O) Washington, DC 20593-0001	U.S. Coast Guard Research and Development Center 1082 Shennecossett Road Groton, CT 06340-6096	13. Type of Report and Period Covered Final Report. Period of Performance: 9 January 1995 to 8 January 1997 14. Sponsoring Agency Code Commandant (G-OPR) U.S. Coast Guard Headquarters Washington, DC 20593-0001

15. Supplementary Notes

The Coast Guard technical contact and COTR is Gary Hover, 860-441-2818.

16. Abstract

The Coast Guard uses Computer Aided Search Planning (CASP) tools to support search and rescue mission planning. CASP target drift algorithms require estimates of the search area ocean currents. Global sea current databases provide this information, however, the data resolution is poor and the data do not always reflect real-time, on-scene conditions. Self Locating Datum Marker Buoys (SLDMB) provide a source of improved sea current data, but the data must be processed into a velocity field format that CASP can use.

This SBIR Phase II research developed and tested statistical techniques known as objective analysis (OA) to compute the ocean current velocity field from SLDMB buoy data.

The following research was completed. OA algorithms were developed, that combine sources of ocean current data distributed irregularly in space and time, to produce an optimal velocity field. A computer program, Ocean Prediction System (OPS), was developed which decodes SLDMB data and calculates the velocity field. An OPS Development Test was conducted in the vicinity of NOAA buoy 44011 in the First Coast Guard District.

Objective analysis techniques successfully estimated ocean surface currents using SLDMB data. OPS algorithms decoded SLDMB transmissions, processed the data, and provided an automated approach to compute ocean current velocity fields from buoy data.

Potential applications of this research are in support of Coast Guard Search and Rescue, Ice Patrol and Environmental Protection missions.

17. Key Words	18. Distribution Statement
current objective analysis search	This document is available to the U.S. public through the National Technical Information Service, Springfield, VA 22161.

19. Security Classif. (of this report)	20. SECURITY CLASSIF. (of this page)	21. No. of Pages	22. Price
UNCLASSIFIED	UNCLASSIFIED		

Form DOT F 1700.7 (8/72) Reproduction of form and completed page is authorized

METRIC CONVERSION FACTORS

Approximate Conversions to Metric Measures

Symbol	When You Know	Multiply By	To Find	Symbol
		LENGTH		
in	inches	*2.5	centimeters	cm
ft	feet	30	centimeters	cm
yd	yards	0.9	meters	m
mi	miles	1.6	kilometers	km
		AREA		
in^2	square inches	6.5	square centimeters	cm^2
ft^2	square feet	0.09	square meters	m^2
yd^2	square yards	0.8	square meters	m^2
mi^2	square miles	2.6	square kilometers	km^2
	acres	0.4	hectares	ha
		MASS (WEIGHT)		
oz	ounces	28	grams	g
lb	pounds	0.45	kilograms	kg
	short tons (2000 lb)	0.9	tonnes	t
		VOLUME		
tsp	teaspoons	5	milliliters	ml
tbsp	tablespoons	15	milliliters	ml
fl oz	fluid ounces	30	milliliters	ml
c	cups	0.24	liters	l
pt	pints	0.47	liters	l
qt	quarts	0.95	liters	l
gal	gallons	3.8	liters	l
ft^3	cubic feet	0.03	cubic meters	m^3
yd^3	cubic yards	0.76	cubic meters	m^3
		TEMPERATURE (EXACT)		
°F	Fahrenheit temperature	5/9 (after subtracting 32)	Celsius temperature	°C

*1 in = 2.54 (exactly).

Approximate Conversions from Metric Measures

Symbol	When You Know	Multiply By	To Find	Symbol
		LENGTH		
mm	millimeters	0.04	inches	in
cm	centimeters	0.4	inches	in
m	meters	3.3	feet	ft
m	meters	1.1	yards	yd
km	kilometers	0.6	miles	mi
		AREA		
cm^2	square centimeters	0.16	square inches	in^2
m^2	square meters	1.2	square yards	yd^2
km^2	square kilometers	0.4	square miles	mi^2
ha	hectares (10,000 m^2)	2.5	acres	
		MASS (WEIGHT)		
g	grams	0.035	ounces	oz
kg	kilograms	2.2	pounds	lb
t	tonnes (1000 kg)	1.1	short tons	
		VOLUME		
ml	milliliters	0.03	fluid ounces	fl oz
l	liters	0.125	cups	c
l	liters	2.1	pints	pt
l	liters	1.06	quarts	qt
l	liters	0.26	gallons	gal
m^3	cubic meters	35	cubic feet	ft^3
m^3	cubic meters	1.3	cubic yards	yd^3
		TEMPERATURE (EXACT)		
°C	Celsius temperature	9/5 (then add 32)	Fahrenheit temperature	°F

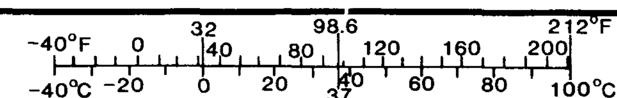

ACKNOWLEDGMENT

We would like to acknowledge the splendid cooperation and direction we received from the Project Officers, LCDR Brian D. Perkins and LT Thomas E. McClay, Coast Guard Research and Development Center.

Technical discussions with Gary Hover, Quincy Robe, Arthur Allen, Dr. Jennifer Dick, Coast Guard R&D Center; Peggy Staubs, Coast Guard OSC; and LT Robert Patton, Coast Guard Headquarters, were helpful throughout the project. Dr. Don Murphy, International Ice Patrol, was helpful in facilitating access to Argos data.

Bernard Petolas, Lorne Vaasjo, and Raymond Mahr, Metocean Data Systems, were helpful in providing four SLDMBs for the OPS Development Test as replacements for buoys which Clearwater Instrumentation, Inc., was unable to provide.

Dr. Joseph Discenza, Daniel H. Wagner, Associates, provided a software patch that allowed OPS data to be used by CASP 2.0.

The project team members were Dr. William J. Browning, Dr. Byron D. Biggs, Dr. Jason J. Brown, Dr. Bryan M. Gorman, Jerald E. Gray, Jennifer L. Isabelle, Lisa A. Skorupski, Dr. Christopher P. Thron, and Thomas E. Wood, Applied Mathematics, Inc; and Dr. Ben Fitzpatrick, North Carolina State University.

The abstract, executive summary, section 1 and section 6 of this report were written by the U.S. Coast Guard Research and Development Center. The remaining sections were written by Applied Mathematics, Inc.

[BLANK]

TABLE OF CONTENTS

LIST OF FIGURES

SECTION 4.0 OPS DEVELOPMENT TEST DESCRIPTION

SECTION 5 OPS DEVELOPMENT TEST RESULTS

APPENDIX A OPS DEVELOPMENT TEST PLAN

APPENDIX B OPS'S USER'S GUIDE

LIST OF TABLES

EXECUTIVE SUMMARY

INTRODUCTION

The Coast Guard uses Computer Aided Search Planning (CASP) tools to support search and rescue mission planning. When generating a search area, CASP uses target drift algorithms that require an estimate of the search area ocean currents. The system can access global sea current databases that provide this information, however, the data spatial resolution is only 1x1 degree on a latitude/longitude grid and the data do not always reflect real-time, on-scene conditions.

The Coast Guard Research and Development Center (R&DC) is developing Self Locating Datum Marker Buoys (SLDMBs). The SLDMB operational concept deploys an array of expendable buoys near the estimated target position. The buoys drift and transmit their positions via satellite. Buoy velocities can be calculated from their reported positions over time. Through this process, SLDMBs can be used to provide up-to-date ocean current information with high resolution in the areas they traverse.

While CASP 1.0 allows for current data to be manually input at specific time/position points, it has no algorithm to interpolate the data to cover a wider "field." A CASP 2.0 prototype has been developed that accepts a sea current velocity field as input. To produce this field manually would be a tedious and error-prone process, consuming an unreasonable amount of time and resources.

What is needed is an automated method to compute the ocean current velocity field from the buoy data. Objective analysis (OA) is a statistical technique used by meteorologists and oceanographers to optimally compute vector fields from observed data. This SBIR Phase II research developed and tested the OA technique and applied it to the problem of computing ocean current velocity fields using SLDMB time/position data.

PHASE II RESEARCH RESULTS

The project developed OA algorithms that determine optimal ocean current velocity fields and associated error fields. Calculations use data from irregularly distributed buoys that transmit position information at different times. A computer program, Ocean Prediction System (OPS), was developed that decodes SLDMB transmissions and provides the data to the objective analysis algorithms. OPS calculates, displays, and saves the velocity and associated error fields. OPS was field tested in the Coast Guard First District using SLDMBs and the test results were analyzed.

CONCLUSIONS

OA techniques can successfully estimate ocean surface currents using SLDMB data. OPS algorithms can decode SLDMB transmissions, process the data, and provide an automated approach to compute ocean current velocity fields from buoy data.

Target position estimates, calculated using CASP 2.0 with OPS processed SLDMB data, were significantly more accurate than the CASP 2.0 estimates calculated from historical global sea current data.

RECOMMENDATIONS

Any implementation of SLDMBs into Coast Guard search planning should consider OPS as the automated approach to calculating required velocity fields.

The preprocessing options in the prototype version of OPS are restricted to SLDMB data. To date, OPS has focused on SLDMBs as the most promising approach to improve calculated search area velocity fields. Several SLDMB questions should be investigated. These include determining the appropriate number of buoys to deploy and the best array configuration.

The OA algorithm is designed to process current measurements and associated uncertainty estimates from any source. Additional ocean current sources need to be investigated.

1.0 INTRODUCTION

The Coast Guard uses Computer Aided Search Planning (CASP) tools to support search and rescue mission planning. When generating a search area, CASP uses target drift algorithms that require an estimate of the search area ocean currents. The system can access global sea current databases that provide this information, however, the data spatial resolution is only 1x1 degree on a latitude/longitude grid and the data do not always reflect real-time, on-scene conditions.

The Coast Guard Research and Development Center (R&DC) is developing Self Locating Datum Marker Buoys (SLDMBs). The SLDMB operational concept deploys an array of expendable buoys near the estimated target position. The buoys drift and transmit their positions via satellite. Buoy velocities can be calculated from their reported positions over time. Through this process, SLDMBs can be used to provide up-to-date ocean current information with high resolution in the areas they traverse.

While CASP 1.0 allows for current data to be manually input at specific time/position points, it has no algorithm to interpolate the data to cover a wider "field." A CASP 2.0 prototype has been developed that accepts a sea current velocity field as input. To produce this field manually would be a tedious and error-prone process, consuming an unreasonable amount of time and resources.

What is needed is an automated method to compute the ocean current velocity field from the buoy data. Objective analysis (OA) is a statistical technique used by meteorologists and oceanographers to optimally compute vector fields from observed data.

This report documents the Small Business Innovative Research (SBIR) Phase II work performed by Applied Mathematics Inc. (AMI) for the U. S. Coast Guard Research and Development Center. The purpose of the Phase II research was to develop and test objective analysis techniques and apply them to the problem of computing ocean current velocity fields using Self Locating Datum Marker Buoy (SLDMB) time/position data.

Organization of Report.

The mathematical theory underlying the OPS algorithm is documented in Section 2.0. A comprehensive introduction to the geostatistics that the OPS algorithm is based on is beyond the scope of this report. However, references are provided for the interested reader.

An overview of the OPS program is given in Section 3.0.

The OPS Development Test is described in Section 4.0.

Analysis results from the OPS Development Test are presented in Section 5.0.

Conclusions and recommendations are given in Section 6.0.

The OPS Development Test Plan is provided as Appendix A.

The OPS User's Guide is provided as Appendix B.

Terminology CASP 2.0 was used exclusively in this project. Accordingly, all references in this report to CASP are to CASP 2.0.

2.0 OPS MODEL DESCRIPTION

The ocean current data blending algorithm used in OPS is based on the method of spatial Kriging commonly used in geostatistics. An introductory exposition of geostatistical methods is given in References [a] and [b]; a more detailed exposition is given in Reference [c].

OPS extends the spatial Kriging method used in geostatistics by including variability in time. Time is treated as a third dimension of space, and the variability models used in geostatistics are extended to treat spatio-temporal correlations.

In Section 2.1, we describe the input data models used in OPS. In Section 2.2, the trend model used in OPS is described. In Section 2.3, the variability model is discussed. Finally in Section 2.4, the algorithm used to determine the optimal field estimate is presented. The notation used in this section for variability models and Kriging follows that of Reference [c].

2.1 INPUT DATA MODEL

Values for the eastward and northward components of velocity, u and v, respectively, are calculated for each buoy from a time-stamped list of buoy positions, $\{t_i, x_i, y_i\}$, using either a constant acceleration model or a constant velocity model. The algorithm includes filters for data spaced too closely in time and calculates a "track quality" value which is used as an indicator of possible outliers.

2.1.1 Buoy Position Error

The latitude (δy_0) and longitude (δx_0) error of a buoy fix position is assigned as a function of the fix quality reported by Argos. Table 2-1 presents the errors assigned to buoy positions by fix quality and the source on which the error value is based. Positions with fix quality zero, A and B are not used in OPS.

Table 2-1. Fix Quality Error

Fix Quality	δx_0 (m)	δy_0 (m)	Source
1 (Argos)	1000	1000	Reference [d]
2 (Argos)	350	350	Reference [d]
3 (Argos)	150	150	Reference [d]
4 (GPS)	50	50	Reference [e]

To prevent anomalies caused by redundant data spaced too closely in time, a minimum time of 15 minutes was chosen to separate consecutive fixes. If a data point is less than 15 minutes from a predecessor, then either the data point or its predecessor is removed based on the following comparison of their fix qualities, Q_{data} and Q_{pred}:

$Q_{\text{data}} \le Q_{\text{pred}}$ $\rightarrow$ Data point removed, and

$Q_{\text{data}} > Q_{\text{pred}}$ $\rightarrow$ Predecessor removed.

2.1.2 Constant Acceleration Model

At any time, t_i, for which a reported position, (x_i, y_i), is bracketed in time by two other position reports, a constant acceleration model is used to determine the velocity. The model assumes that over a reasonably short time period (less than two hours) the buoys move with roughly constant acceleration, $\boldsymbol{a} = (a, b)$. Under this assumption, the equation of motion is modeled as

$$\boldsymbol{r}(t) = \boldsymbol{r}_0 + \boldsymbol{v}_0(t - t_0) + \frac{1}{2}\boldsymbol{a}(t - t_0)^2, \tag{2.1}$$

where $\boldsymbol{r}(t) = (x(t), y(t))$, $\boldsymbol{r}_0 = \boldsymbol{r}(t_0)$, and $\boldsymbol{v}_0 = (u(t_0), v(t_0))$. Let t_0 be the time of a given position report. The velocity at t_0 is determined from positions at t_0 and at the nearest times, t_+ and t_-, such that, $t_- < t_0 < t_+$. The equations of motion at times $t = t_0$, $t = t_+$, and $t = t_-$ are solved simultaneously for the acceleration,

$$\boldsymbol{a} = \frac{2}{t_+ - t_-}\left(\frac{\boldsymbol{r}_+ - \boldsymbol{r}_0}{t_+ - t_0} - \frac{\boldsymbol{r}_0 - \boldsymbol{r}_-}{t_0 - t_-}\right), \tag{2.2}$$

and for the velocity, at time t_0,

$$\boldsymbol{v}_0 = \left(\frac{1}{t_+ - t_0} - \frac{1}{t_+ - t_-}\right)(\boldsymbol{r}_+ - \boldsymbol{r}_0) + \left(\frac{1}{t_0 - t_-} - \frac{1}{t_+ - t_-}\right)(\boldsymbol{r}_0 - \boldsymbol{r}_-). \tag{2.3}$$

The errors in the velocity components, δu_0 and δv_0, are calculated by first-order differential approximation of Equation (2.3), assuming three independent normally distributed variables, (x_+, x_0, x_-) or (y_+, y_0, y_-), giving

$$\delta u_0 = \left[\left(\frac{1}{t_+ - t_0} - \frac{1}{t_+ - t_-}\right)^2 (\delta x_+)^2 + \left(\frac{1}{t_+ - t_0} - \frac{1}{t_0 - t_-}\right)^2 (\delta x_0)^2 + \left(\frac{1}{t_0 - t_-} - \frac{1}{t_+ - t_-}\right)^2 (\delta x_-)^2\right]^{1/2}, \text{ and} \tag{2.4}$$

$$\delta v_0 = \left[\left(\frac{1}{t_+ - t_0} - \frac{1}{t_+ - t_-}\right)^2 (\delta y_+)^2 + \left(\frac{1}{t_+ - t_0} - \frac{1}{t_0 - t_-}\right)^2 (\delta y_0)^2 + \left(\frac{1}{t_0 - t_-} - \frac{1}{t_+ - t_-}\right)^2 (\delta y_-)^2\right]^{1/2}. \tag{2.5}$$

2.1.3 Constant Velocity Model

At the times of the first and last reported positions, a constant velocity model is used to determine velocity for these times. The model assumes that over a reasonably short time period (less than one hour) the buoys move with roughly constant velocity, $\boldsymbol{v}$. Under this assumption, the equation of motion is modeled as

$$\boldsymbol{r}(t) = \boldsymbol{r}_0 + \boldsymbol{v}(t - t_0), \tag{2.6}$$

The velocity is determined from positions at two successive times, t_+ and t_-, such that $t_- < t_+$. The equations of motion at times $t = t_+$ and $t = t_-$ are solved simultaneously for the velocity,

$$\boldsymbol{v} = \frac{\boldsymbol{r}_+ - \boldsymbol{r}_-}{t_+ - t_-}. \tag{2.7}$$

The errors in the velocity components, δu_0 and δv_0, are calculated by first-order differential approximation of Equation (2.7), assuming two independent normally distributed variables x_+ and x_-, or y_+ and y_-, with standard deviations δx_+ and δx_-, or δy_+ and δy_-, giving

$$\delta u_0 = \frac{\sqrt{(\delta x_+)^2 + (\delta x_-)^2}}{t_+ - t_-} \tag{2.8}$$

$$\delta v_0 = \frac{\sqrt{(\delta y_+)^2 + (\delta y_-)^2}}{t_+ - t_-} \tag{2.9}$$

2.1.4 Acceleration Statistics

Acceleration confidence intervals are calculated using accelerations, $\boldsymbol{a}_i = (a_i, b_i)$, calculated from buoy positions using Equation (2.2). The acceleration covariance matrix is constructed,

$$C = \begin{bmatrix} \sigma_a^2 & \sigma_{ab} \\ \sigma_{ab} & \sigma_b^2 \end{bmatrix}, \tag{2.10}$$

where the (co)variances are constructed as follows. The acceleration distribution is modeled as a bivariate normal distribution with zero mean, so that

$$\sigma_a^2 = \frac{\sum_{i=1}^{N} a_i^2}{N-1}, \tag{2.11}$$

$$\sigma_b^2 = \frac{\sum_{i=1}^{N} b_i^2}{N-1}, \text{ and} \tag{2.12}$$

$$\sigma_{ab} = \frac{\sum_{i=1}^{N} a_i b_i}{N-1}, \tag{2.13}$$

where N is the total number of accelerations calculated from all buoys.

The covariance matrix is diagonalized to find the lengths of the semimajor and semiminor axes of the 1σ confidence interval. The solutions of the characteristic equation are

$$L_{\text{maj}} = \sqrt{\frac{1}{2}\left(\sigma_a^2 + \sigma_b^2 + \sqrt{(\sigma_a^2 - \sigma_b^2)^2 + 4\sigma_{ab}^2}\right)} \tag{2.14}$$

$$L_{\text{min}} = \sqrt{\frac{1}{2}\left(\sigma_a^2 + \sigma_b^2 - \sqrt{(\sigma_a^2 - \sigma_b^2)^2 + 4\sigma_{ab}^2}\right)} \tag{2.15}$$

and the slope of the major axis is

$$M_{\text{maj}} = \frac{2\sigma_{ab}}{\sigma_a^2 - \sigma_b^2 + \sqrt{(\sigma_a^2 - \sigma_b^2)^2 + 4\sigma_{ab}}} \tag{2.16}$$

The $K\sigma$ confidence region is an ellipse parameterized by a center at the origin, a major axis of length $2KL_{\text{maj}}$, a minor axis of length $2KL_{\text{min}}$, and a major axis slope of M_{maj}.

The rule by which data should be removed as outliers depends on the desired probability of false alarm, P_{fa} values, which is the probability of marking a valid point as an outlier. Table 2-2 shows the outlier threshold K representing the $K\sigma$ confidence interval outside which points are discarded, based on P_{fa} for circular-normally distributed data. For elliptic-normally distributed data, the values of K in Table 2-2 represent an upper bound on the confidence interval.

Table 2-2. Confidence Interval Corresponding to a Given P_{fa}

P_{fa}	K
0.01	3.04
0.001	3.72
0.0001	4.29
0.00001	4.80
0.000001	5.26

For each reported buoy position, OPS calculates a value called the "track quality" (TQ), which is defined as

$$\text{TQ} = \max\left(0, \left[4 - \sqrt{\left(\frac{a \cdot z_{\text{maj}}}{L_{\text{maj}}}\right)^2 + \left(\frac{a \cdot z_{\text{min}}}{L_{\text{min}}}\right)^2}\right]\right) \tag{2.17}$$

where z_{maj} and z_{min} are the normalized major and minor axes of the confidence interval and $\lceil \ \rceil$ is the ceiling function. The quantity under the square root is, therefore, a magnitude of the acceleration as measured in confidence intervals, and TQ is an integer that is

4, if $\boldsymbol{a}$ is within 1 σ,

3, if $\boldsymbol{a}$ is between 1 σ and 2 σ,

2, if $\boldsymbol{a}$ is between 2 σ and 3 σ,

1, if $\boldsymbol{a}$ is between 3 σ and 4 σ, and

0, if $\boldsymbol{a}$ is outside 4 σ.

The OPS program includes an automatic outlier removal procedure. This procedure iteratively removes data for which TQ = 0, recomputing the confidence interval based on the remaining data until no outliers are left.

2.2 TREND MODEL

After buoy velocity estimates have been obtained, OPS chooses those estimates that are within the user-defined area and within a user-defined "influential" time window. Observations outside these limits are not used in the calculation of the velocity field estimates. In Phase I (Reference [f]), a fixed number of influential data points (20) were used.

Denote a spatio-temporal vector as $\boldsymbol{s} = (x, y, t)$ and the observed surface current velocities as $\boldsymbol{v}_i = \boldsymbol{v}(\boldsymbol{s}_i)$. The set $\{\boldsymbol{v}_i\}_{i=1}^{n}$, where n is the number of velocity points within the influential time window, is modeled as a partial realization of a random field, $\{\boldsymbol{V}(\boldsymbol{s})\}$, that is decomposable as

$$\boldsymbol{V}(\boldsymbol{s}) = \boldsymbol{\mu}(t) + \boldsymbol{\delta}(\boldsymbol{s}), \tag{2.18}$$

where $\mu_j(t)$, $j = 1, 2$ are deterministic functions of time, and $\delta_j(\boldsymbol{s})$, $j = 1, 2$ are, in general, a zero-mean cross-correlated error field. The deterministic component is modeled as an m-order polynomial, so that $\mu_j(t) = \Sigma_{k=0}^{m} M_{jk} t^k$. In Phase I, μ was modeled as a constant. With matrices V, T and Δ defined by their elements as

$$V_{ji} = (\boldsymbol{v}_i)_j, \tag{2.19}$$

$$T_{ik} = t_i^k, \text{ and} \tag{2.20}$$

$$\Delta_{ji} = (\boldsymbol{\delta}(\boldsymbol{s}_i))_j, \tag{2.21}$$

Equation (2.18) can be written in matrix notation as

$$V = MT^T + \Delta . \tag{2.22}$$

The OPS program calculates ordinary (non-weighted) least squares estimates for the parameters comprising M by minimizing the sample variance of the residuals. Denoting $\boldsymbol{\delta} = \boldsymbol{\delta}(s_i)$, the sample variance of the residuals is

$$\sum_{i=1}^{n} \Delta_{ji}^2 = \sum_{i=1}^{n} \left| V_{ji} - \sum_{k=0}^{m} M_{jk} t_i^k \right|^2 , \qquad j = 1, 2 . \tag{2.23}$$

Setting the partial derivatives of Equation (2.23) with respect to each element of M equal to zero, we have for all k,

$$\sum_{i=1}^{n} \sum_{l=0}^{m} M_{jl} t_i^l t_i^k = \sum_{i=1}^{n} V_{ji} t_i^k , \qquad j = 1, 2 \text{, or} \tag{2.24}$$

$$MT^T T = VT . \tag{2.25}$$

The parameters are, therefore, given by $M = VT(T^T T)^{-1}$.

2.3 VARIABILITY MODEL

Kriging methods use a calculated statistic called the *variogram* to measure the spatial dependence of correlation in data collected at different locations. In OPS, time is added as a third parameter to ensure that spatio-temporal correlations are also modeled. The procedure used in OPS to estimate the variogram is based on Reference [g].

Given a spatio-temporally dependent measured quantity drawn from a random field $\boldsymbol{Z}(s)$, the variogram, $2\gamma_Z(\boldsymbol{h})$, represents the variance of measured differences in the measured quantity between locations separated by a given distance vector,

$$2\gamma_Z(s_1 - s_2) = \operatorname{cov}(\boldsymbol{Z}(s_1) - \boldsymbol{Z}(s_2)) . \tag{2.26}$$

The variogram is usually a function of some distance measure, $d(\boldsymbol{h})$. Kriging, therefore, depends on fields for which both the decomposition of Equation (2.18) and the spatial invariance of Equation (2.26) hold. When these two conditions hold, we call the field $Z(s)$ *intrinsically stationary.*

2.3.1 Residual Decomposition

The residual velocity data is assumed to be decomposable as

$$\delta(s) = W(s) + \eta(s) + \varepsilon(s). \tag{2.27}$$

The small-scale variation, $W(s)$, is an L_2-continuous, intrinsically stationary random field whose characteristic correlation distances are comparable to the sampling resolution. The micro-scale variation, $\eta(s)$, is an intrinsically stationary random field whose characteristic correlation distances are smaller than the sampling resolution. A white-noise error field, $\varepsilon(s)$, represents measurement error. The microscale variation is assumed to be negligible since the velocities are calculated as averages over a path of length comparable to the sampling resolution. Since variances add linearly, we have the decomposition

$$2\gamma_\delta(h) = 2\gamma_W(h) + 2\sigma_\varepsilon^2, \tag{2.28}$$

where σ_ε^2, the sample mean of measurement error covariance from Equations (2.4), (2.5), (2.8) and (2.9), is given by

$$\sigma_\varepsilon^2 = \left(\frac{1}{n}\sum_{i=1}^{n}(\delta v_0)_i^2\right) I_2, \tag{2.29}$$

with n, the number of velocities measured in the search area or in the time window, and I_2, a 2×2 identity matrix.

In the following discussion, the vector $v = (u, v)$ refers to the residual value, δ, of the current.

2.3.2 Sample Variogram

To construct a sample variogram from the irregularly spaced velocity data, OPS computes a distance-weighted average of squared velocity component differences on a regular grid. First, a spatio-temporal difference vector, $h_k = s_{i(k)} - s_{j(k)}$, is computed for each unique pair, $(i(k), j(k))$, $i(k) \neq j(k)$, $k = 1, \ldots, \binom{n}{2}$, of velocity reports. The pairs are ordered so that $t_{i(k)}$ is always greater than $t_{j(k)}$.

A domain is defined in the space of $\boldsymbol{h}$ as a rectangular box, extending from $-\frac{1}{2}\Delta x_{max}$ to $+\frac{1}{2}\Delta x_{max}$, from $-\frac{1}{2}\Delta y_{max}$ to $+\frac{1}{2}\Delta y_{max}$, and from 0 to $\frac{1}{2}\Delta t_{max}$, where Δx_{max}, Δy_{max}, and Δt_{max} are the greatest distances found from any pair of data points along the x, y, and t axes. A number of vertices, N_v, is chosen such that $\sqrt[3]{N_v}$ is the next odd integer greater than the cube root of the number of data points. The vertices are distributed in the domain to form $(\sqrt[3]{N_v} - 1)^3$ rectangular boxes similar to the domain.

At each vertex, a weighted average of velocity differences squared is computed to estimate the sample variogram at the vertex. Given a vertex $\boldsymbol{h}_n = (\Delta x_n, \Delta y_n, \Delta t_n)$, the weight for a pair with distance $(\Delta x_k, \Delta y_k, \Delta t_k)$ is taken from a Cressman form,

$$w_k = \begin{cases} \left(\dfrac{1-d^2}{1+d^2}\right) & (d < 1) \\ 0 & (d \geq 1) \end{cases} \tag{2.30}$$

where d is a normalized distance, so that

$$d^2 = \frac{\left(\dfrac{\Delta x_k - \Delta x_n}{\Delta x_v}\right)^2 + \left(\dfrac{\Delta y_k - \Delta y_n}{\Delta y_v}\right)^2 + \left(\dfrac{\Delta t_k - \Delta t_n}{\Delta t_v}\right)^2}{\left(\dfrac{\Delta x_n}{\Delta x_v}\right)^2 + \left(\dfrac{\Delta y_n}{\Delta y_v}\right)^2 + \left(\dfrac{\Delta t_n}{\Delta t_v}\right)^2}, \tag{2.31}$$

where $(\Delta x_v, \Delta y_v, \Delta t_v)$ are the distances along x, y, and t between adjacent vertices.

The weighted averages yielding the sample variogram estimates are

$$2\gamma^{uu}(\boldsymbol{h}_n) = \frac{\sum_k w_k^{uu}(u_{i(k)} - u_{j(k)})^2}{\sum_k w_k^{uu}} \tag{2.32}$$

$$2\gamma^{vv}(\boldsymbol{h}_n) = \frac{\sum_k w_k^{vv}(v_{i(k)} - v_{j(k)})^2}{\sum_k w_k^{vv}}, \text{ and} \tag{2.33}$$

$$2\gamma^{uv}(\boldsymbol{h}_n) = \frac{\sum_k w_k^{uv}(u_{i(k)} - v_{j(k)})^2}{\sum_k w_k^{uv}}. \tag{2.34}$$

2.3.3 Model Variogram

Each of the variograms in Equations (2.32), (2.33), and (2.34) is parametrically modeled based on a multivariate Gaussian correlation function, so that each semivariogram, $\gamma(\boldsymbol{h})$, is

$$\gamma(\boldsymbol{h}) = \sigma_\varepsilon^2 + \sigma^2\left[1 - \exp\left(-\frac{1}{2}\,\boldsymbol{h}\; A\; \boldsymbol{h}\right)\right], \tag{2.35}$$

where A is a symmetric positive-definite 3×3 matrix, σ_ε^2 is an element of the measurement error covariance, and σ^2 is a scalar parameter. The semivariogram sill, defined as $\lim_{\|h\| \to \infty} \gamma(\boldsymbol{h})$, is taken as the highest value of $\gamma(\boldsymbol{h})$ calculated in the domain defined in Section 2.3.2. In Phase I, the matrix A was diagonal, so that latitude-longitude and spatio-temporal correlations of velocities were not treated. Also, the covariance function at zero distance, $C(0)$, which is equivalent to the semivariogram sill, was estimated from the variance of velocity components from a small number of highly correlated "influential" points, which led to underestimated errors.

With σ^2 determined from the sill, the elements of A are found using the empirical estimates of the normalized second moments, m_{pq} of the correlogram,

$$\rho(\boldsymbol{h}) = 1 - \frac{\gamma(\boldsymbol{h})}{\sigma_\varepsilon^2 + \sigma^2}, \tag{2.36}$$

which are

$$m_{pq} = \frac{\sum_n h_{np} h_{nq} \rho(\boldsymbol{h}_n)}{\sum_n \rho(\boldsymbol{h}_n)}, \tag{2.37}$$

where p and q each refer to a spatio-temporal component, x, y, or t, of the distance, and n refers to a vertex. Assuming that the multivariate Gaussian form is a good approximation to $\rho(\boldsymbol{h})$, and that the current data has been sampled over a region including essentially uncorrelated data, we have the approximation,

$$m_{pq} \cong \frac{\int h_p h_q \rho(\boldsymbol{h}) d\boldsymbol{h}}{\int \rho(\boldsymbol{h}) d\boldsymbol{h}} \tag{2.38}$$

$$= \frac{\int h_p h_q \mathrm{Gau}(\boldsymbol{h};\Sigma) d\boldsymbol{h}}{\int \mathrm{Gau}(\boldsymbol{h};\Sigma) d\boldsymbol{h}} \tag{2.39}$$

$$= \Sigma_{pq}, \tag{2.40}$$

where Σ is the covariance matrix associated with the Gaussian function $\mathrm{Gau}(\boldsymbol{h};\Sigma)$. The matrix A is

$$A = \Sigma^{-1/2} , \tag{2.41}$$

which is computable from the moments m_{pq}. The values of $\sigma_\varepsilon^2, \sigma^2$, and the matrix A are stored for each pairing of velocity components, (u, u), (u, v), and (v, v).

2.4 OPTIMAL FIELD ESTIMATION

For each point on the user-defined grid, the ten (10) most influential data points are chosen. The most influential points are those for which the model variograms have the lowest value. If the set of influential points are not identical for all variograms, points are added until the ten most influential points from every variogram are included. A linear system is then constructed to minimize the mean-squared prediction error of the grid point estimate under the constraint that the estimate is unbiased.

The predicted current at a grid point, s_g, is modeled as a linear combination of the current velocity components of the influential points,

$$u(s_g) = \sum_{i=1}^{10} \alpha_i^{uu} u(s_i) + \alpha_i^{uv} v(s_i), \tag{2.42}$$

$$v(s_g) = \sum_{i=1}^{10} \alpha_i^{vu} u(s_i) + \alpha_i^{vv} v(s_i), \tag{2.43}$$

where s_i refers to the spatio-temporal position of the influential point i. Let z_1 and z_2 represent the two velocity components in either order. The weights giving the optimal field at s_g are those that minimize the mean-squared prediction error,

$$\sigma_{1e}^2 = \left\langle \left(z_1(s_g) - \sum_i \alpha_i^{11} z_1(s_i) + \alpha_i^{12} z_2(s_i) \right)^2 \right\rangle, \tag{2.44}$$

subject to the constraints of unbiasedness,

$$\sum_i \alpha_i^{11} = 1\text{, and} \tag{2.45}$$

$$\sum_i \alpha_i^{12} = 0. \tag{2.46}$$

Denoting $z_{1g} = z_1(s_g)$, $z_{1i} = z_1(s_i)$, and $z_{2i} = z_2(s_i)$, and using the constraints given in Equations (2.45) and (2.46), the squared predicted error is

$$\left(z_{1g} - \sum_i \alpha_i^{11} z_{1i} + \alpha_i^{12} z_{2i} \right)^2 = z_{1g}^2 - 2 z_{1g} \sum_i (\alpha_i^{11} z_{1i} + \alpha_i^{12} z_{2i}) \tag{2.47}$$

$$+ \sum_{ij} (\alpha_i^{11} \alpha_j^{11} z_{1i} z_{1j} + 2\alpha_i^{11} \alpha_j^{12} z_{1i} z_{2j} + \alpha_i^{12} \alpha_j^{12} z_{2i} z_{2j})$$

$$= z_{1g}^2 - \sum_i [\alpha_i^{11}(z_{1g}^2 + z_{1i}^2 - (z_{1g} - z_{1i})^2) + \alpha_i^{12}(z_{1g}^2 + z_{2i}^2 - (z_{1g} - z_{2i})^2)] \quad (2.48)$$

$$+\frac{1}{2}\sum_{ij}[\alpha_i^{11}\alpha_j^{11}(z_{1i}^2 + z_{1j}^2 - (z_{1i} - z_{1j})^2) + 2\alpha_i^{11}\alpha_j^{12}(z_{1i}^2 + z_{2j}^2 - (z_{1i} - z_{2j})^2)$$

$$+ \alpha_i^{12}\alpha_j^{12}(z_{2i}^2 + z_{2i}^2 - (z_{2i} - z_{2j})^2)]$$

$$= \sum_i [\alpha_i^{11}(z_{1g} - z_{1i})^2 + \alpha_i^{12}(z_{1g} - z_{2i})^2] \quad (2.49)$$

$$-\frac{1}{2}\sum_{ij}[\alpha_i^{11}\alpha_j^{11}(z_{1i} - z_{1j})^2 + 2\alpha_i^{11}\alpha_j^{12}(z_{1i} - z_{2j})^2 + \alpha_i^{12}\alpha_j^{12}(z_{2i} - z_{2j})^2]$$

Lagrange multipliers are used to find $(\alpha_i^{11}, \alpha_i^{12})$ values that minimize Equation (2.44) subject to the constraints given by Equations (2.45) and (2.46). The optimal weights, $\{\alpha_i^{11}\}$ and $\{\alpha_i^{12}\}$, are found by minimizing

$$\sigma_{1e}^2 - 2m^{11}\left(\sum_i \alpha_i^{11} - 1\right) - 2m^{12}\sum_i \alpha_i^{12} = \sum_i [\alpha_i^{11}\gamma^{11}(s_g - s_i) + \alpha_i^{12}\gamma^{12}(s_g - s_i)] \quad (2.50)$$

$$-\frac{1}{2}\sum_{ij}[\alpha_i^{11}\alpha_j^{11}\gamma^{11}(s_i - s_j) + 2\alpha_i^{11}\alpha_j^{12}\gamma^{12}(s_i - s_j)$$

$$+ \alpha_i^{12}\alpha_j^{12}\gamma^{22}(s_i - s_j)]$$

$$- 2m^{11}\left(\sum_i \alpha_i^{11} - 1\right) - 2m^{12}\sum_i \alpha_i^{12}.$$

Setting the partial derivatives of Equation (2.50) with respect to each weight equal to zero results in a linear system. Combining the linear system for $u = 1$ and $v = 2$ with the system for $v = 1$ and $u = 2$ results in the following system of equations:

$$\gamma_i^{uu} = m^{uu} + \sum_j \Gamma_{ij}^{uu}\alpha_j^{uu} + \Gamma_{ij}^{uv}\alpha_j^{uv} \quad (2.51)$$

$$\gamma_i^{uv} = m^{uv} + \sum_j \Gamma_{ij}^{uv}\alpha_j^{uu} + \Gamma_{ij}^{vv}\alpha_j^{uv} \quad (2.52)$$

$$\gamma_i^{vu} = m^{vu} + \sum_j \Gamma_{ij}^{vu}\alpha_j^{vv} + \Gamma_{ij}^{uu}\alpha_j^{vu} \quad (2.53)$$

$$\gamma_i^{vv} = m^{vv} + \sum_j \Gamma_{ij}^{vv}\alpha_j^{vv} + \Gamma_{ij}^{vu}\alpha_j^{vu}, \quad (2.54)$$

where m^{uu}, m^{uv}, m^{vu}, and m^{vv} are Lagrange multipliers. The left-handed sides of Equations (2.51) through (2.54) are given by

$$\gamma_i^{uu} = \gamma^{uu}(s_g - s_i), \quad (2.55)$$

$$\gamma_i^{uv} = \gamma^{uv}(s_g - s_i), \quad (2.56)$$

$$\gamma_i^{vu} = \gamma^{vu}(s_g - s_i), \text{ and} \quad (2.57)$$

$$\gamma_i^{vv} = \gamma^{vv}(s_g - s_i). \quad (2.58)$$

The matrices Γ^{uu}, Γ^{uv}, Γ^{vu}, and Γ^{vv} in Equations (2.51) through (2.54) are given by

$$\Gamma_{ij}^{uu} = \gamma^{uu}(s_i - s_j), \quad (2.59)$$

$$\Gamma_{ij}^{uv} = \gamma^{uv}(s_i - s_j), \quad (2.60)$$

$$\Gamma_{ij}^{vu} = \gamma^{vu}(s_i - s_j), \text{ and} \quad (2.61)$$

$$\Gamma_{ij}^{vv} = \gamma^{vv}(s_i - s_j). \quad (2.62)$$

The residual current components are given by Equations (2.42) and (2.43), and the estimated variances are

$$\sigma_u^2 = \sigma_{ue}^2 - \sigma_\varepsilon^2, \quad (2.63)$$

$$\sigma_v^2 = \sigma_{ve}^2 - \sigma_\varepsilon^2. \quad (2.64)$$

The mean value of the current, $\mu(t)$, is added to the residual current estimate at the grid point to give the current estimate at that point.

The models tested for the cross-variogram, $\gamma^{uv} = \gamma^{vu}$, which relates different velocity components in varying spatio-temporal separations, do not necessarily obey the Schwarz inequality for covariance matrix components. This failure can lead to instability in the Kriging solution, so the cross-variogram is not used, and the weights α^{uv} and α^{vu} are set to zero in OPS. In Phase I, the cross-correlogram, which is the analog to the cross-variogram in objective analysis, was also not used.

3.0 OPS PROGRAM DESCRIPTION

The Ocean Prediction System (OPS) is designed to generate statistical estimates in real time of ocean surface current using Self Locating Data Marker Buoy (SLDMB) data.

The OPS program is a prototype system. Calculations and displays are available for the Coast Guard First District. The OA algorithm is designed to process current measurements and associated uncertainty estimates from any source. However, the OA preprocessing options in OPS are restricted to SLDMB data.

The program includes the following subprograms.

3.1 BUOY DATA RETRIEVAL

The program contacts the Argos data center using either the Internet or Tymnet dialup, downloads the GPS and Argos fix data for the requested buoy IDs, removes redundant data, translates the downloaded data into buoy fix times, positions, and fix type/quality. The downloaded data is then merged with existing fix data for the requested buoys and saved for use as input to the current field calculation.

3.2 BUOY DATA PROCESSING

Buoy data processing allows the operator to examine downloaded buoy fix data graphically and numerically, view calculated buoy velocities, delete bad data points from the data set, and re-save the buoy data for later use as current field calculation input.

3.3 SURFACE CURRENT FIELD GENERATION AND DISPLAY

The current field generation program allows the operator to specify Objective Analysis (OA) parameters, calculate and save a current field, and display the current field graphically and numerically.

The operator can display a newly calculated or previously saved current vector field, RMS error, contoured current values, buoy tracks, and buoy velocities. Overlay options include display of Coast Guard First District boundaries and digital charts. Numerical displays include input parameters, and calculated current values with RMS error. The user may also write an output file containing the current information which may be used as input to an appropriately modified version of CASP (Reference [h]).

The operator may also generate, save, and replay slide shows containing current field images at different times in order to observe the time-evolution of the current field.

The OPS User's Guide is provided as Appendix B.

4.0 OPS DEVELOPMENT TEST DESCRIPTION

The OPS Development Test consisted of three phases:

Phase I Buoy Deployment,
Phase II Real Time Estimation, and
Phase III Data Collection.

The test plan is provided as Appendix A. Analysis results are discussed in Section 5.0.

4.1 PHASE I. BUOY DEPLOYMENT

Buoy deployment was delayed 48 hours due to poor weather conditions. Deployment of buoys 1-11 took place from 010949Z - 011441Z JUN 96 in the vicinity of NOAA buoy 44011 in accordance with the test plan. Weather conditions at time of launch were: winds less than 10 knots from the southwest and wave height less than 3 feet.

Transmissions from all buoys were received by the Gonio Radio Direction Finder on board prior to launch. Buoys 7 and 10 did not transmit after they were launched. Buoy 1 transmissions were erratic and unreliable. Buoy 5 did not transmit following the first hour after launch. Good data was received from the remaining seven buoys. Images taken during Phase I are shown in Figures 4-1 through 4-8.

4.2 PHASE II. REAL TIME ESTIMATION

During Phase II, buoy data was downloaded and surface current fields and Area of Uncertainty (AOU) propagations were calculated in near real time. An image of the workstation used to run OPS is shown in Figure 4-9.

Phase II results were posted on the Internet at www.applmath.com for viewing by authorized users.

4.3 PHASE III. DATA COLLECTION

Phase II ended and Phase III began at 081200Z JUN 96. Buoy 1 stopped reporting GPS fixes at 031345Z JUN 96, but continued to report Argos fixes. Buoy 3 stopped reporting GPS fixes at 050431Z JUN 96, and stopped reporting Argos fixes at 090715Z JUN 96. Buoy 4 reported several invalid GPS fix times between 091200Z and 101200Z JUN 96, and stopped reporting GPS fixes at 160537Z JUN 96. Buoy 6 stopped reporting GPS fixes at 011527Z JUN 96, and reported its last Argos fix at 132152Z JUN 96. With the exception of brief data dropouts, buoys 1, 2, and 4 continued to report Argos fixes, and buoys 8, 9, and 11 continued to report good GPS and Argos fixes throughout the remainder of Phase III.

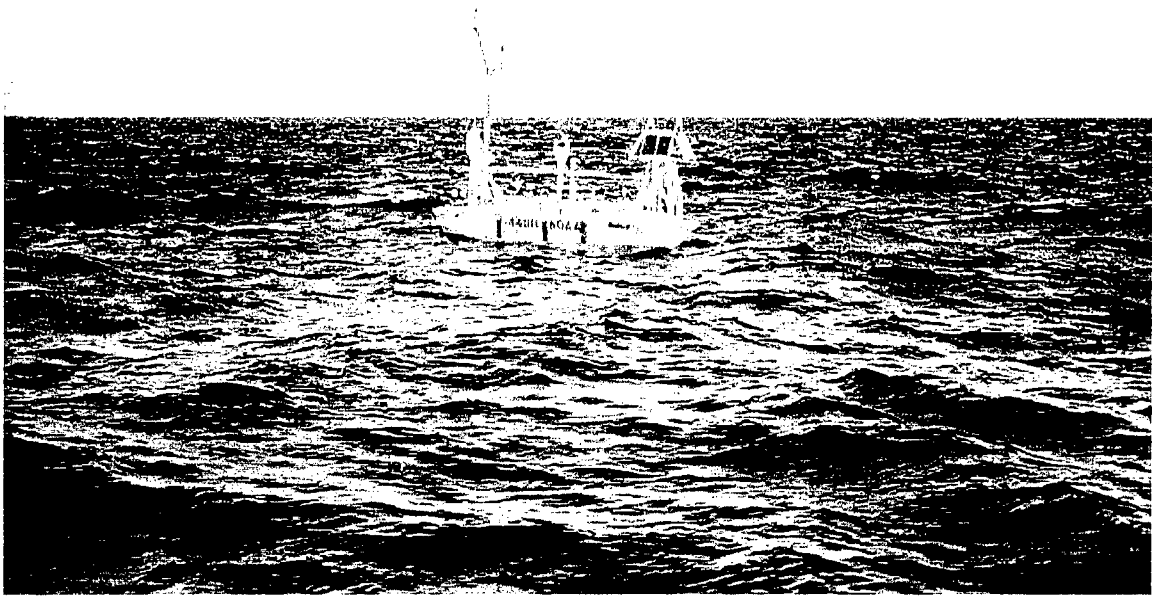

Figure 4-1. NOAA Buoy 44011 at Time of Buoy #1 Deployment

Figure 4-2. Metocean Buoy on the Deck of M/Y High Seas

Figure 4-3. Deployment of Metocean Buoy

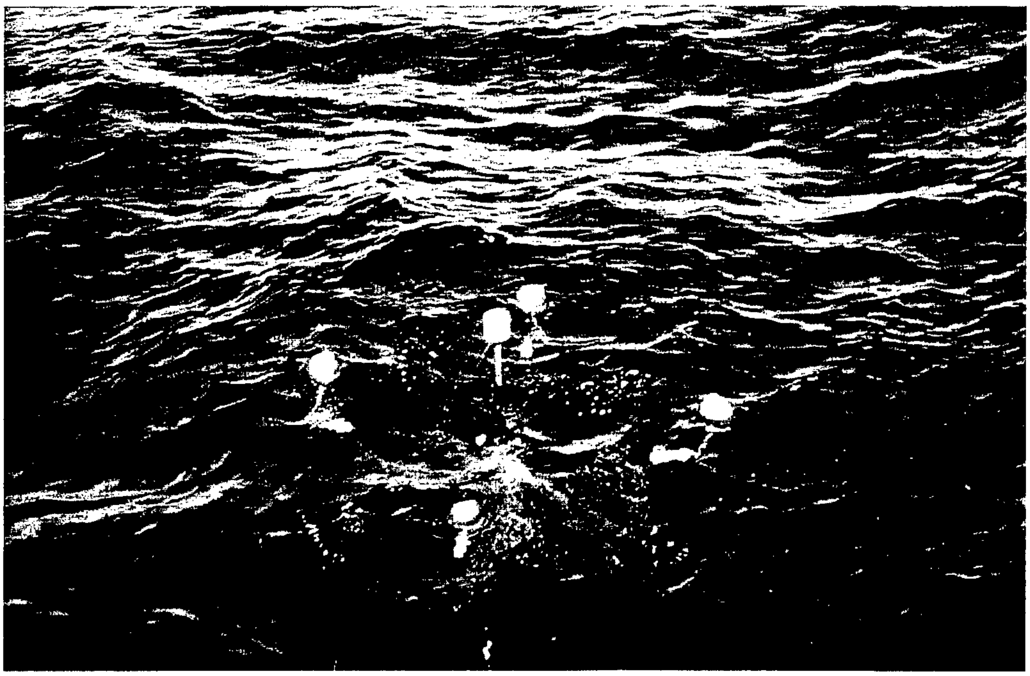

Figure 4-4. Metocean Buoy in Water

Figure 4-5. Metocean Buoy in Water

Figure 4-6. Deployment of Clearwater Buoy

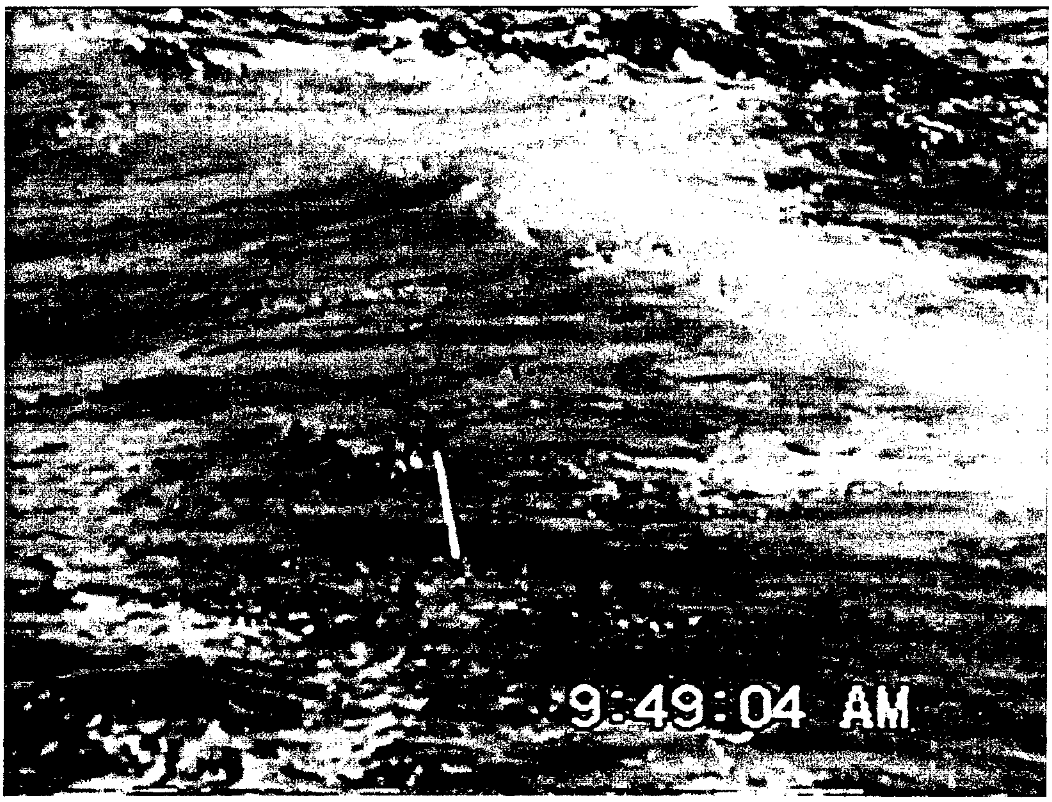

Figure 4-7. Clearwater Buoy in Water

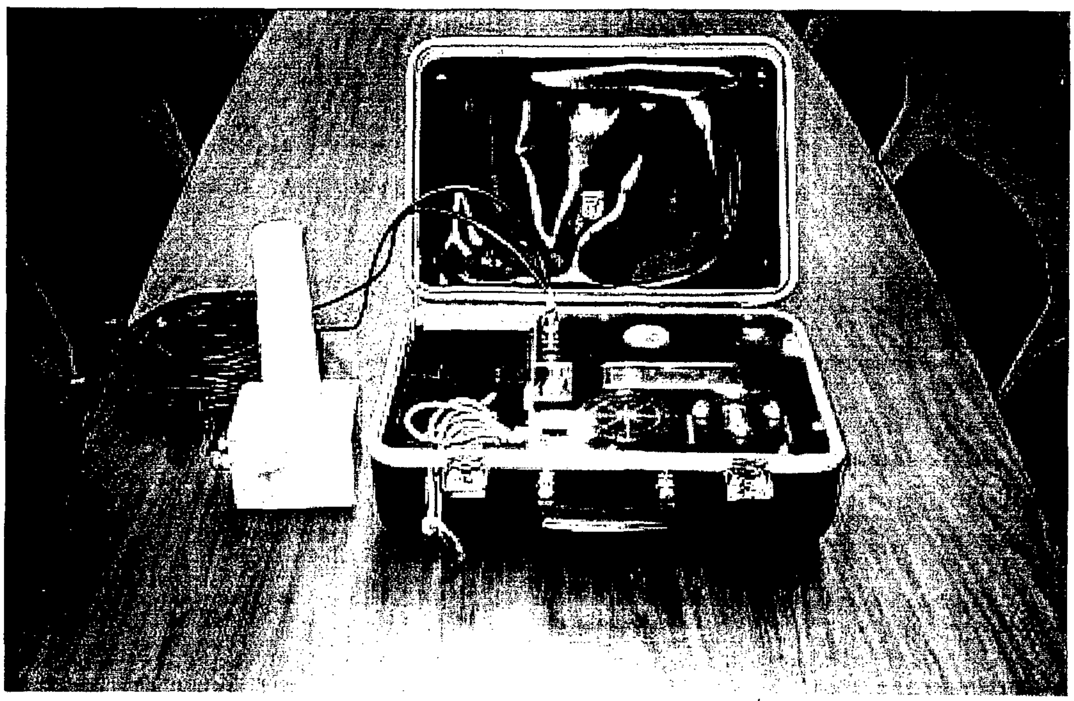

Figure 4-8. Gonio Radio Direction Finder Used to Monitor Buoy Transmissions During Deployment

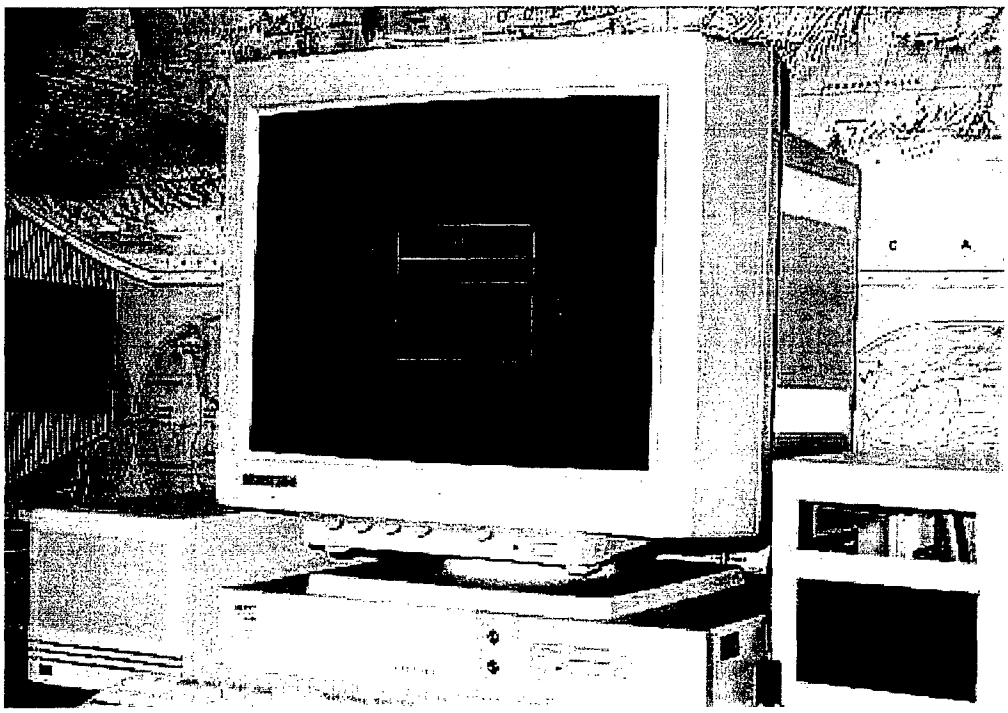

Figure 4-9. HP Workstation Used for OPS

Phase III ended at 281200Z JUN 96. At this time, buoys 1, 2, and 4 continued to report Argos fixes, and buoys 8, 9, and 11 continued to report both GPS and Argos fixes. A timeline of the fixes received from each buoy throughout the buoys' lifetimes is shown in Figure 4-10.

Additional data was collected and archived until 011700Z September 1996 at which time all buoys had ceased transmitting.

Weather data (atmospheric pressure, wind direction, wind speed, and wave height) reported hourly by NOAA buoy 44011 during the buoy lifetimes are shown in Figures 4-11 through 4-14. This data was retrieved via the Internet in near real time at www.ems.psu.edu and www.met.fsu.edu.

The Metocean buoys (buoys 8-11) reported their battery voltages as part of the data stream. The buoys were predicted to operate until the battery voltage reached 8.5 volts. The battery voltages as a function of time for buoys 8, 9, and 11 (buoy 10 failed immediately after launch) are shown in Figure 4-15.

Following launch, the buoys generally spiraled toward the WestSouthwest throughout Phase III. Following the end of Phase III, buoys 1, 2, and 4 continued to spiral to the Southwest. Buoys 1 and 2 eventually turned toward the East, and then toward the North before they stopped transmitting. Buoy 4 stopped transmitting while still spiraling toward the Southwest. While buoy 11 continued to spiral toward the WestSouthwest until it stopped transmitting, buoys 8 and 9 turned toward the North, then toward the Northeast before they stopped transmitting. The buoy tracks for the duration of the buoys' lifetimes are shown in Figure 4-16. Note that the buoys stopped transmitting at different times. The last buoy stopped transmitting at 011700Z SEP 96.

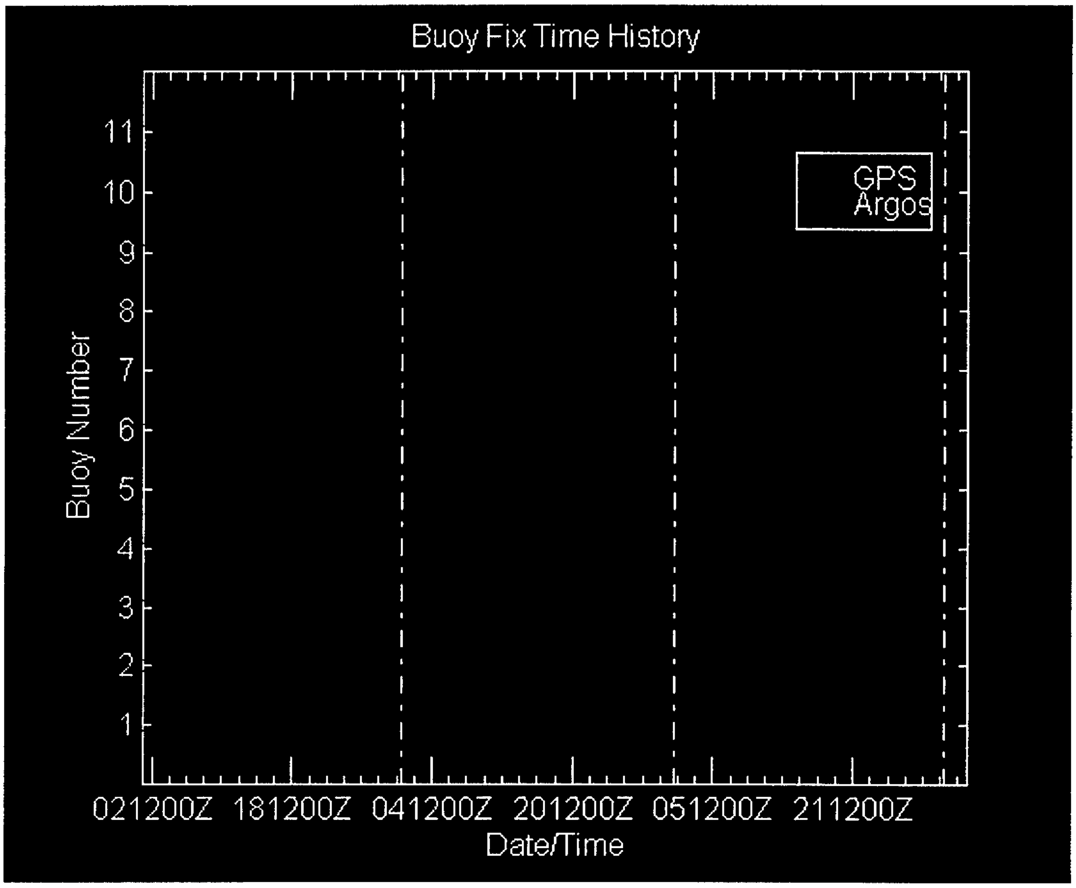

Figure 4-10. SLDMB Timeline: June to September 1996

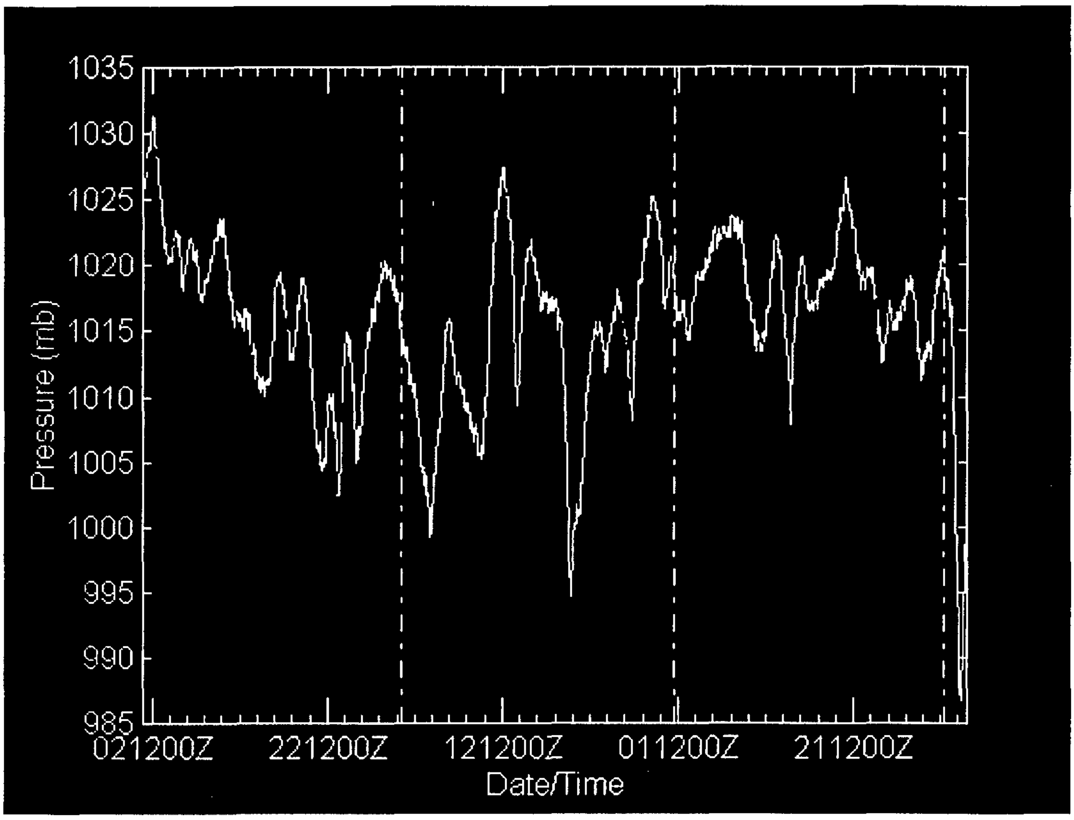

Figure 4-11. NOAA Buoy 44011 Atmospheric Pressure Hourly Data: June to September 1996

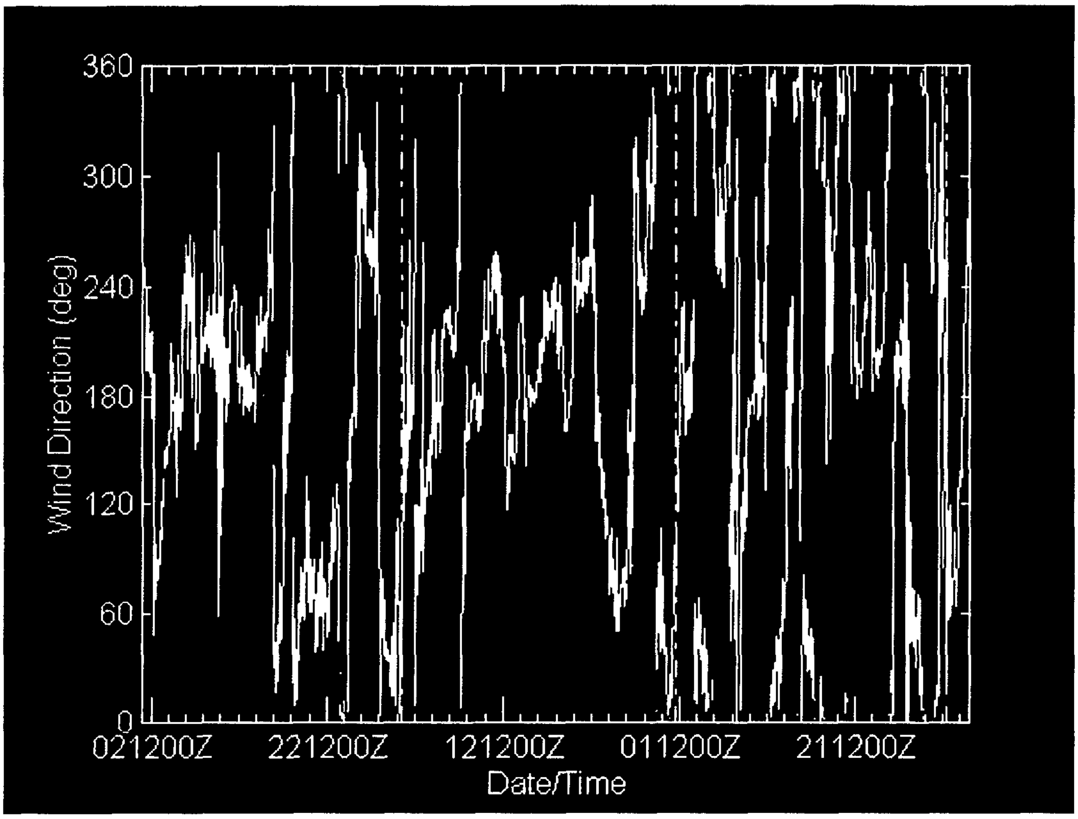

Figure 4-12. NOAA Buoy 44011 Wind Direction Hourly Data: June to September 1996

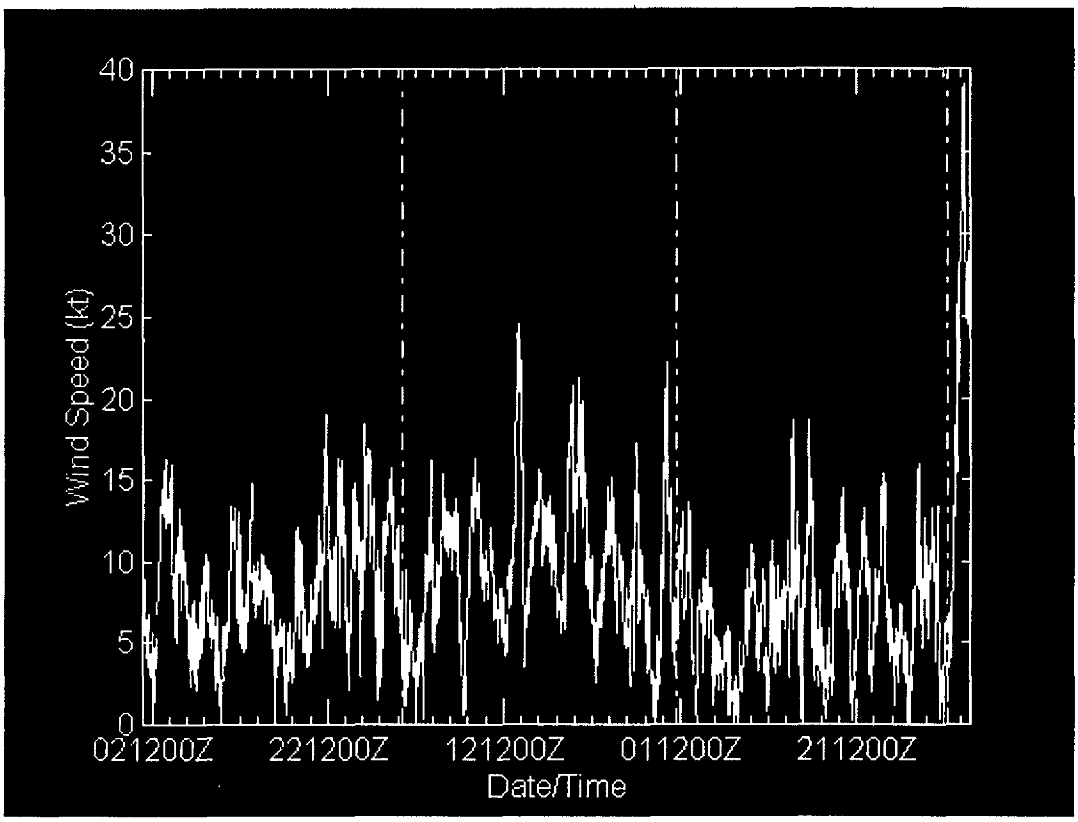

Figure 4-13. NOAA Buoy 44011 Wind Speed Hourly Data: June to September 1996

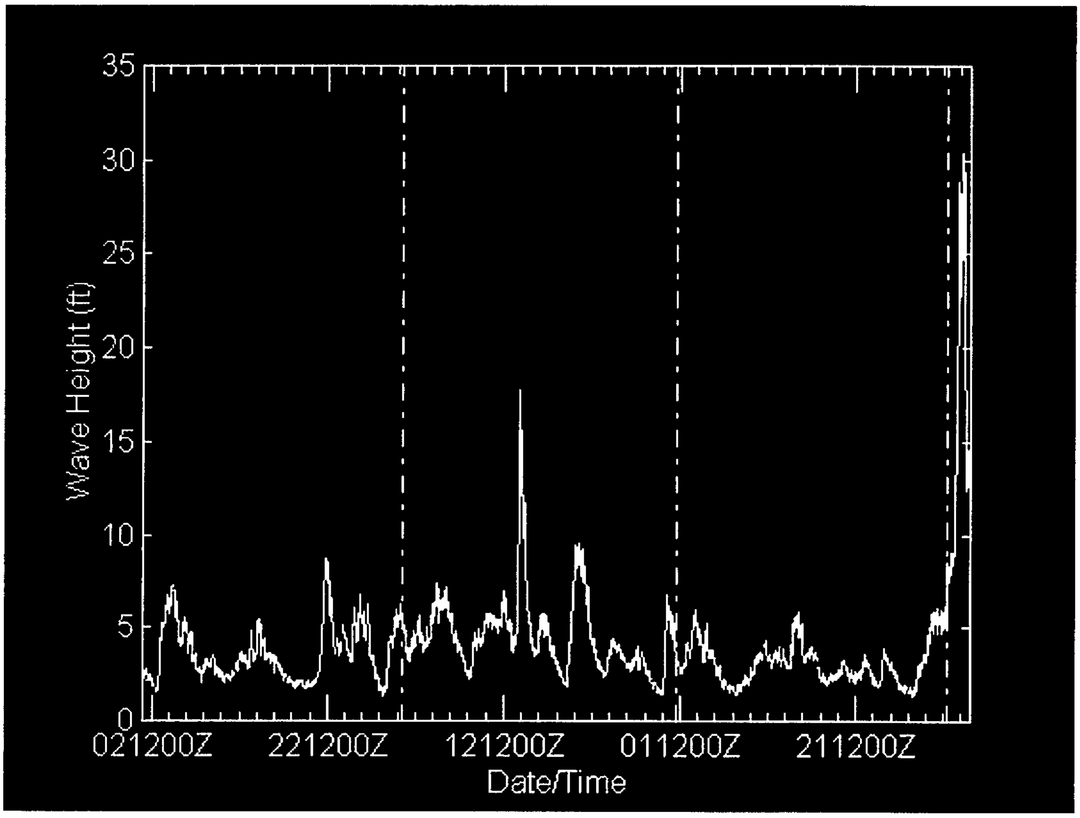

Figure 4-14. NOAA Buoy 44011 Wave Height Hourly Data: June to September 1996

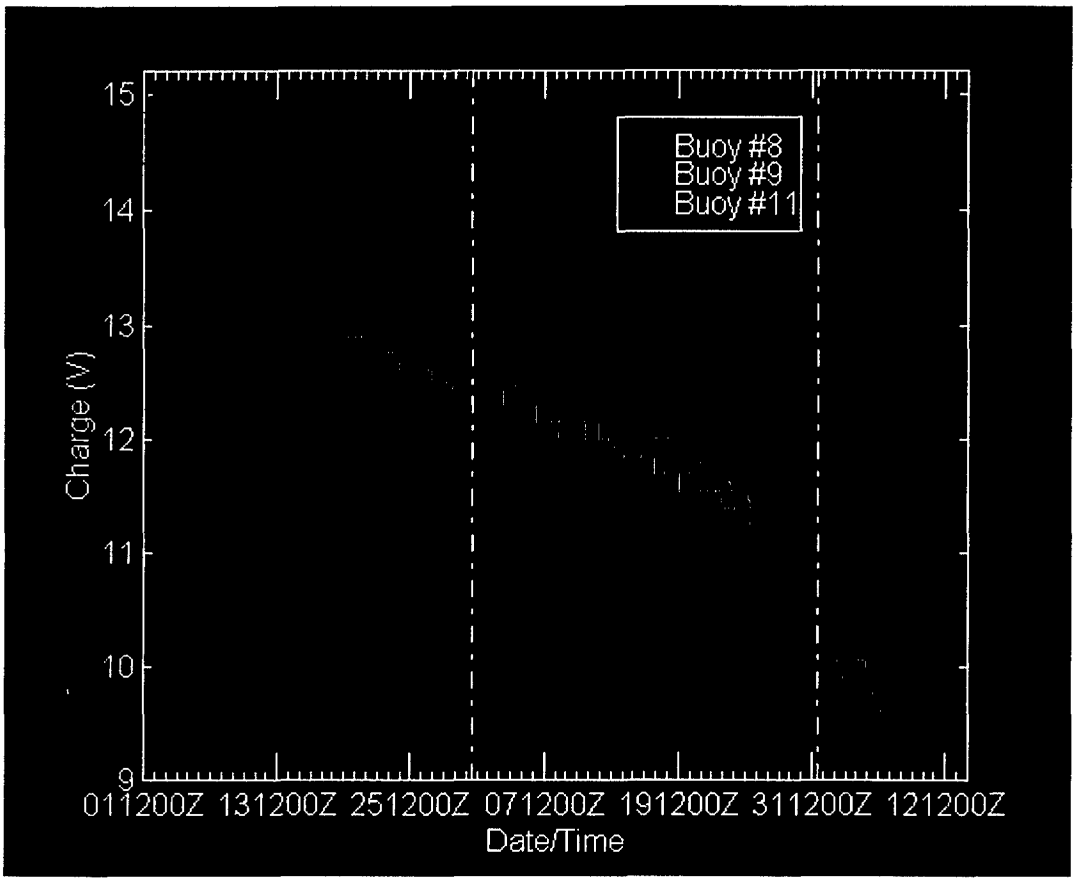

Figure 4-15. Metocean SLDMB Battery Voltages

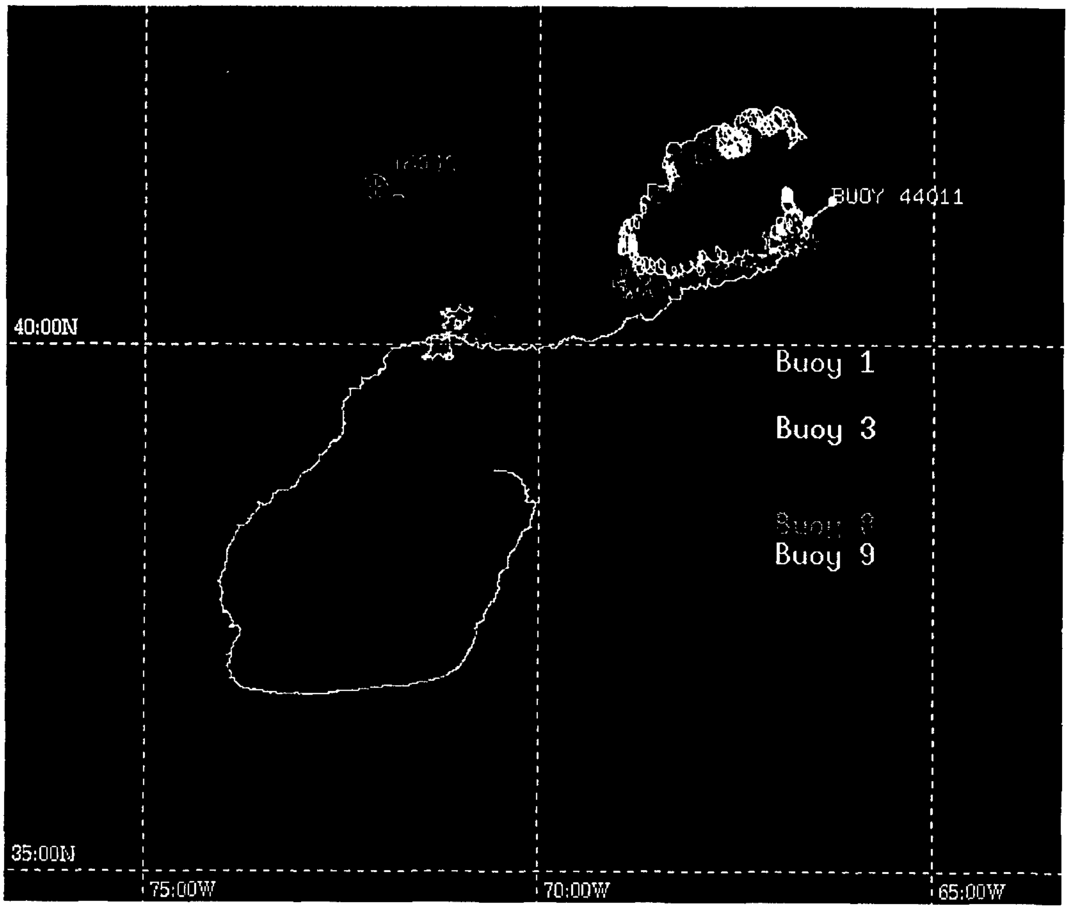

Figure 4-16. Cumulative Tracks from 011200Z JUN 96 to 011700Z SEP 96

5.0 OPS DEVELOPMENT TEST RESULTS

The main results from the OPS Development Test are as follows:

SLDMB PERFORMANCE (Section 5.1)

- 2/7 Clearwater and 1/4 METOCEAN buoys failed within 1 hour.
- Of the remaining buoys, 2/5 Clearwater and 3/3 METOCEAN gave reliable GPS data.
- GPS transmissions from Clearwater buoys ceased within 17 days.
- 3/5 Clearwater and 3/3 METOCEAN buoys continued reporting after 17 days.
- GPS and Argos data from the remaining METOCEAN buoys continued for 65-69 days.
- Argos data from the remaining Clearwater buoys continued for 85-92 days.

SLDMB DATA QUALITY (Section 5.2)

- 83.5% of data were GPS fixes, and 16.5% were Argos fixes.
- 336 of 12,163 data points (2.76%) were marked as outliers by the OPS input data processing algorithm.

SLDMB TRACKS (Section 5.3)

- Tracks bifurcated in the shelf water near 40 30 N, 69 00 W.
- Two tracks converged in the Gulf Stream near 36 30 N, 73 00 W.
- There was no significant correlation between buoy drift velocity and wind velocity.
- The tracks had a strong cyclic component with approximately a 12.5 hour period.

OPS PERFORMANCE (Section 5.6)

- CASP predictions of the motion of Buoy 1 and its AOU using OPS currents were accurate, whereas CASP predictions using historical currents were highly biased.
    - CASP AOUs for Buoy 1 using historical currents contained the target at 90% “confidence” in 2/48 cases (4%).
    - CASP AOUs for Buoy 1 using OPS currents contained the target at 90% “confidence” in 43/48 cases (90%).

- CASP predictions of the motion of Buoy 11 and its AOU using OPS currents were less accurate than those for Buoy 1, but still far less biased than CASP predictions using historical currents.
    - CASP AOUs for Buoy 11 using historical currents contained the target at 90% “confidence” in 0/24 cases (0%).
    - CASP AOUs for Buoy 11 using OPS currents contained the target at 90% “confidence” in 13/24 cases (54%).
- CASP AOUs using OPS currents grew faster than CASP AOUs using historical data, due to higher uncertainty calculated by OPS.
    - Area of 92 - 99% CASP AOU for Buoy 1 using historical currents was 31 square miles after 72 hours.
    - Area of 92 - 99% CASP AOU for Buoy 1 using OPS currents was 403 square miles after 72 hours.
    - Area of smallest CASP AOU containing Buoy 1 using historical currents was 893 square miles after 72 hours.
    - Area of smallest CASP AOU containing Buoy 1 using OPS currents was 155 square miles after 72 hours.

OPS SENSITIVITY ANALYSIS (Section 5.7)

- Overall estimated uncertainty was minimized when the buoys were separated by at least 5 nm in latitude and longitude.
- OPS performed better when the drifter buoys surrounded the target.
- OPS performance was somewhat improved with the use of buoy data taken both before and after the time at which the current is estimated.
- OPS performance was sensitive to the time window used. OPS performed best in this test for time windows between 6 and 12 hours.
- OPS performance was sensitive to the order of the polynomial used to model the average current in time. OPS performed best in this test with a cubic model.
- OPS performance was not sensitive to the use of a Shapiro filter to spatially smooth the current field estimate.
- OPS performance was not sensitive to the number of influential points used in the Kriging procedure.

Analysis Methodology. CASP was used to assess OPS effectiveness.

The probability map feature in CASP was used to drift a target with CASP historical current data files and, using a software patch provided by Daniel H. Wagner, Associates (Reference [h]), with OPS currents. The target parameters were PIW without PFD; size 5.8 feet; leeway factor 0; drift 0; displacement: light, no drogue. The position data parameters were credibility 1; time error 0; position error matching SLDMB fix error.

The software patch was used because the DMB option in CASP 2.0 is not operational.

The measures used to analyze OPS performance were the distance from the AOU center of mass to the target as a measure of predictor accuracy, the AOU probability level at the target position as a measure of error accuracy, and the area of the smallest AOU containing the target as a measure of effectiveness.

In the following sections, we provide support for these conclusions.

5.1 SLDMB PERFORMANCE

The eleven buoys were deployed on 1 June 1996 from 0949Z to 1441Z at the locations specified in the test plan. Transmissions were received from each buoy by the Gonio RDF on board M/Y HIGH SEAS at least 30 minutes prior to launch. A timeline of buoy fixes is given in Figure 4-10. Buoys 7 and 10 ceased transmission immediately after launch, and Buoy 5 ceased after one hour in the water. GPS positions from Buoy 1 were erratic and ceased altogether after 52 hours, but its Argos fixes were reasonable. Buoy 6 ceased GPS transmissions three hours after launch, but continued to report intermittent Argos fixes for twelve days. Buoy 3 ceased GPS transmissions after nearly four days, but continued to report Argos fixes for another four days.

GPS transmissions from the three remaining Clearwater buoys ceased within 17 days from launch, but Argos fixes were reported for more than 85 days after launch. GPS transmissions from each of the three remaining METOCEAN buoys continued for roughly the life of the battery, more than 65 days. Figure 4-15 shows the battery voltages of the three METOCEAN buoys as a function of time. Argos fix reports from the METOCEAN buoys did not last more than two days after the end of GPS transmissions.

5.2 SLDMB DATA QUALITY

Table 5-1 gives the distribution of all usable buoy position data retrieved by OPS and their reported fix qualities. A total of 12,163 data points were used. GPS fixes accounted for more than 83 percent of all position data, primarily because the GPS data rate tended to be much higher than the Argos rate. Table 5-2 gives the distribution of velocity data by track quality, as defined in Section 2.1.4. Position reports giving track qualities of zero were considered outliers and were removed from further processing. Approximately 336 points, or 2.76 percent of all points were marked as outliers. Assuming a bivariate Gaussian acceleration distribution, the outliers would have been removed with at most 0.03 percent probability (per point) of false alarm.

Table 5-1. Distribution of Usable SLDMB Data by Fix Quality

Fix Quality	Percentage
1 Argos	6.1
2 Argos	6.8
3 Argos	3.6
4 GPS	83.5

Table 5-2. Distribution of SLDMB Data by Source and Track Quality

Track Quality	Percentage		
	of GPS	of Argos	Overall
0	3.1	1.3	2.8
1	2.2	0.3	1.9
2	14.0	2.0	12.0
3	45.5	12.7	40.1
4	35.2	83.7	43.2

The empirical distribution function of acceleration values is plotted in Figure 5-1 as a distribution over confidence levels R. A χ^2 distribution is also plotted, which results from considering the acceleration distribution as a bivariate Gaussian distribution. The two distributions differ at the 1-percent significance level, the empirical distribution being more tailed than the χ^2 distribution for R and more kurtotic within about 1.5 confidence intervals.

5.3 SLDMB TRACKS

The complete tracks of the eight buoys remaining more than one hour after launch are shown in Figure 4-16. The combined tracks illustrate features of the shelf-water currents, the slope-water currents, and the Gulf Stream. Regions of strong current and weak current can be seen by comparing the relative sizes of the loops created by short-period cycles. A bifurcation point can be seen near 40 30 North latitude, 69 00 West longitude, at which Buoys 8 and 9 split from the rest of the group. A convergence of buoy tracks 1 and 2 can be seen near 36 30 North latitude, 73 00 West longitude, as the buoys enter and follow the Gulf Stream.

Figure 5-2 shows the same tracks as Figure 4-16 for the first five days after deployment. Dropouts in the data, visible in the tracks of Buoys 1, 6, 9, and 11, are filled with a straight line track for continuity on the plot. The periodic cycles can easily be seen in Figure 5-2.

Two features of currents were examined using velocity estimates from the complete set of buoy tracks. The buoy velocities were first correlated with winds measured at NOAA Buoy 44011 in order to gauge the effect of winds on the surface drifters. The observed periodic motion of the buoys was also examined by spectral analysis.

Wind speed and direction, which are reported hourly by NOAA Buoy 44011, were correlated with each velocity (u_i, v_i) estimated from n drifter buoy positions. The wind speeds were converted into eastward and northward components, u_w and v_w, respectively.

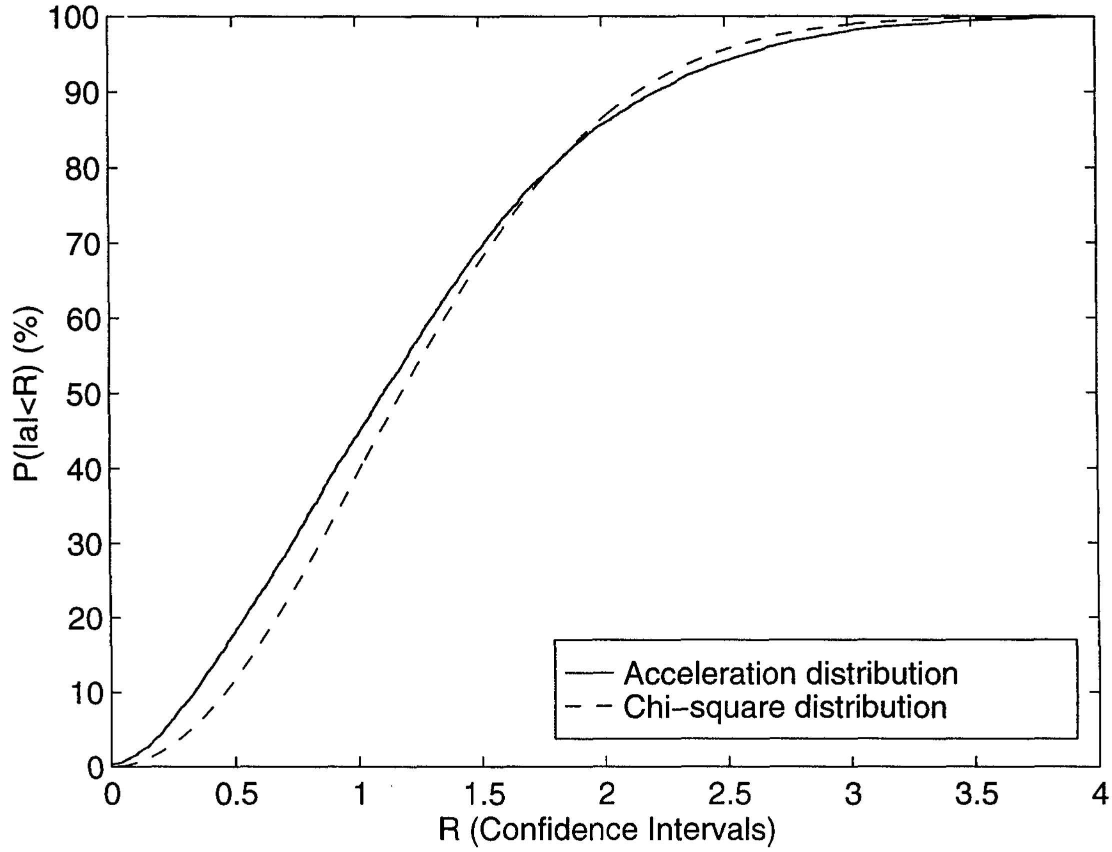

Figure 5-1. Distribution of Acceleration Values

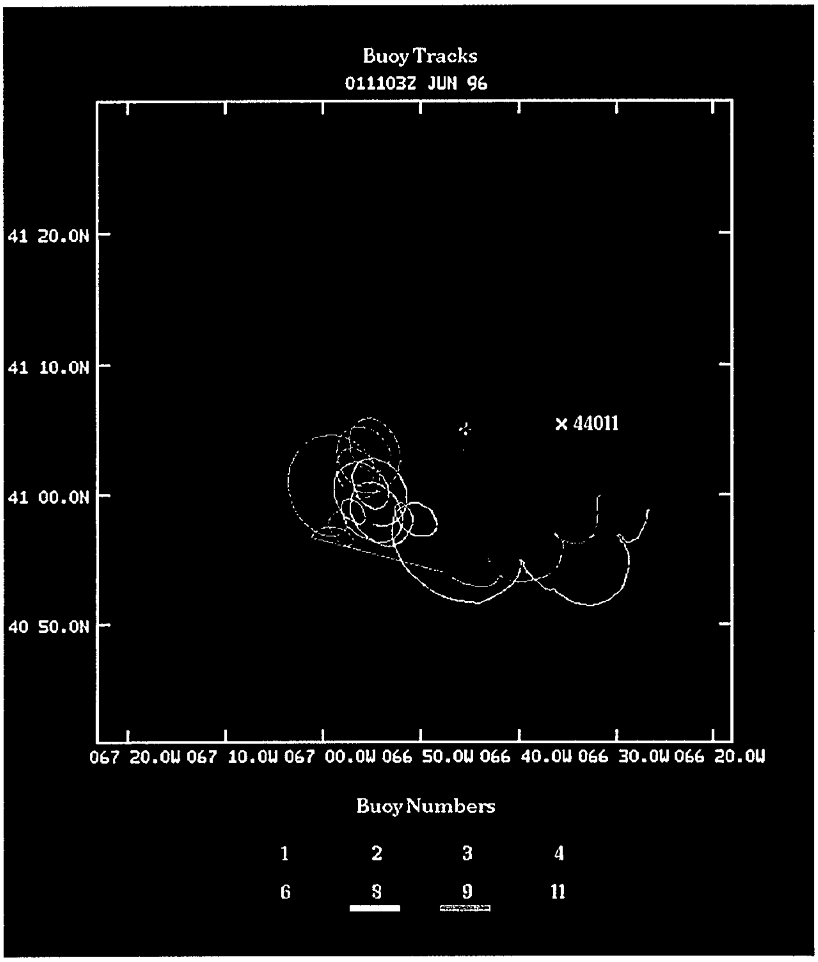

Figure 5-2. Buoy Tracks from 011200Z to 061200 JUN 96

The correlation coefficients r_u and r_v were then computed as

$$r_u = \frac{\sum_{i=1}^{n} (u_i - \bar{u})(u_{wi} - \bar{u}_w)}{\sqrt{\sum_{i=1}^{n} (u_i - \bar{u})^2 + (u_{wi} - \bar{u}_w)^2}} \tag{5.1}$$

$$r_v = \frac{\sum_{i=1}^{n} (v_i - \bar{v})(v_{wi} - \bar{v}_w)}{\sqrt{\sum_{i=1}^{n} (v_i - \bar{v})^2 + (v_{wi} - \bar{v}_w)^2}} \tag{5.2}$$

where (u_{wi}, v_{wi}) is the average wind velocity over a predefined time interval, Δt, interpolated linearly in time to the time of the buoy velocity report, (u_i, v_i), and the bar denotes an average over the n points.

Table 5-3 gives the correlation coefficients computed using six and twelve-hour time intervals. A radius of influence, R, defines a disk outside of which buoy velocity reports are excluded from the sums in Equations (5.1) and (5.2). For both time intervals, there was no significant correlation found between the wind velocity and the buoy drift velocity. The sample size, n, for each calculation is listed in Table 5-3.

Table 5-3. Correlation Coefficients for Wind Velocity and Buoy Velocity

Δt (hr)	R (nm)	n	r_u	r_v
6	5	202	+0.10	+0.16
6	10	1027	-0.10	+0.01
6	20	2538	-0.07	-0.09
6	50	4480	-0.10	-0.08
12	5	201	+0.12	+0.23
12	10	1023	-0.11	+0.08
12	20	2534	-0.05	-0.01
12	50	4480	-0.07	-0.03

The cyclic motion of the buoys was examined using the GPS positions from the five buoys, Buoys 2, 4, 8, 9, and 11, that were transmitting reasonable GPS fixes. The Fourier transforms, $U(f)$ and $V(f)$, of the velocity components were calculated by approximating the transform integrals using the midpoint rule,

$$U(f) = \sum_{i=1}^{n-1} \frac{1}{2}(u_i + u_{i+1})\exp[i\pi f(t_i + t_{i+1})] \tag{5.3}$$

$$V(f) = \sum_{i=1}^{n-1} \frac{1}{2}(v_i + v_{i+1})\exp[i\pi f(t_i + t_{i+1})] . \tag{5.4}$$

The moduli of $U(f)$ and $V(f)$ are plotted in Figures 5-3 and 5-4, versus period, or inverse frequency. The sharp peaks at approximately 12.5 hours indicate a strong tidal component in the current.

5.4 OPS CURRENT FIELD ESTIMATES

Figure 5-5 shows the OPS current field estimate every four hours for the first twenty hours of the test, 011200Z JUN96 to 020800Z JUN96. The arrow lengths and directions indicate the estimated current speed and direction. The color indicates the root-mean-square (RMS) error of the two velocity components. The regions of lowest error are, as expected, close to the location of the buoys at the solution time.

Figures 5-6 and 5-7 show the OPS current field estimates for the first four days of the test, 011200Z JUN96 to 051200Z JUN96. Note that by the fourth day the buoys have collapsed nearly onto a line. The lack of data separation in space causes difficulty in characterizing the error distribution accurately in both spatial dimensions, so the error estimates increase.

5.5 AREA OF UNCERTAINTY PROPAGATION

Using the position of NOAA Buoy 44011 as an initial position at time 011200Z JUN96 for a drifting target with a one nautical mile uncertainty radius, the area of uncertainty (AOU) was propagated.

AMI AOU Propagation. Figures 5-8, 5-9, and 5-10 show the progression of the AOU at six times during the first four days of the test. Each color level indicates the probability of containing the target within the region enclosed by that color. The AOU is colored from areas of highest probability density to areas of lowest probability density, so every color level defines the smallest search area with a given probability of containing the target.

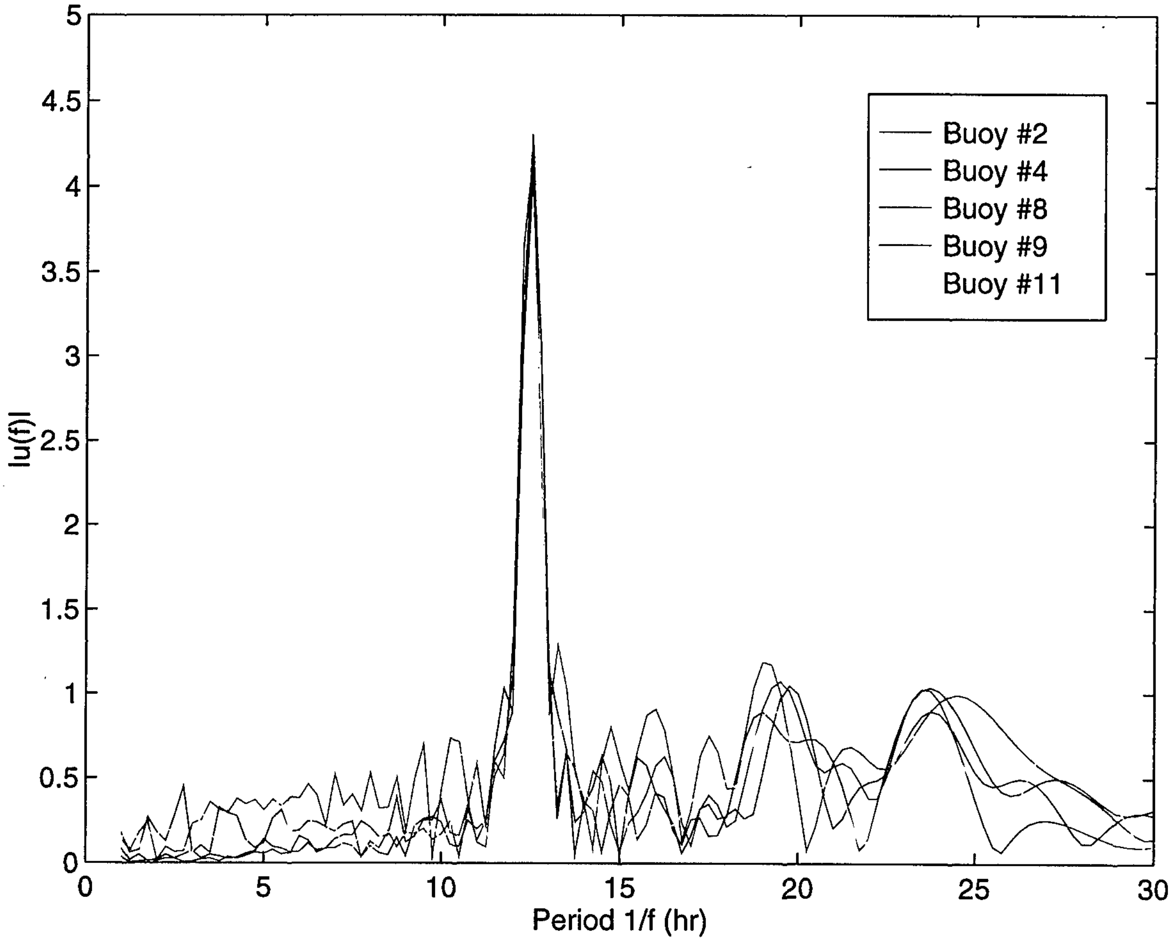

Figure 5-3. Modulus of $U(f)$ for Five Buoys vs. Period

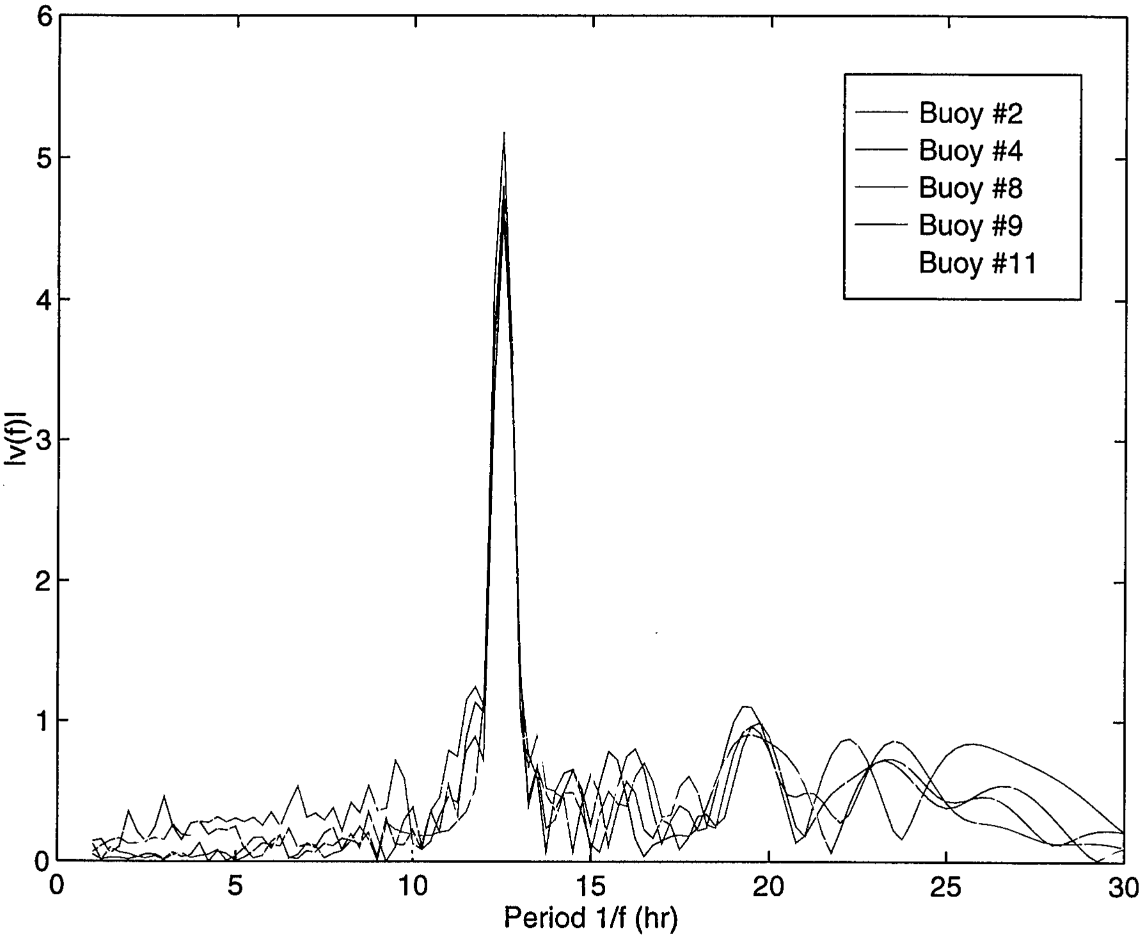

Figure 5-4. Modulus of $V(f)$ for Five Buoys vs. Period

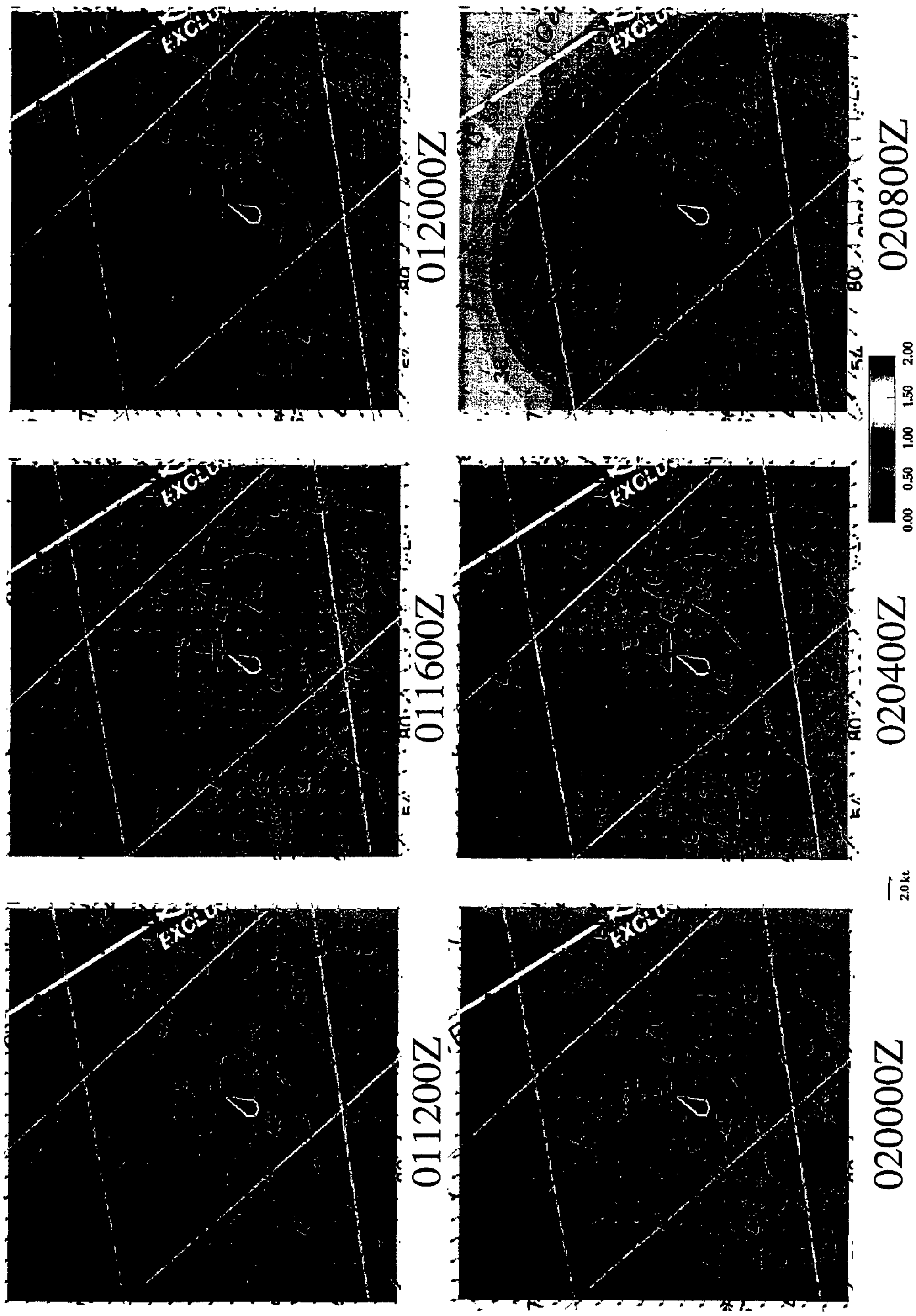

Figure 5-5. OPS Current Field Estimate, 011200Z - 020800Z JUN 96

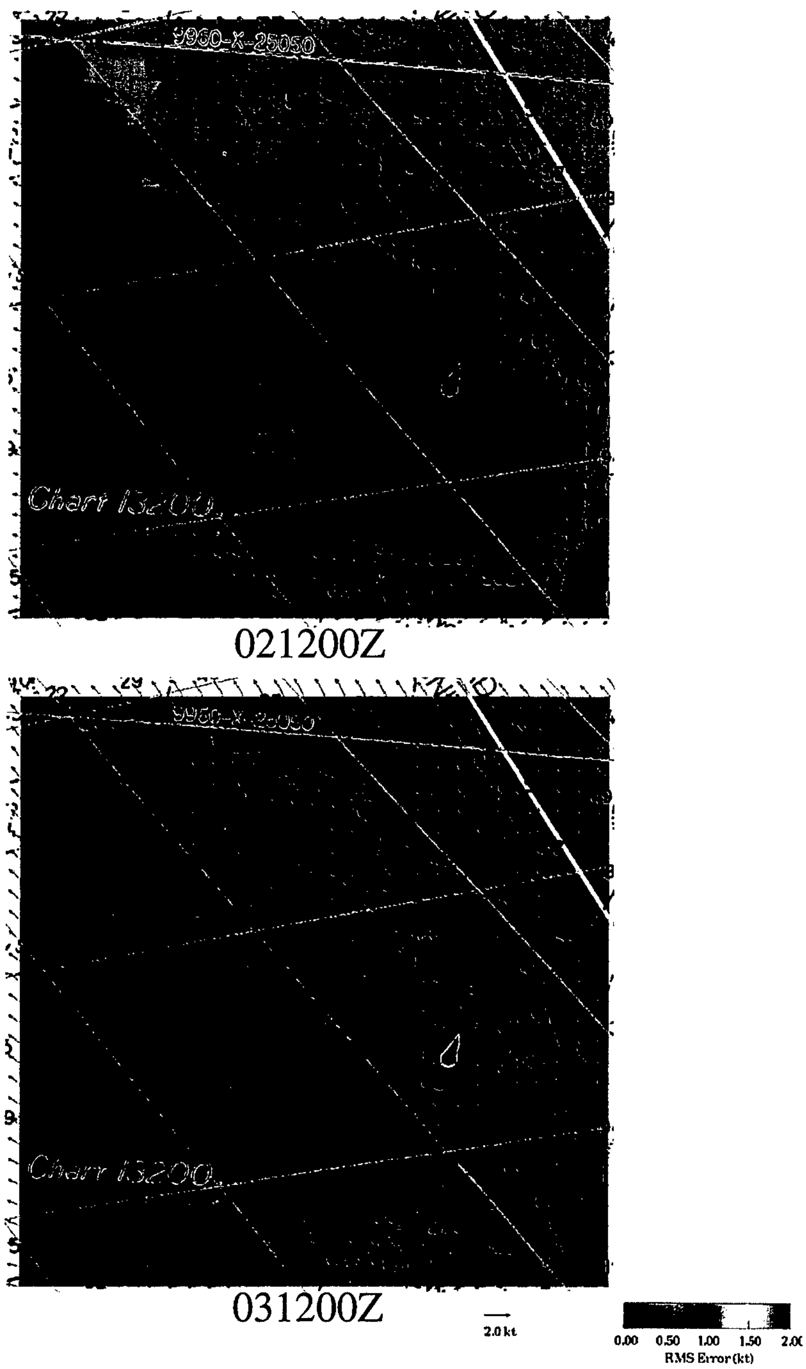

Figure 5-6. OPS Current Field Estimate, 021200Z - 031200Z JUN 96

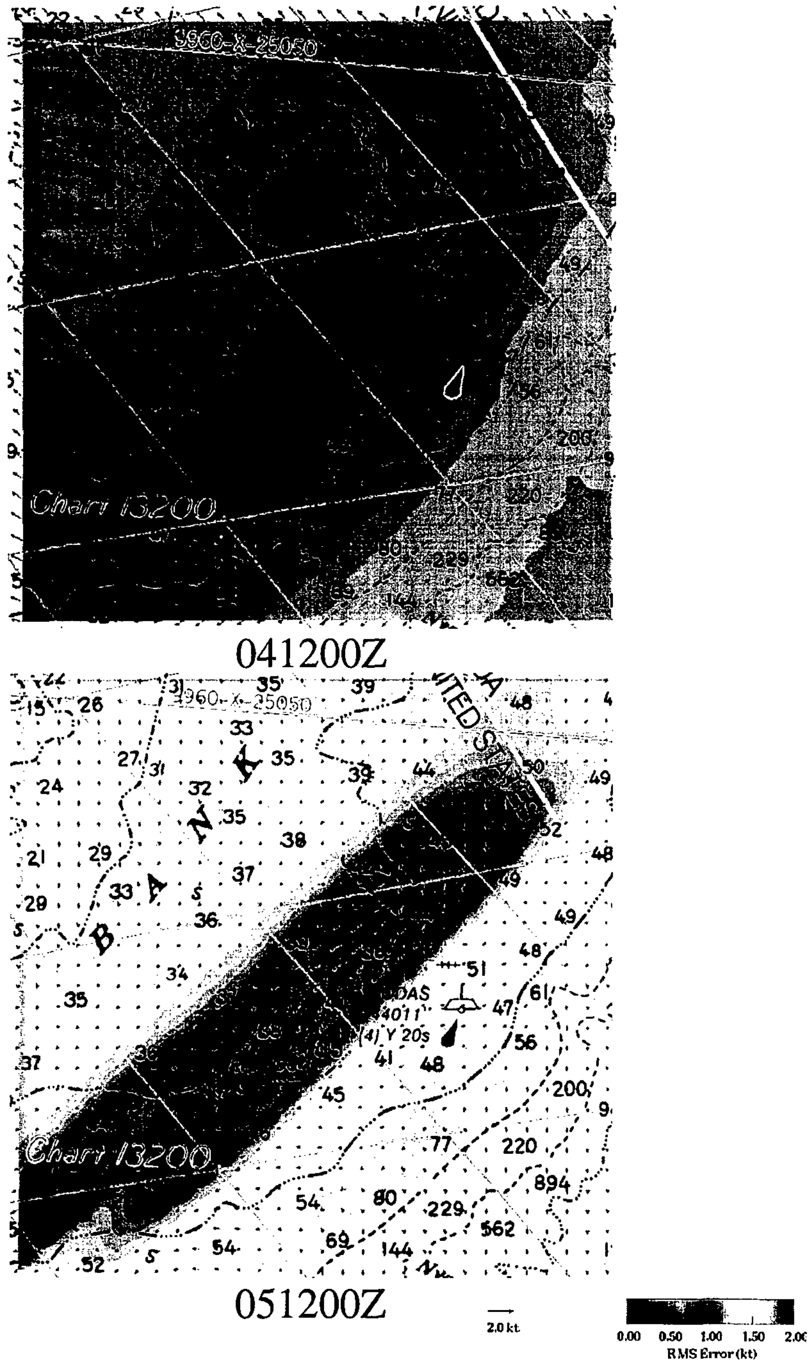

Figure 5-7. OPS Current Field Estimate, 041200Z - 051200Z JUN 96

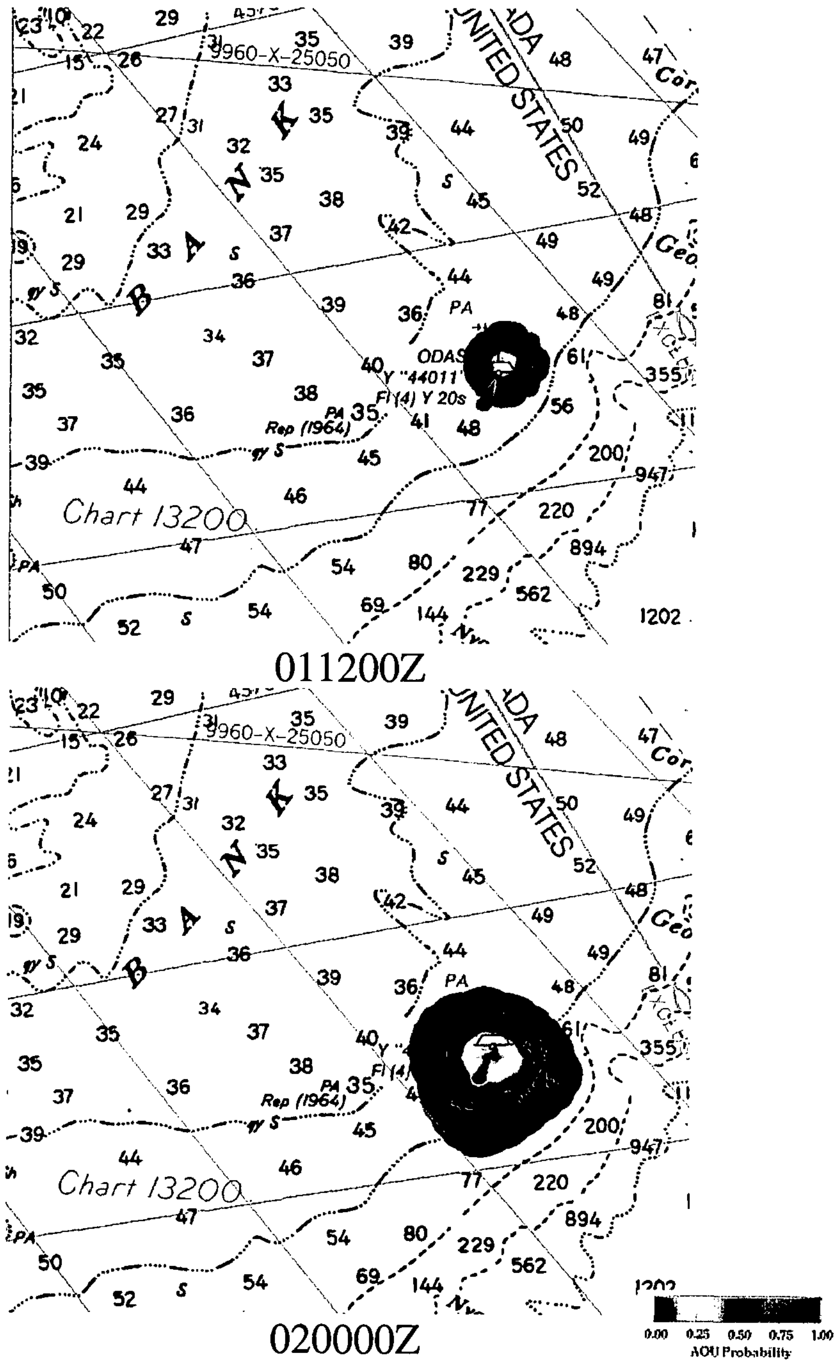

Figure 5-8. Example of AOU Propagation Using AMI Propagation Algorithm, 011200Z - 020000Z JUN 96

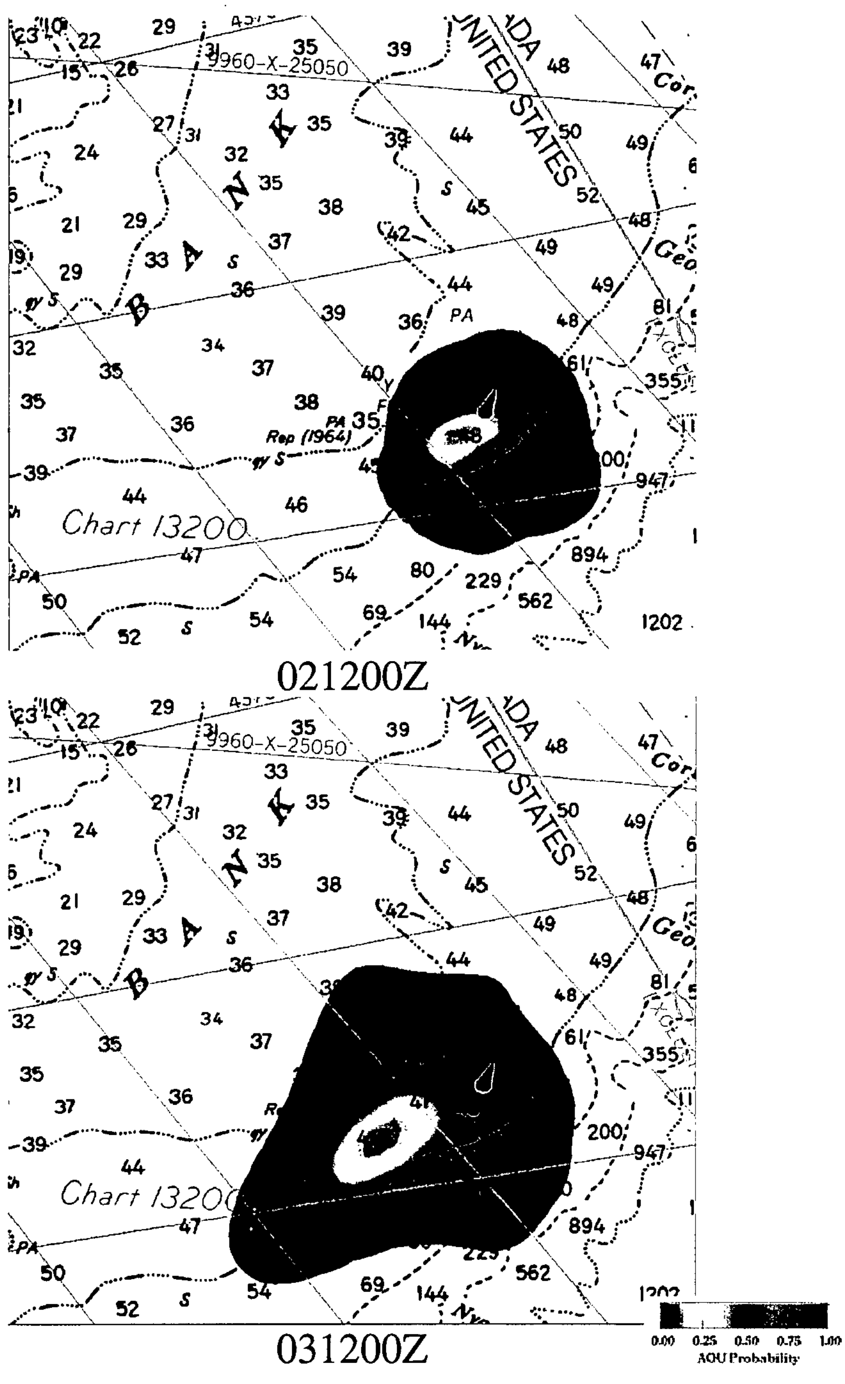

Figure 5-9. Example of AOU Propagation Using AMI Propagation Algorithm, 021200Z - 031200Z JUN 96

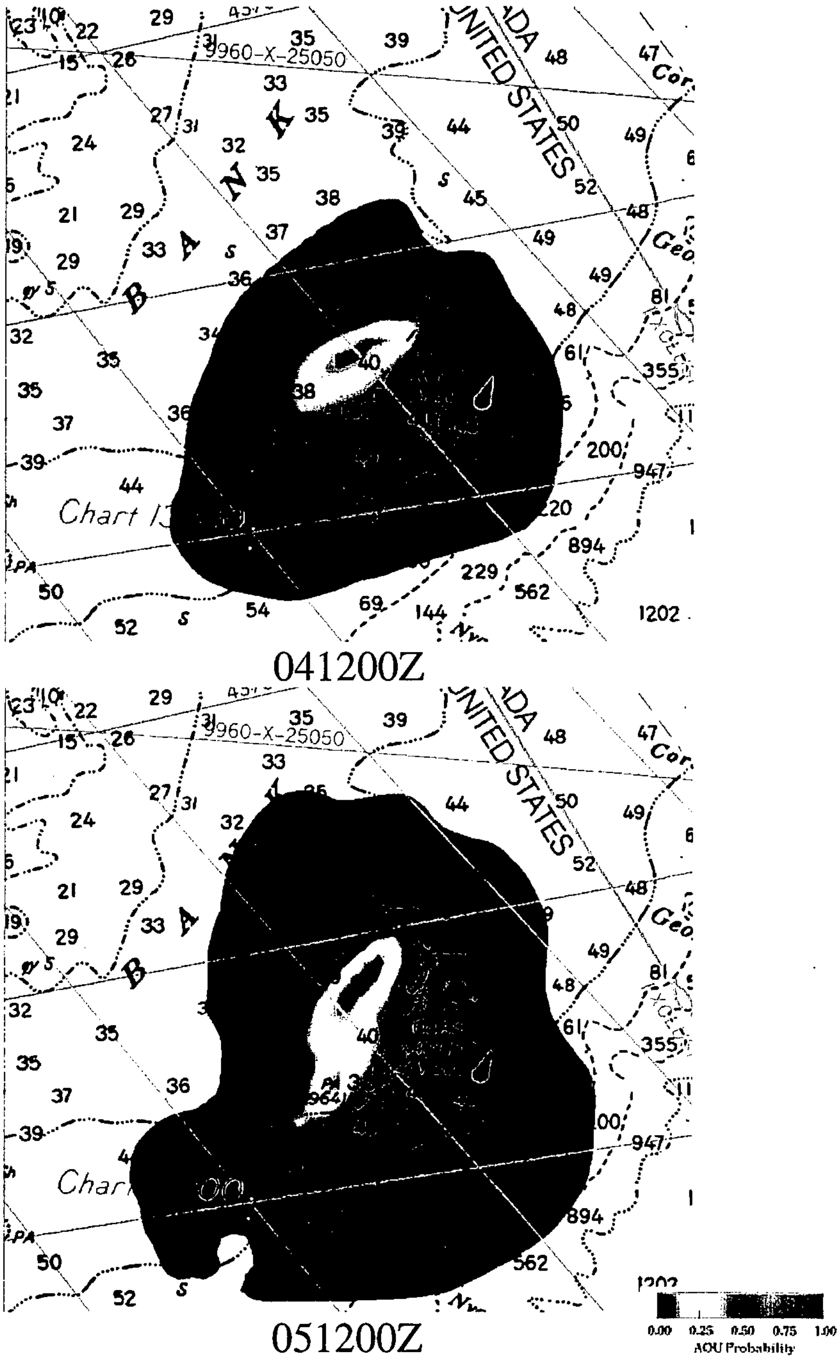

Figure 5-10. Example of AOU Propagation Using AMI Propagation Algorithm, 041200Z - 051200Z JUN 96

The AOUs shown in Figures 5-8, 5-9, and 5-10 were generated using an algorithm developed by Applied Mathematics, Inc. The algorithm models the AOU as a coarse-grained probability density and integrates the Fokker-Planck equation for its time evolution. The Fokker-Planck equation is discussed in Reference [i].

CASP AOU Propagation. Figures 5-11 and 5-12 show the progression of the AOU using CASP probability map feature for the same target and at the same times as in Figures 5-8, 5-9, and 5-10.

5.6 OPS PERFORMANCE

OPS performance was assessed using CASP probability map feature to predict the motion of two buoys, Buoys 1 and 11. These two buoys were chosen to identify differences in performance between a case in which the buoys surround the target (i.e., Buoy 1) and a case in which the buoys lie to one side of the target (i.e., Buoy 11). Table 5-4 gives the initial positions used, including the uncertainties assigned, δx_0 and δy_0.

Table 5-4. Initial Positions of Buoys 1 and 11

Buoy	Time	Latitude	Longitude	$\delta x_0, \delta y_0$ (m)
1	011133Z	41 04.5 N	66 35.4 W	1000
11	011500Z	41 37.5 N	66 44.7 W	200

Data from the selected buoy was excluded from consideration by the OPS algorithm and the buoy position was used as the true position of a target. The target's initial position was set to the first known position of the buoy. Using data from the remaining buoys in OPS, a set of current fields were generated every two hours starting one hour from the initial time. The fields were sent to CASP and the AOU was propagated in four-hour increments over four days.

Buoy 1 as Target. Figures 5-13 shows a set of AOU snapshots every twelve hours of Buoy 1 as target generated from the CASP AOU using the currents provided by OPS. Figure 5-14 shows a set of AOU snapshots of Buoy 1 as target generated from the CASP AOU using historical current data. In both figures, the actual position of Buoy 1 is marked with a black circle and white crosshairs. Where this position was unavailable at the time of the snapshot, a position was estimated by linear interpolation between the nearest Buoy 1 position reports in time. The AOUs based on OPS-estimated currents are seen to grow much faster than those based on historical cur-

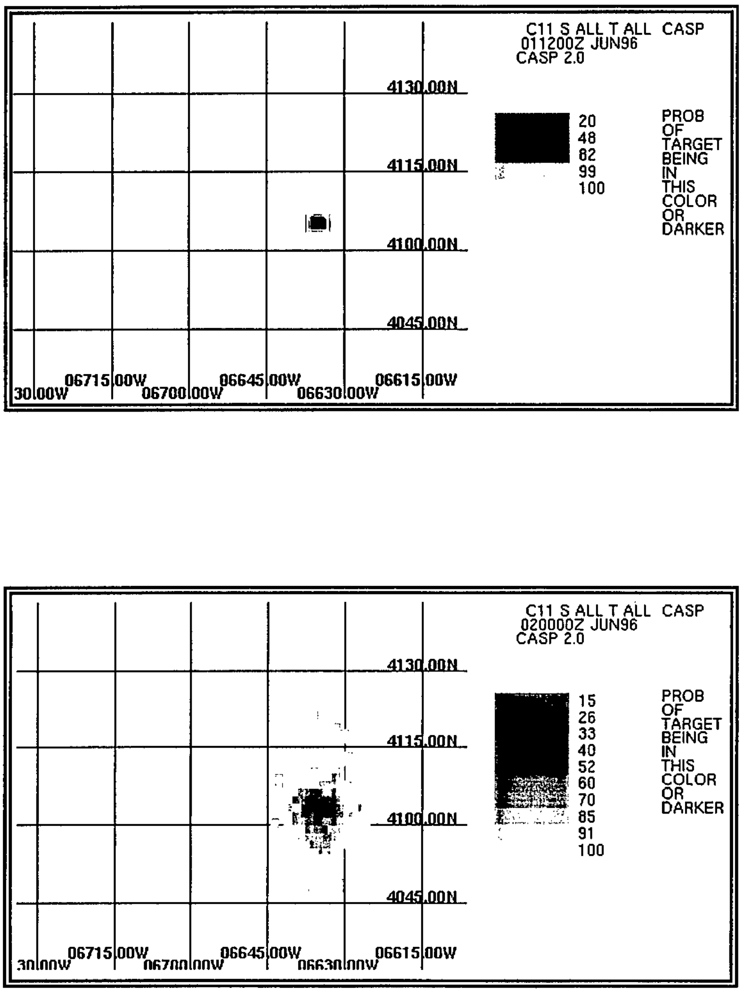

Figure 5-11. Example of CASP AOU Propagation, 011200Z - 020000 JUN 96

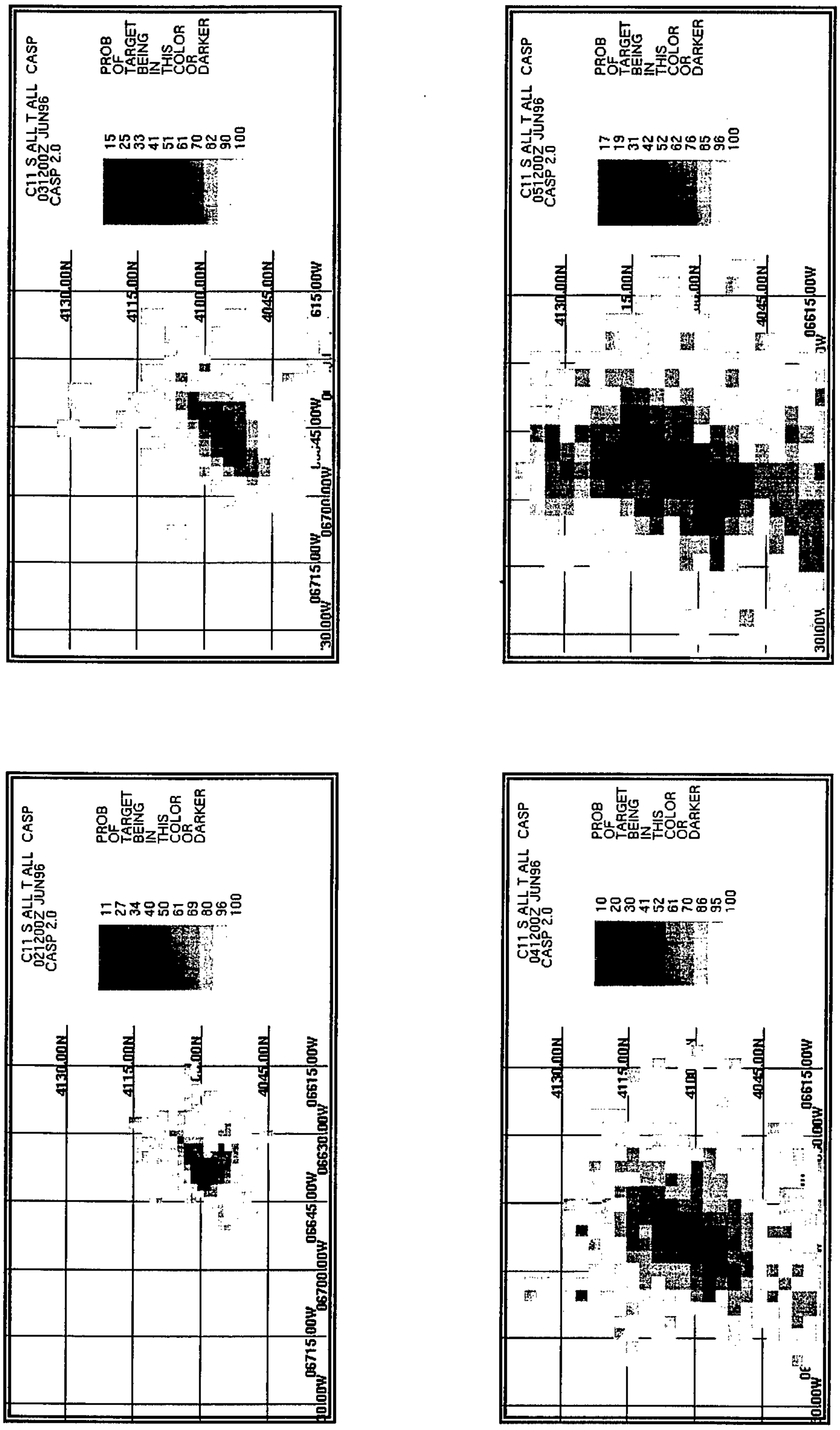

Figure 5-12. Example of CASP AOU Propagation, 011200Z - 051200 JUN 96

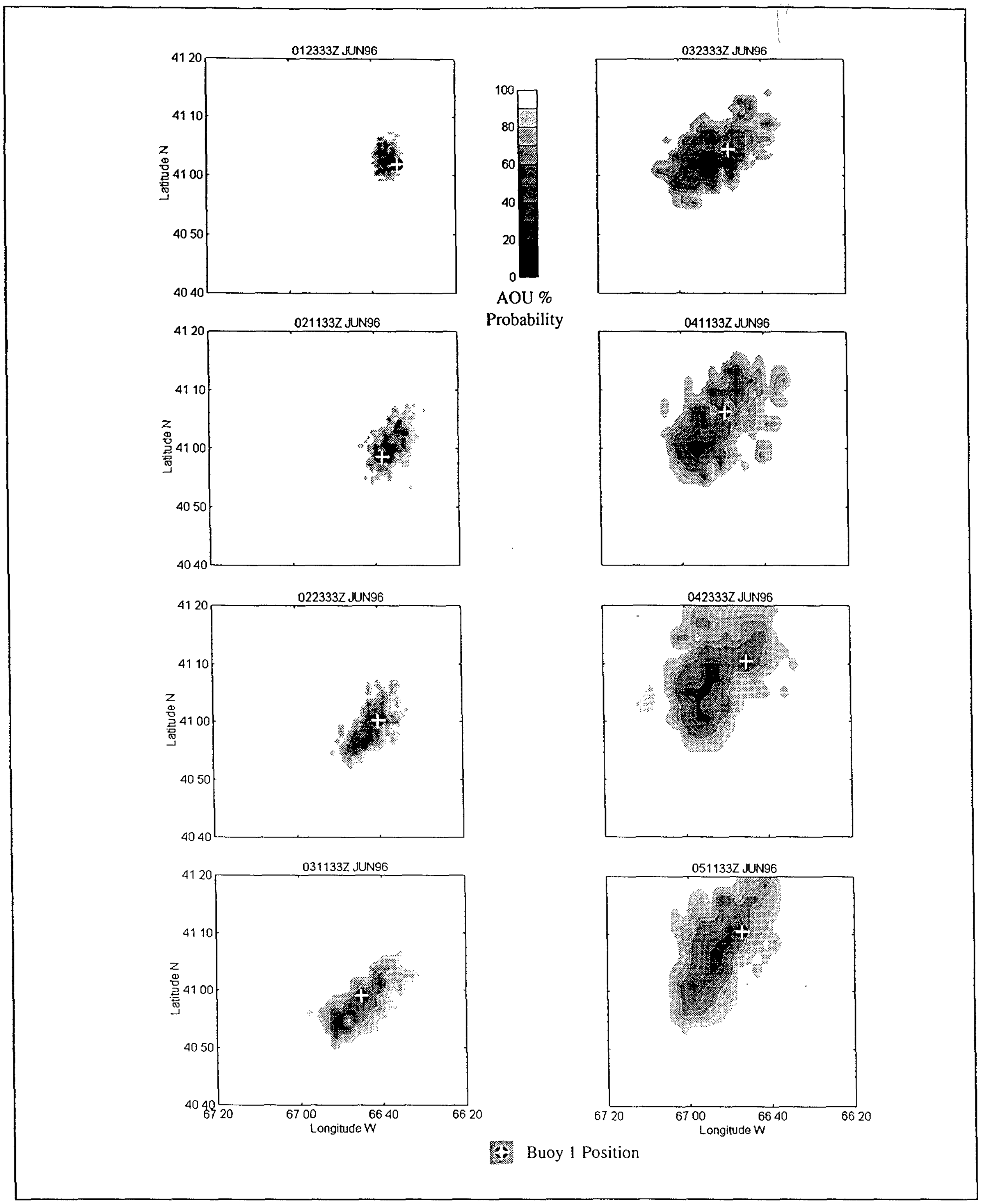

Figure 5-13. AOUs for Buoy 1 as Target Using OPS Current Field, 012333Z - 051133Z JUN 96

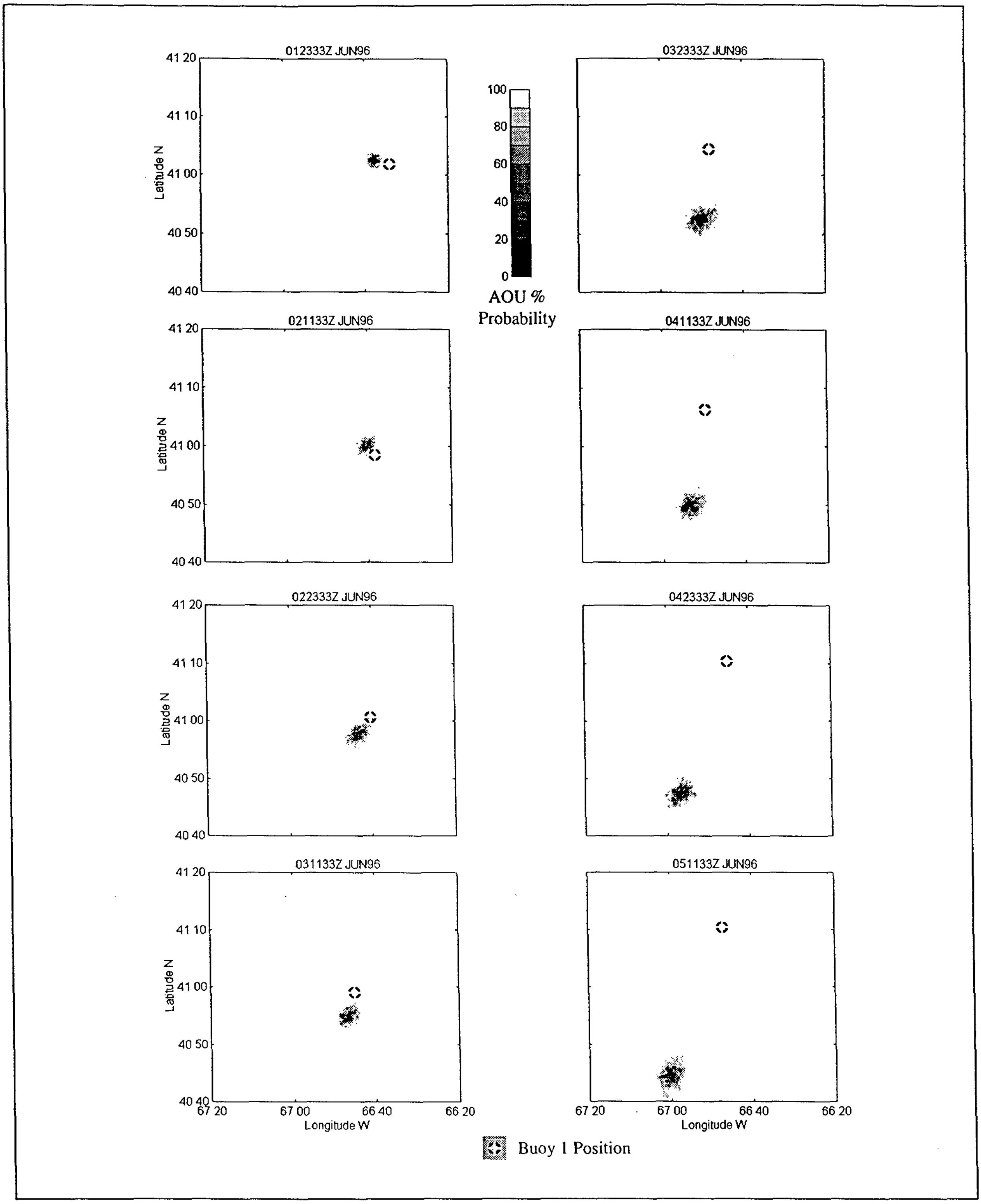

Figure 5-14. AOUs for Buoy 1 as Target Using CASP Historical Current Field, 012333Z - 051133Z JUN 96

rents. To quantify this difference in AOU growth rates, a plot of CASP AOU size versus time every four hours for the first 56 hours of the test is shown in Figure 5-15. Table 5-5 gives values of the CASP AOU size for levels between 90 and 99 percent at four times.

Table 5-5. CASP AOU Size for Buoy 1 as Target

Time (hrs)	Size of CASP 90-99% AOU (sq nm)	
	Historical Current	OPS Current
24	11	125
48	23	252
72	31	403
96	30	602

The higher rate of AOU growth using OPS occurs because the uncertainties reported by OPS are higher than those used by CASP with the historical databases. However, the AOUs based on OPS-estimated currents agree with the reported positions much better than those based on historical currents.

From a number of AOU propagations over a period of time, the percentage of positions found within any given confidence level was determined. Ideally, the resulting cumulative distribution function (CDF) is a straight line from (0%,0%) to (100%,100%). If the predicted positions are biased, the distribution will lie below that line, indicating that the AOU is a poor predictor of the buoy's location. If the error is overestimated, the distribution will lie above the line, indicating that the AOU leads to excessively large search areas. For comparison, the same procedure can be followed with the AOU propagated according to historical data in CASP in order to measure the effectiveness of OPS relative to the use of historical data.

Figure 5-16 presents CDFs of reported positions of Buoy 1 versus AOU confidence levels. Four propagations were made, two using OPS to predict currents, and two using historical currents. The CDFs from the two sets of propagations are plotted in the figure. The AOUs with OPS-estimated currents are accurate AOUs, in that each confidence level contains roughly the expected probability of finding the target. The null hypothesis that the AOU represents the true target distribution cannot be rejected, even at the 20-percent significance level.

The AOUs based on historical current data, however, show extremely high bias and do not represent the target's AOU. The null hypothesis that these AOUs represent the true target distribution can be rejected at better than the 1-percent significance level. In comparison, CASP AOUs for Buoy 1 using historical currents contained Buoy 1 at 90 percent "confidence" in 2 of 48 cases, or with 4 percent probability. CASP AOUs for Buoy 1 using OPS-estimated currents contained Buoy 1 at 90 percent "confidence" in 43 of 48 cases, or with 90 percent probability.

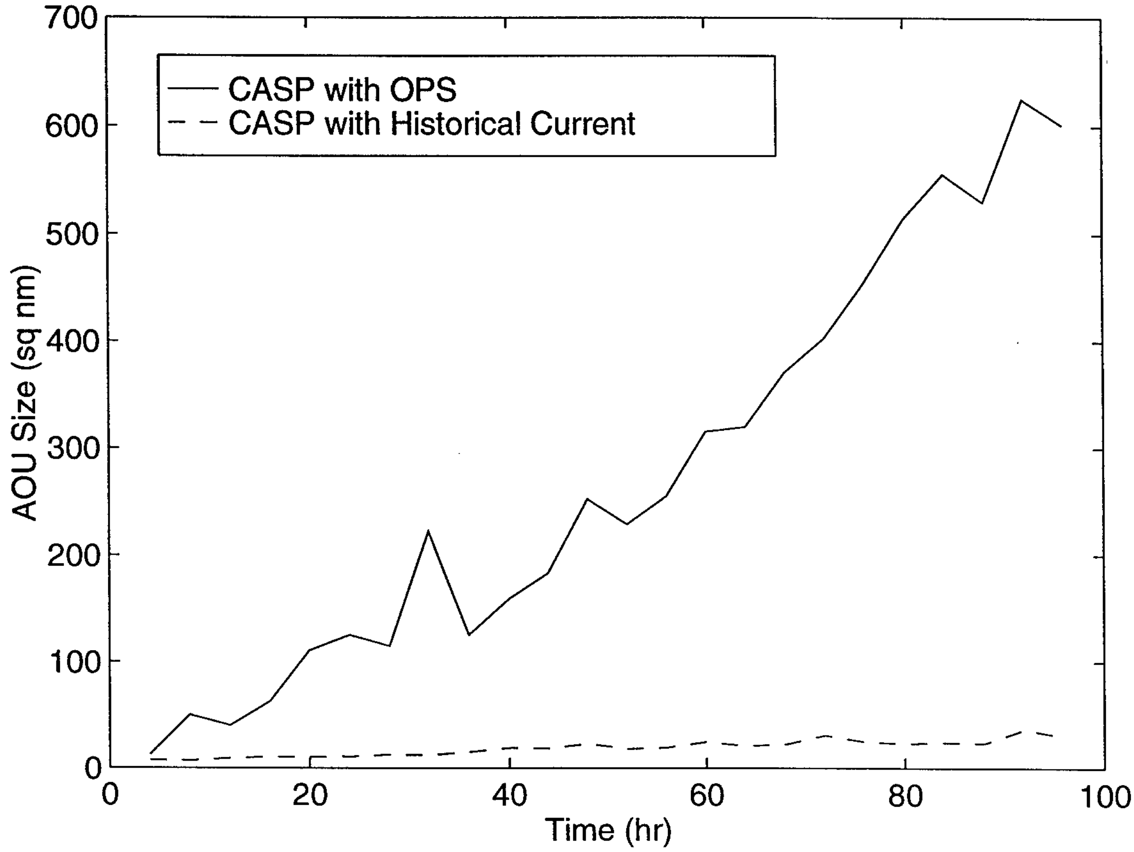

Figure 5-15. CASP AOU Size at 90 - 99% Level vs. Time for Buoy 1

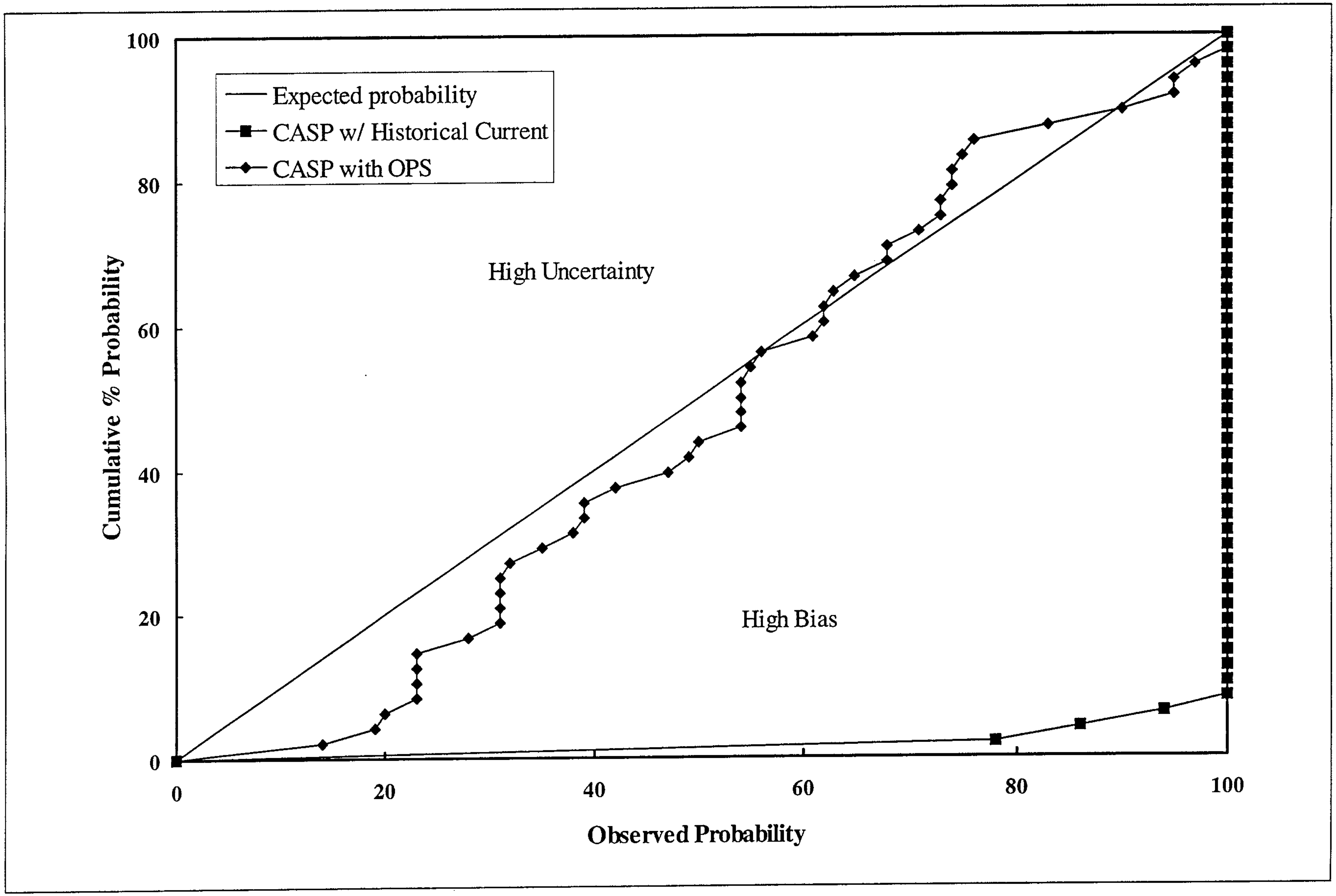

Figure 5-16. CDF of Buoy 1 Positions vs. AOU Confidence Level

As a measure of effectiveness in predicting buoy motion, we consider the size of the smallest AOU containing the buoy with 100 percent probability. A plot of the size of the smallest AOU that contains Buoy 1 versus time every four hours for the first 96 hours of the Test is shown in Figure 5-17. Table 5-6 gives the values at four times. Some of the buoy positions were outside of the colored region of the CASP AOU. An area could not be determined directly from the CASP AOU for these cases, so the area reported in Table 5-6 and Figure 5-11 is that of a disk of diameter *R* equal to the distance between the buoy position and the center of mass of the AOU.

Table 5-6. Size of Smallest CASP AOU Size that Contains Buoy 1

Time (hrs)	Size of Smallest CASP AOU Containing Buoy 1 (sq nm)	
	Historical Current	OPS Current
24	11	12
48	53	49
72	873	120
96	2384	49

Buoy 11 as Target. Figure 5-18 gives CDFs of reported positions of Buoy 11 versus AOU confidence levels. Two propagations were made, one using OPS to predict currents, and one using CASP historical currents. The CDFs for the two propagations are shown in Figure 5-18. CASP predictions of the motion of Buoy 11 and its AOU using OPS-estimated currents were less accurate than those for Buoy 1. However, they were far less biased than CASP predictions using historical currents. CASP AOUs for Buoy 11 using historical currents contained the target at 90 percent "confidence" in 0 of 24 cases, or with 0 percent probability. CASP AOUs for Buoy 11 using OPS currents contained the target at 90 percent "confidence" in 13 of 24 cases, or with 54 percent probability.

It is not surprising that OPS is less able to estimate current at locations outside the perimeter of available data than inside. The current at a given location is correlated with currents in all directions, so when data is available in only one sector, OPS cannot account for any structure of nearby currents in the remaining sectors.

5.7 OPS SENSITIVITY ANALYSIS

The sensitivity of OPS performance to data processing methods and to choice of input parameters was examined by comparing AOU propagations of Buoy 1 as target for the first four days of the test. The same measures of performance (MOP), used in Section 5.6,

1. the distance from the AOU center of mass to the buoy,
2. the AOU probability level at the buoy position, and
3. the area of the AOU up to that probability level,

were also used to compare alternatives.

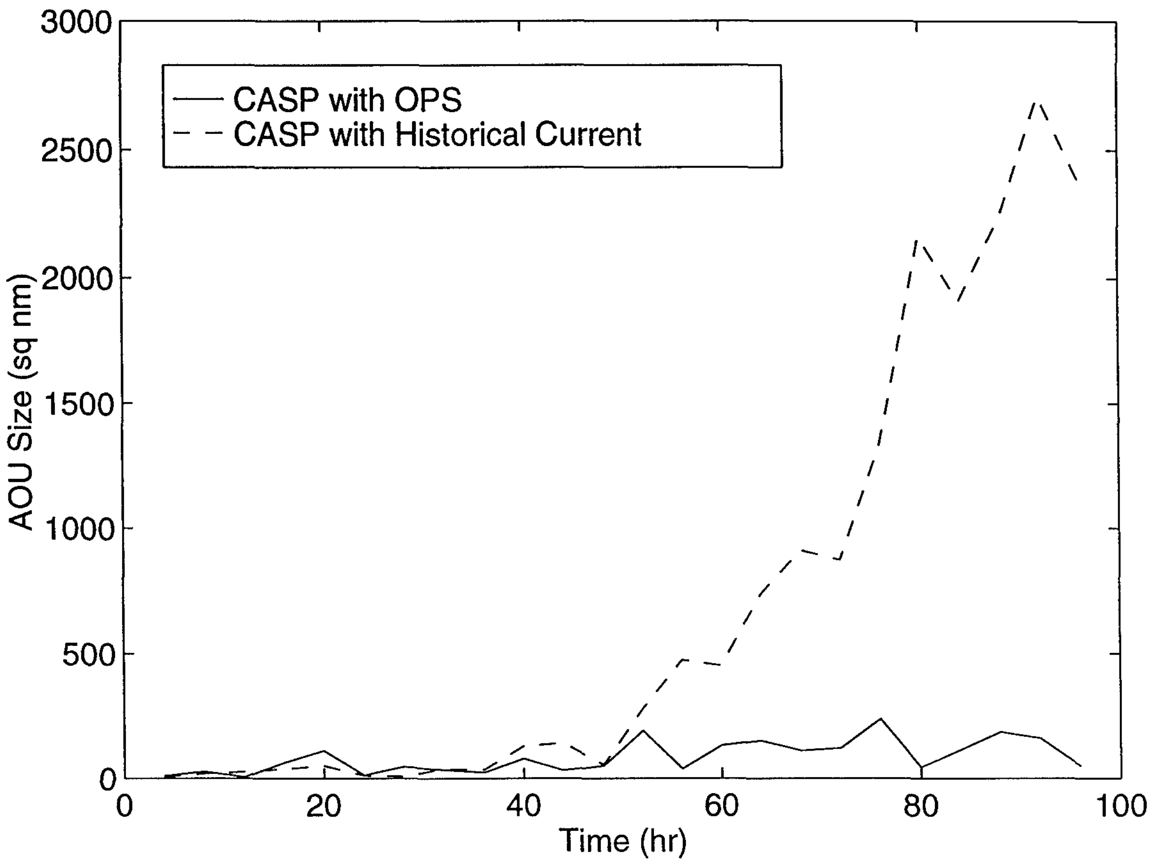

Figure 5-17. Smallest CASP AOU Size Containing Buoy 1

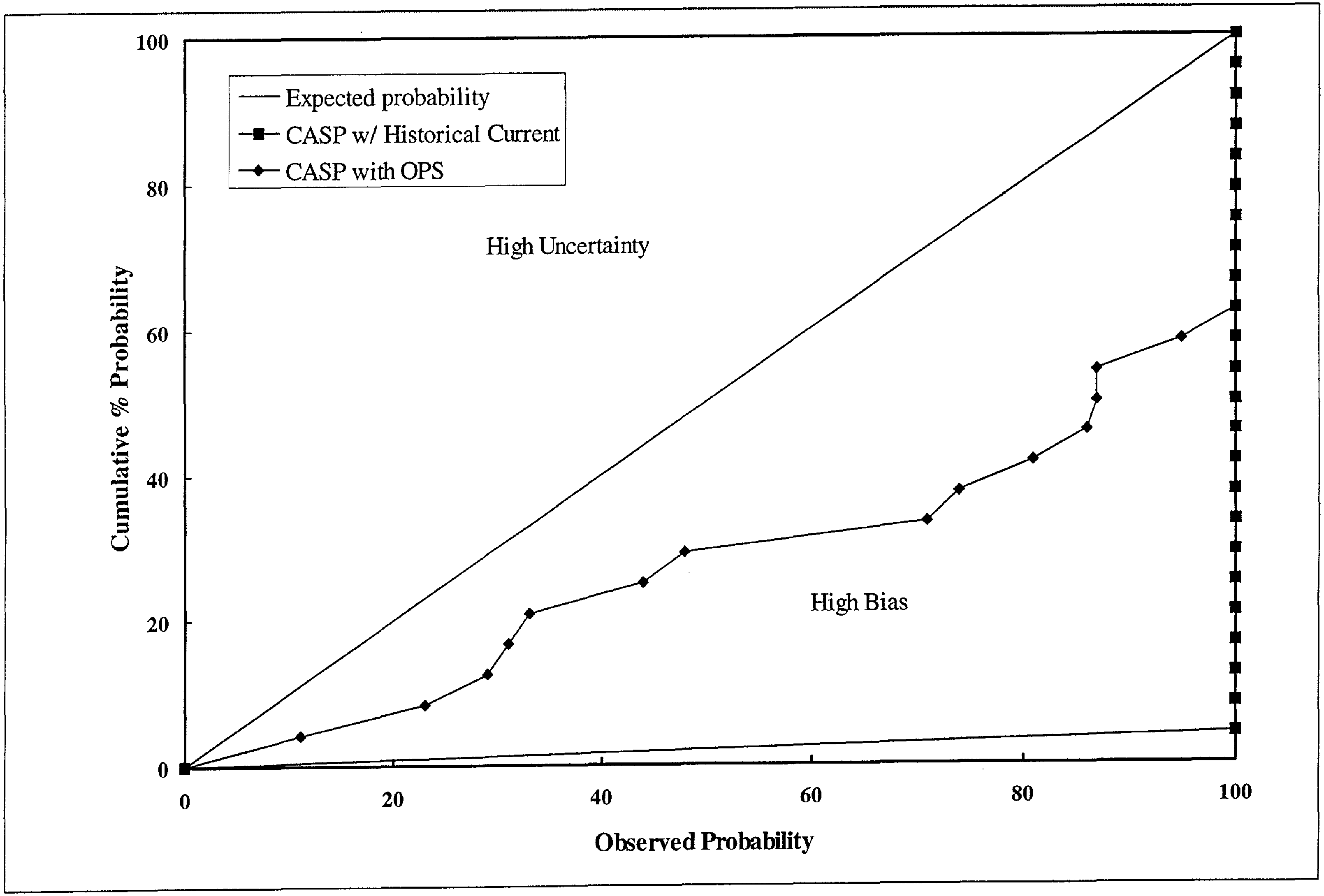

Figure 5-18. CDF of Buoy 11 Positions vs. AOU Confidence Levels

MOP 1 measures the accuracy of spatial prediction, MOP 2 measures the accuracy of reported error, and MOP 3 estimates overall effectiveness by giving the smallest AOU area containing the buoy with 100 percent probability.

Prior and Posterior Data. Figure 5-19 shows performance results of AOU propagations in which an influential time window of six hours was used to define a set of input data consisting either of prior data only, or both prior and posterior data. The influential time window for the prior and posterior case extended three hours in either direction from the time of the current estimate. The distance of the AOU center from the buoy was not drastically altered, but the area of the AOU containing the buoy grew more slowly when both prior and posterior data were admitted as input. By default, OPS uses any posterior data available within the influential time window.

Influential Time Window. Figure 5-20 shows the performance results of AOU propagations in which influential time windows of 6, 12, and 24 hours were used. All cases included prior and posterior data. Above twelve hours, the influential time window had a great effect on all three measures, most clearly in the area of the containing AOU. From six to twelve hours, the differences were smaller, with the six-hour case showing somewhat less bias, and thus lower AOU probability levels.

GPS vs. Argos Data. Figure 5-21 shows the performance results of AOU propagations in which GPS fix data was used compared to those in which only Argos fix data were used. Not using GPS data results in highly biased predictions, comparable to the bias of AOUs when using historical current data. The sharp decrease in the AOU probability level is due to high reported errors in current, resulting in an AOU growth rate faster than the departure rate of the AOU center from the buoy position. This difference in performance results from the inaccuracy and sparseness of Argos data compared with GPS.

Polynomial Trend Model. Figure 5-22 shows the performance results of AOU propagations in which the polynomial trend model used to determine current from the buoy position data is a quadratic, cubic, and quartic (i.e., 2nd, 3rd, and 4th order polynomial). The influential time window used in this comparison was six hours. The cubic and quartic models resulted in less bias, and thus higher effectiveness, than the quadratic model. Although the quartic model seems to result in lower bias than the cubic model, the effectiveness gain is not uniform, as can be seen in Figure 5-23, which compares the results from cubic and quartic models for a twelve-hour influential time window. Here the quartic model shows higher bias, resulting in larger AOU areas containing the buoy. OPS currently uses the cubic model.

Influential Points. Figure 5-24 shows performance results of AOU propagations in which twenty influential points are used in the Kriging procedure and a propagation in which only ten influential points are used. The resulting change in performance was not significant.

Shapiro Filter. Figure 5-25 shows performance results of AOU propagations in which a smoothing (Shapiro) filter (Reference [j]) is used on the current estimates against a propagation in which no output filter is applied. The Phase I algorithm used a Shapiro filter to smooth the output. Both propagations in Figure 5-25 use ten influential points. The change in performance was not significant.

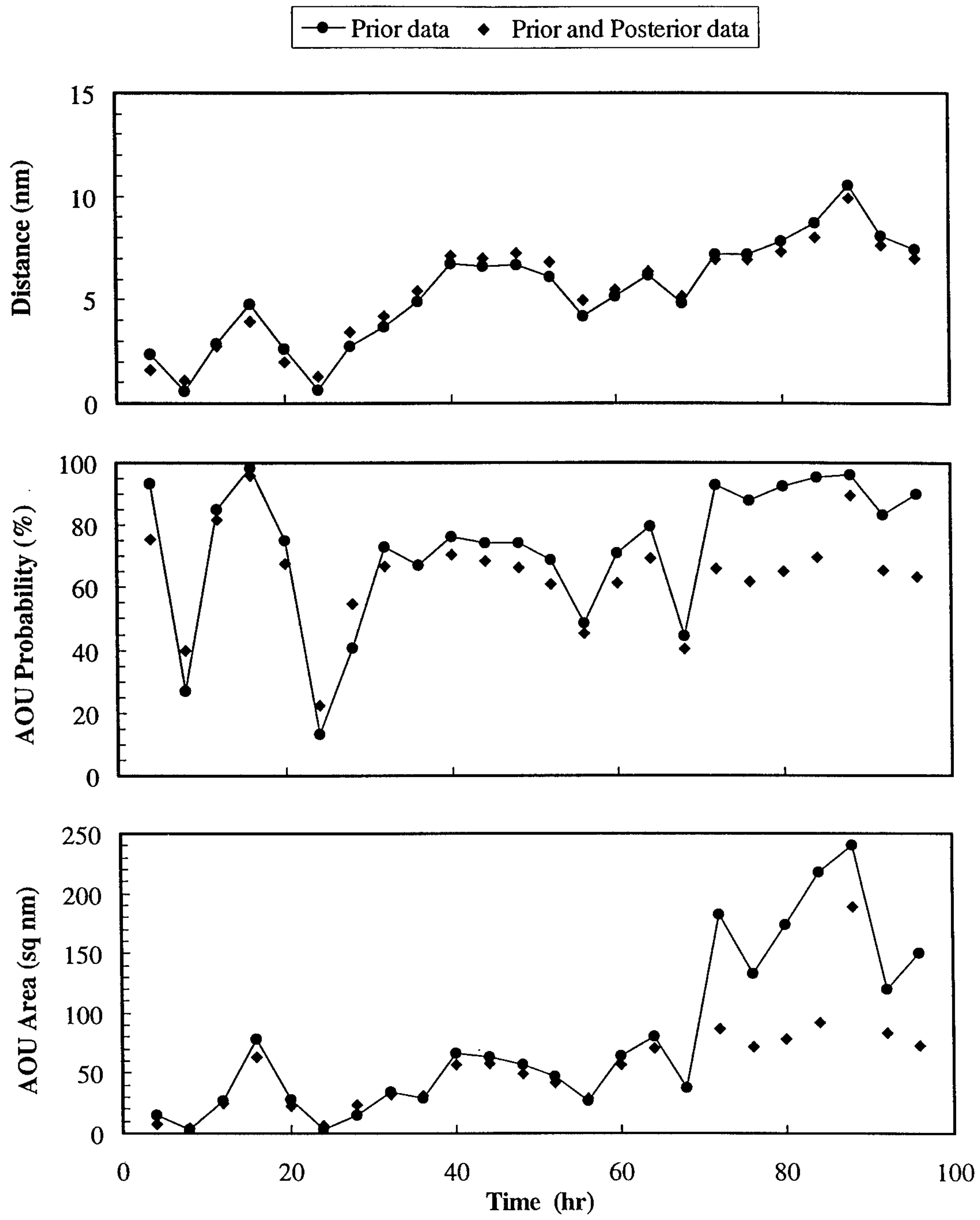

Figure 5-19. Performance Results for Prior Data Only and Prior and Posterior Data

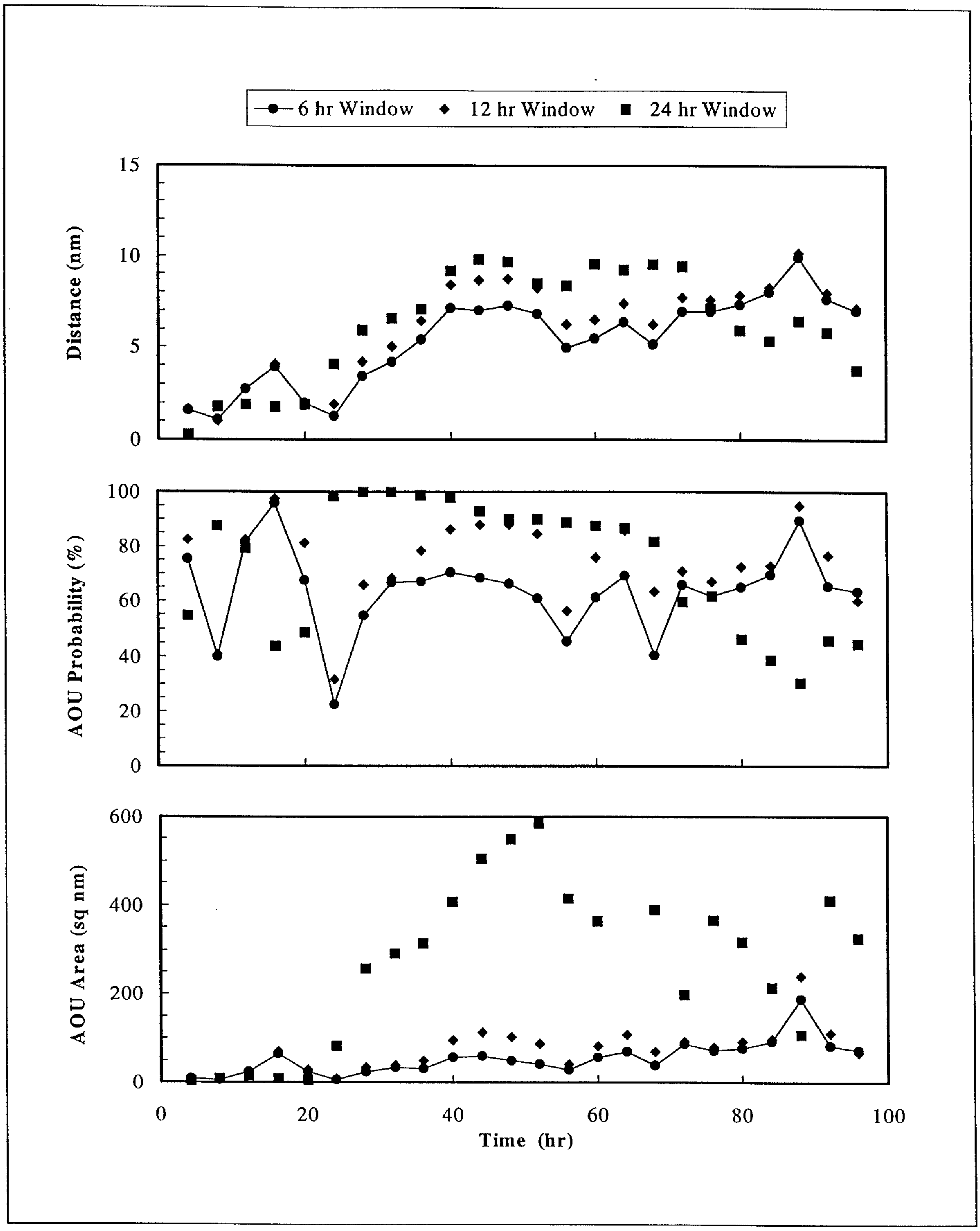

Figure 5-20. Performance Results for Three Influential Time Windows

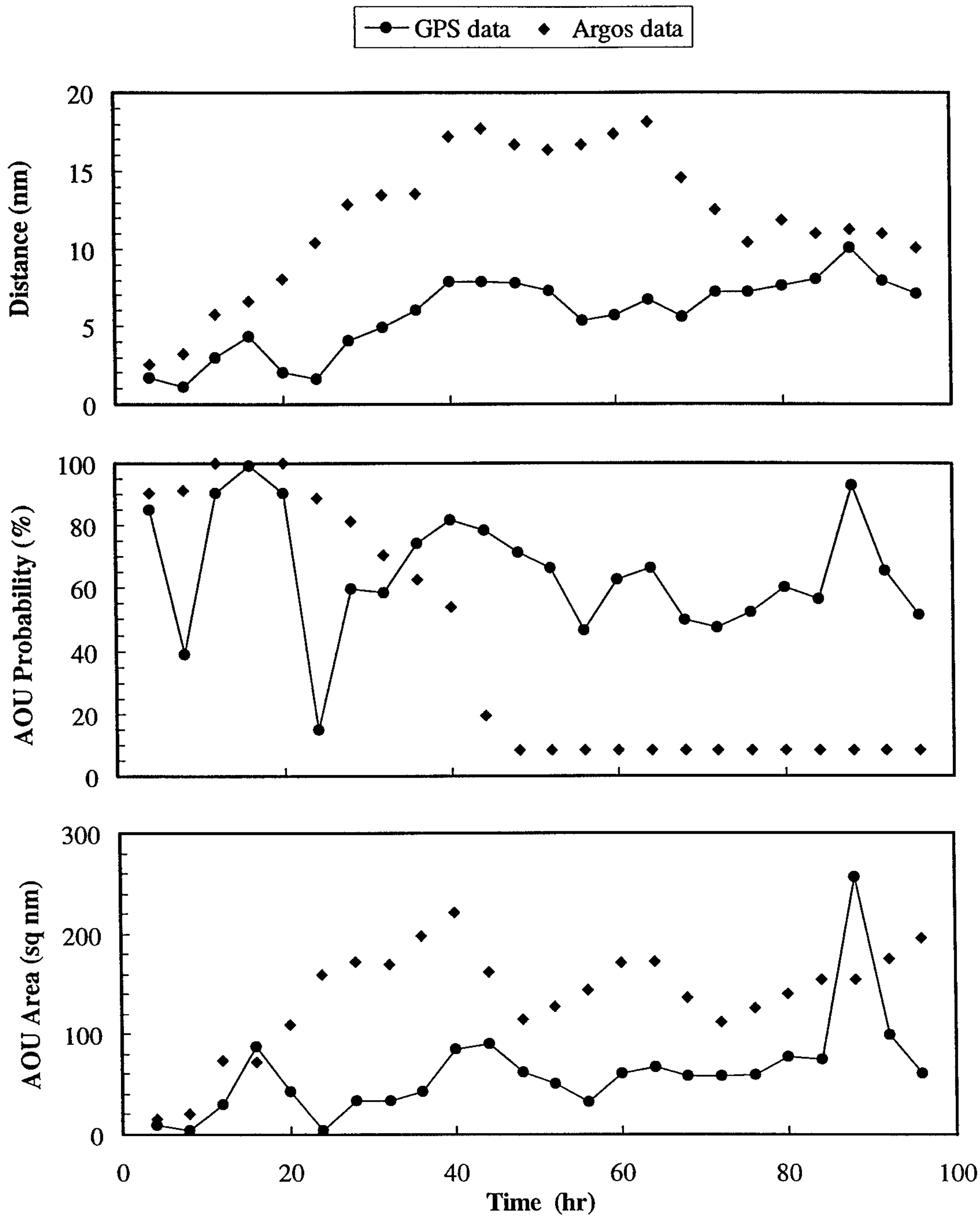

Figure 5-21. Performance Results Using GPS Data and Argos Data

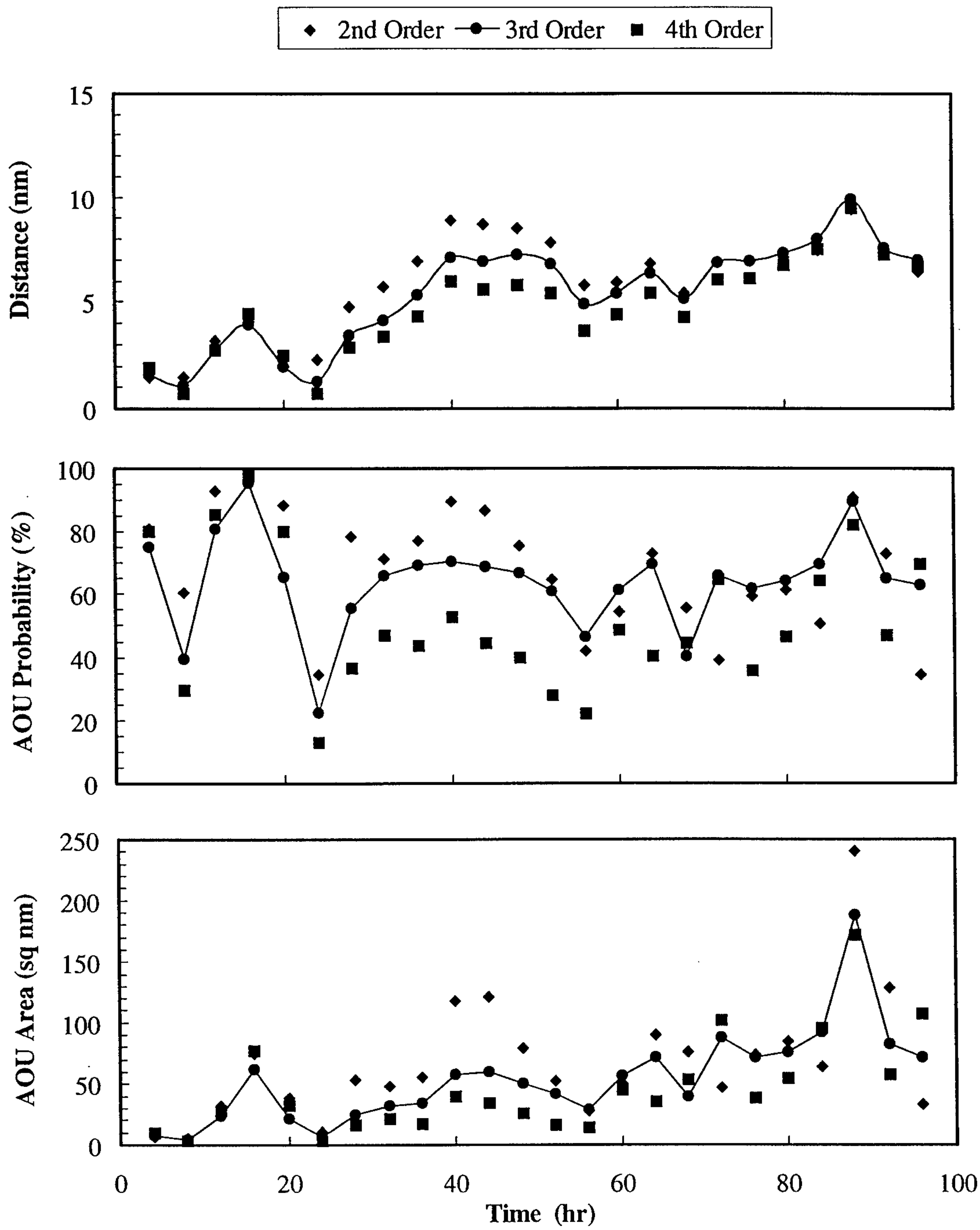

Figure 5-22. Performance Results Using Three Trend Models, with a 6 hr Influential Time Window

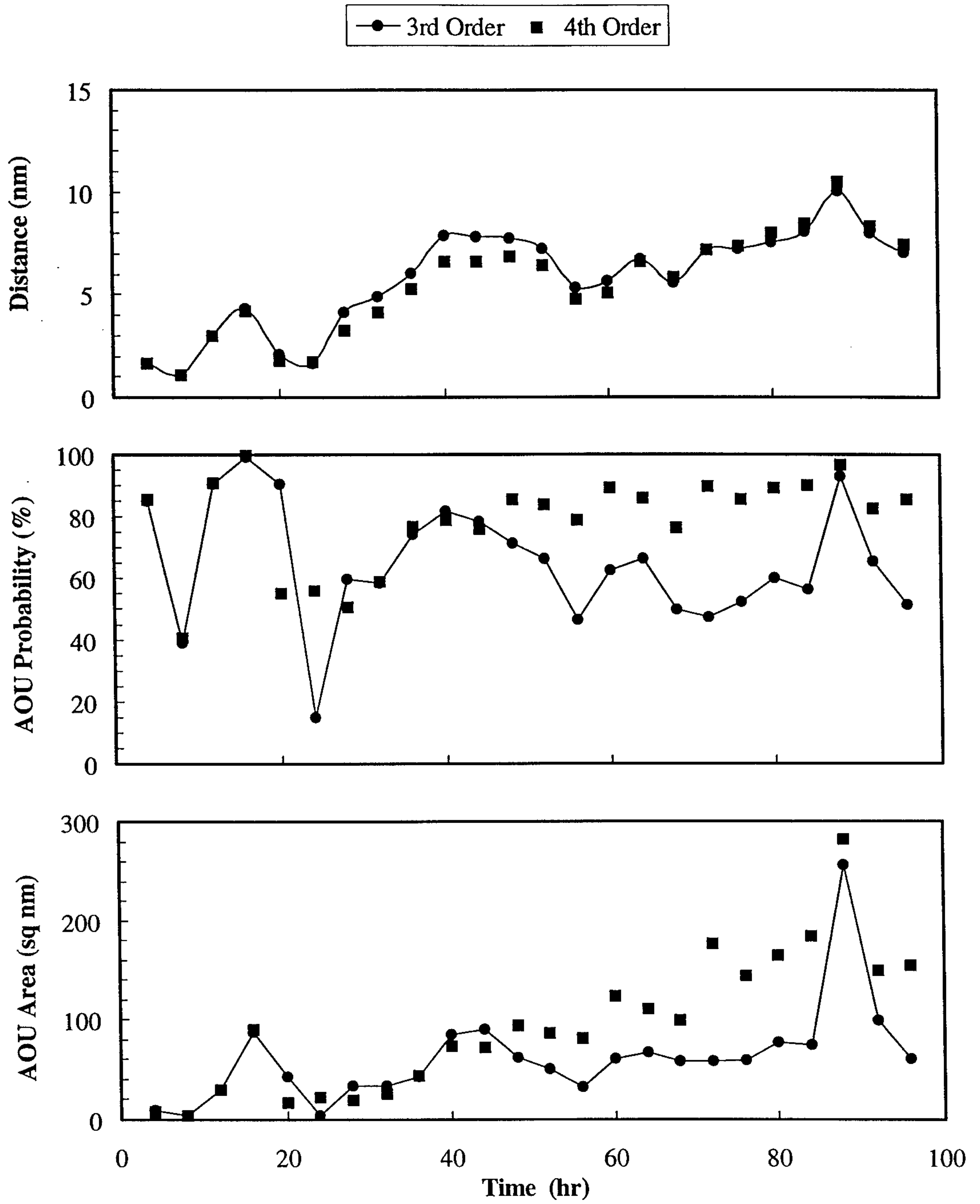

Figure 5-23. Performance Results Using Two Trend Models, with a 12 hr Influential Time Window

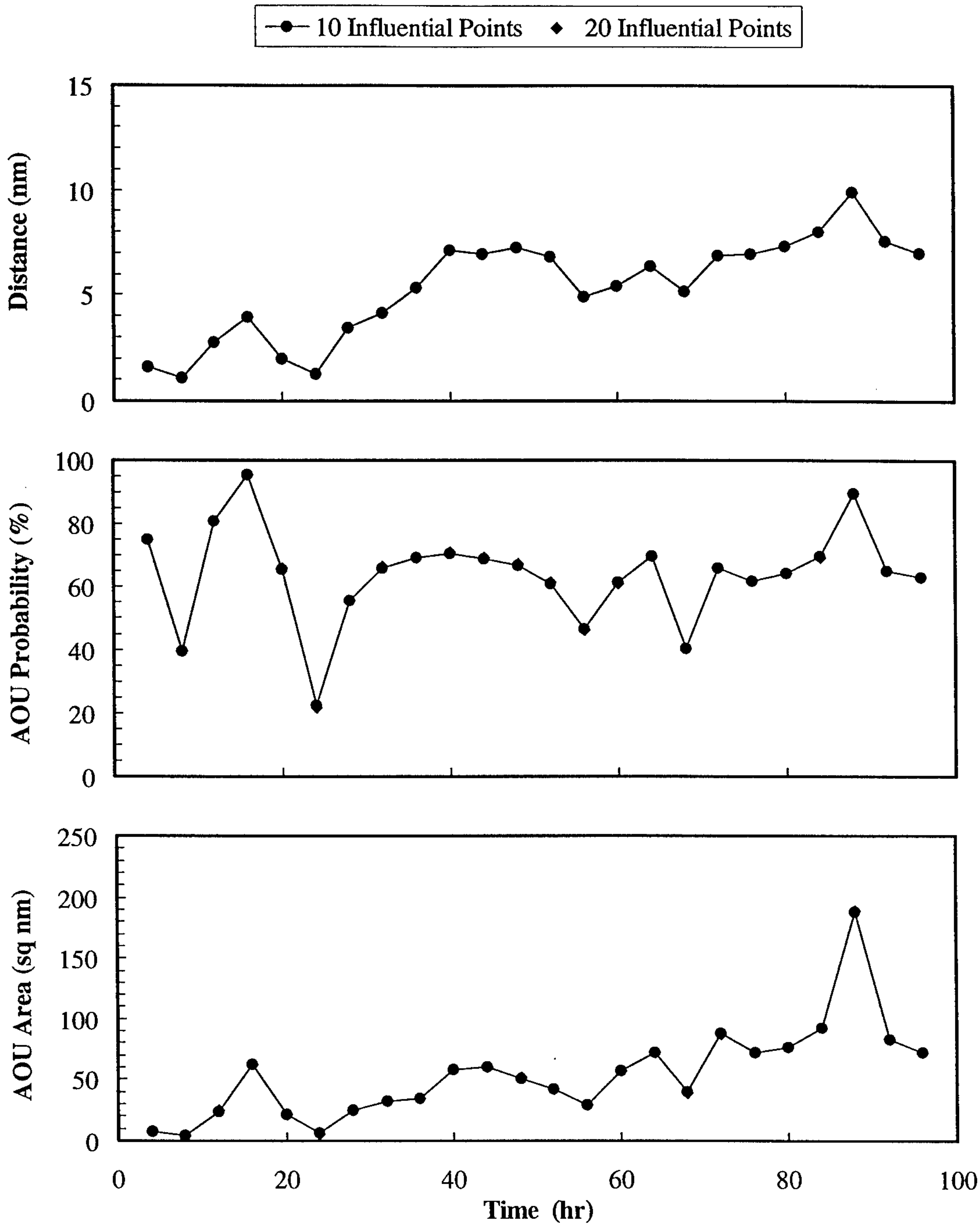

Figure 5-24. Performance Results for Two Sets of Influential Points

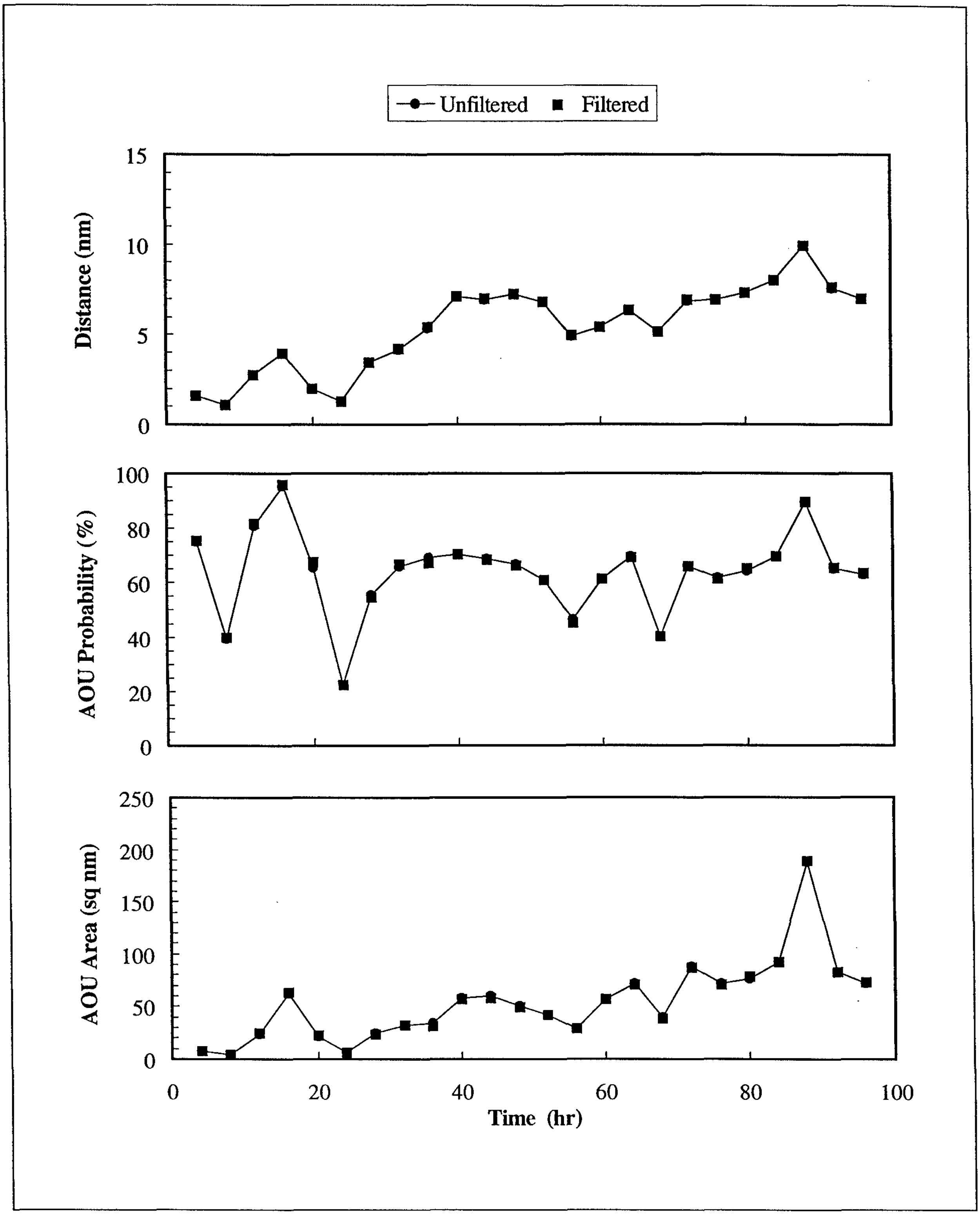

Figure 5-25. Performance Results with and without Output Filter

6.0 CONCLUSIONS AND RECOMMENDATIONS

In this section, we present conclusions and recommendations resulting from the Phase II research effort.

6.1 CONCLUSIONS

- OA techniques can successfully estimate ocean surface currents using SLDMB data.

- The OPS Development Test demonstrated that OPS algorithms can decode SLDMB transmissions, process the data, and provide an automated approach to compute ocean current velocity fields from buoy data.

- Target position estimates, calculated using CASP 2.0 with OPS processed SLDMB data, were significantly more accurate than the CASP 2.0 estimates calculated from historical global sea current data.

- The Internet was successfully used to allow the Coast Guard and OPS Developers to view results and on-scene weather data during the OPS Development Test.

6.2 RECOMMENDATIONS

Any implementation of SLDMBs into Coast Guard search planning should consider OPS as the automated approach to calculating required velocity fields.

The OA algorithm is designed to process current measurements and associated uncertainty estimates from any source. Additional ocean current sources need to be investigated.

The OA preprocessing options in the prototype version of OPS are restricted to SLDMB data. OPS has focused on SLDMBs as the most promising approach to improve calculated search area velocity fields. Several SLDMB questions should be investigated. These include determining the appropriate number of buoys to deploy and the best array configuration.

6.2.1 Integration of OPS and CASP

A software patch was used to input OPS current fields into CASP during the Development Test. This code was inefficient in generating AOU projections.

Code should be written to allow efficient input of OPS data into CASP.

6.2.2 Model Improvements

Improvements to the OPS model are recommended in the following areas:

Input Data Model. The constant acceleration and constant velocity models can be replaced with a cubic spline model. This would allow OPS to generate sample velocities at any point in time and would ensure consistency of physical parameters throughout each buoy track. An empirical model for the buoy velocity and acceleration statistics would allow removal of outliers with a known probability of false alarm.

Trend Model. Improvements can be made to the trend model by combining the physics of the ocean surface with the buoy track data. Known periodicities, like the tidal cycles observed during the OPS Development Test, can be more effectively removed from consideration by using digital notch filters. The weighted least squares algorithm for the trend model could also take position error into account. Using models of the ocean surface physics, a procedure could be developed to determine the optimal influential time window, which depends on the accuracy of the trend model. This would eliminate the need for a user-entered time window.

Variogram Model. Improvements can be made to the variogram model and variogram calculation procedure. For example, the cross-variogram, which relates different velocity components in varying spatio-temporal separations, does not have a model that necessarily obeys the Schwarz inequality for covariance matrix components. This leads to instability in the Kriging solution, so it is not used in the OPS calculation. A better cross-variogram model would properly treat anisotropy in the velocity vector correlation structure. If a stable feedback of the variogram model into the global statistics of the data is possible, then a more stable estimate of the variogram sill could be made based on all of the data instead of a subset of the data.

REFERENCES

a. Isaaks, Edward H. and R. Mohan Srivastava, An Introduction to Applied Geostatistics, Oxford University Press, New York, 1989.

b. Deutch, Clayton V. and Andre G. Journel, GSLIB Geostatistical Software Library and User's Guide, Oxford University Press, New York, 1992.

c. Cressie, Noel A.C., Statistics for Spatial Data. Wiley, New York, 1993.

d. Basic Description of Argos System, INTERNET Access at address http://www.argosinc.com.

e. Logsdon, Tom, The NAVSTAR Global Positioning System, Van Nostrand Reinhold, New York, 1992.

f. "Objective Analysis Of Oceanic Data For Coast Guard Trajectory Models", Applied Mathematics, Inc., Phase I Final Report, 23 March 1994.

g. "Estimation of a Multidimensional Covariance Function in Case of Anisotropy", Leon Borgman and Li Chao, Mathematical Geology, Vol. 26, No. 2, 1994.

h. README.UserData dated May 08 15:00 1996, Daniel H. Wagner, Associates, Inc., Hampton, VA.

i. Gardiner, C.W., Handbook of Stochastic Methods. Springer-Verlag, New York, 1983.

j. "Smothing Filtering, and Boundary Effects", Ralph Shapiro, Reviews of Geophysics and Space Physics, Vol. 8, No. 2, 1970.

APPENDIX A
OPS DEVELOPMENT TEST PLAN

1.0 INTRODUCTION

Ocean Prediction System (OPS) is under development to provide estimates of ocean surface current fields for use in real time by search and rescue planners.

These estimates are intended for use by CASP 2.0 to develop search plans and evaluate search effectiveness. Searches using OPS should be more efficient and more effective because in-situ small scale dynamic data instead of large scale historical data will be used to drift the search area.

Search effectiveness is expected to increase due to:

- a greater likelihood that the search region will contain the search object, and
- a reduction in the growth of the search area of uncertainty.

The purpose of the OPS Development Test is to assist in the development of OPS. Analysis of test results and lessons learned will be used to help improve and validate the algorithms, to assist in selection of algorithm parameters, and to assess the utility of specific program options and displays.

The OPS Development Test will be conducted by Applied Mathematics, Inc., personnel under the direction of Dr. William J. Browning, Test Director.

2.0 TEST OBJECTIVES

Test objectives are to evaluate:

- OPS mathematical algorithms for objective analysis of SLDMB data,
- OPS software for acquiring/processing SLDMB data from Service Argos,
- OPS/CASP 2.0 interface, and
- OPS program operability.

2.1 Specific Test Objectives

Specific test objectives are:

2.1.1 Algorithm Performance

- Examine algorithm performance as a function of
    - number of buoys,
    - buoy relative position,
    - time,
    - buoy spacing (average nearest-neighbor distance),
    - buoy spatial configuration (perimeter or lattice type),
    - the time lag used to estimate buoy velocity,
    - the time window, and
    - the number of influential points.

    Algorithm performance will be examined by selectively removing buoy data and by changing parameters in the algorithm. We will use the current field as input to CASP 2.0 and assume that the excluded buoy(s) is the target. The displacement of the buoy from its predicted position will be tracked in time and compared to distance expected for different velocity uncertainties.

- Evaluate algorithms for blending two current fields.

2.1.2 Argos/SLDMB/OPS Interface

- Verify ability to correctly download/process SLDMB data.
- Evaluate procedures for downloading data.
- Determine best way to handle
    - removal or reconstruction of noisy input,
    - cross-checking of multiple data reports, and
    - reconciliation of conflicting data reports.

The outlier reporting code in OPS will be used to determine the fraction of unusable data points being sent from the interface code to OPS.

2.1.3 OPS/CASP 2.0 Interface

- Verify ability to input real-time current data into CASP.
- Assess whether the use of OPS increases the likelihood that the search region contains the target compared to use of historical current data.
- Assess whether the use of OPS reduces the growth of the search area compared to use of historical current data.
- Evaluate effect of buoy pattern on CASP search area growth with time.
- Evaluate CASP 2.0 drift time step when using OPS.

2.1.4 Evaluate OPS Program Features

We will address the following questions:

- Are the main features readily available to the user?
- Are the commands easy to identify?
- Are the entry fields in dialog boxes arranged and grouped by categories?
- Is it clear what input is expected in each entry field?
- Do error (warning) dialogs explain the reason for the error (warning) clearly?
- Does the program respond within a reasonable amount of time to user input, even if the program needs time to process?

- Is it easy to request and receive Argos/GPS data?
- Is it easy to request OA data be sent to CASP?
- Are the graphical displays useful for visualizing the current field and its estimated error?
- Are there any desirable displays or features missing?
- Is it easy to use the data archive mode?
- Is it easy to recall saved parameters and results?

3.0 TEST CONDUCT

The test will be conducted in three phases:

Phase I. Buoy deployment. Eleven (11) self locating data marker buoys will be deployed in a 5 nm lattice pattern centered at NOAA buoy # 44011 moored on Georges Bank at 41.0500N, 66.3500W (see Figure 1). Seven (7) ClearSat-1 Surface Layer Drifter (GPS option) buoys manufactured by Clearwater Instrumentation, Inc., and four (4) Argos GPS surface current Davis drifters manufactured by METOCEAN Data Systems, Ltd., will be used.

Phase I will start 29 May 1300Z and end 31 May 1700Z.

Phase II. Real time estimation of ocean surface current fields. SLDMB GPS data will be downloaded from Argos. Calculations of OPS surface current field and probability maps of uncertainty area will be made daily.

Phase II will start 30 May 1700Z. Phase II will continue as long as information useful for OPS development is obtained. Test results will be reviewed, 7 June, and an option to extend Phase II until 13 June 2100Z will be considered at that time.

Phase III. SLDMB data collection. In Phase III, SLDMB data will be collected, reviewed and archived. Phase III will begin at the completion of Phase I. The only difference between Phase II and Phase III is that, in Phase III, real time estimation will not be made. Phase III will end 2200Z 28 June or when the buoys cease transmitting, whichever time is earlier. The estimated buoy battery endurance is shown in Table 1.

Table 1. Buoy Battery Endurance

Buoy	Buoy ID	Voltage Level	Estimated Run Time (days)
1	9176	9.5	15
2	4574	9.5	15
3	9178	8.6	5 - 7
4	4575	9.5	15
5	9177	9.6	15
6	4552	9.6	15
7	4546	9.5	15
8	9881	15	48
9	9882	15	48
10	9883	15	48
11	9884	15	48

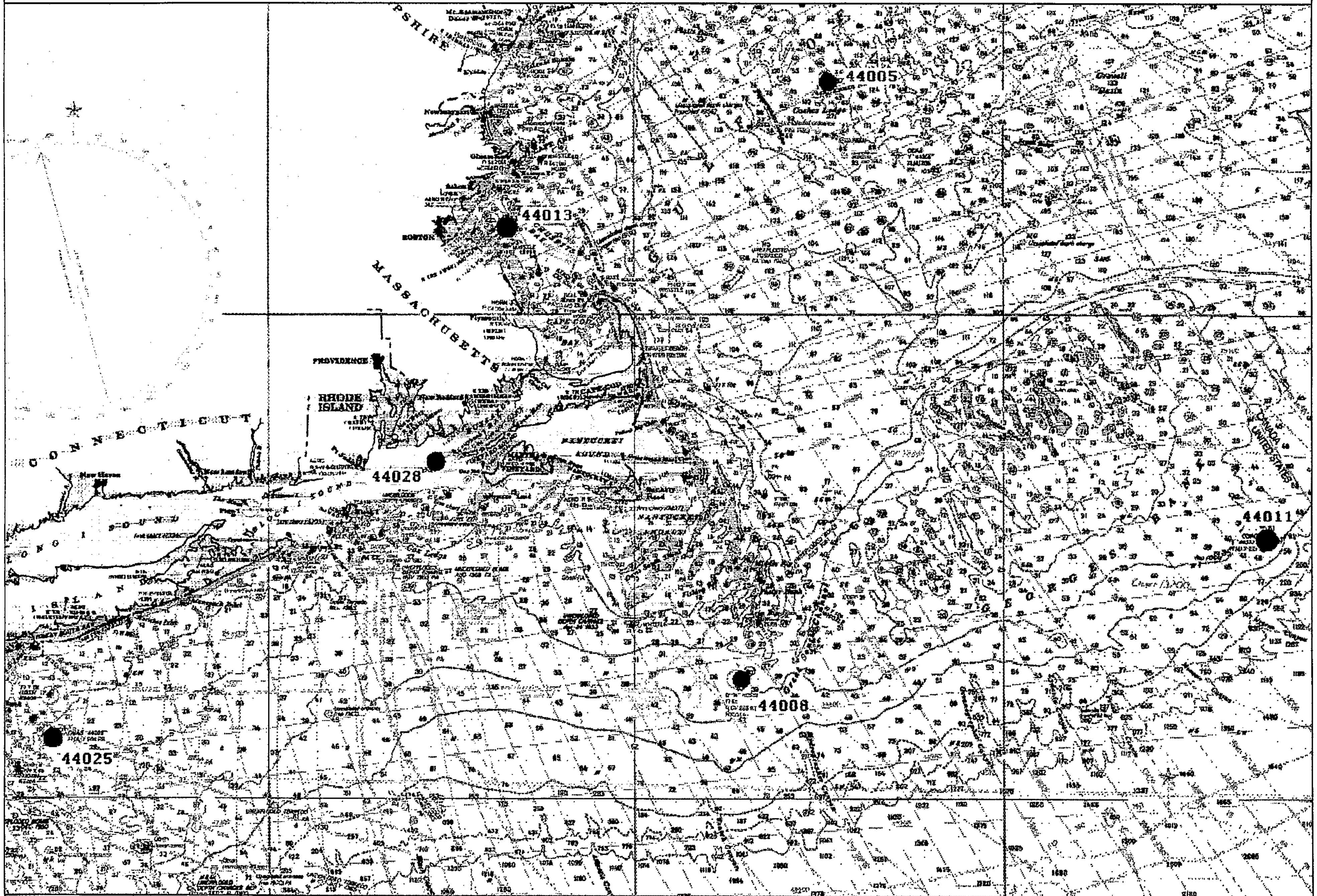

Figure 1. NOAA Buoy Locations

3.1 Test Schedule

The test schedule is shown in Table 2.

Table 2. OPS Test Schedule

Phase	Description	Start	End
I	Buoy deployment	29 May 1300Z	31 May 1700Z
II	Real time estimation	30 May 1700Z	13 June 2200Z
III	Data collection	30 May 1700Z	28 June 2200Z

The test time line is shown in Figure 2.

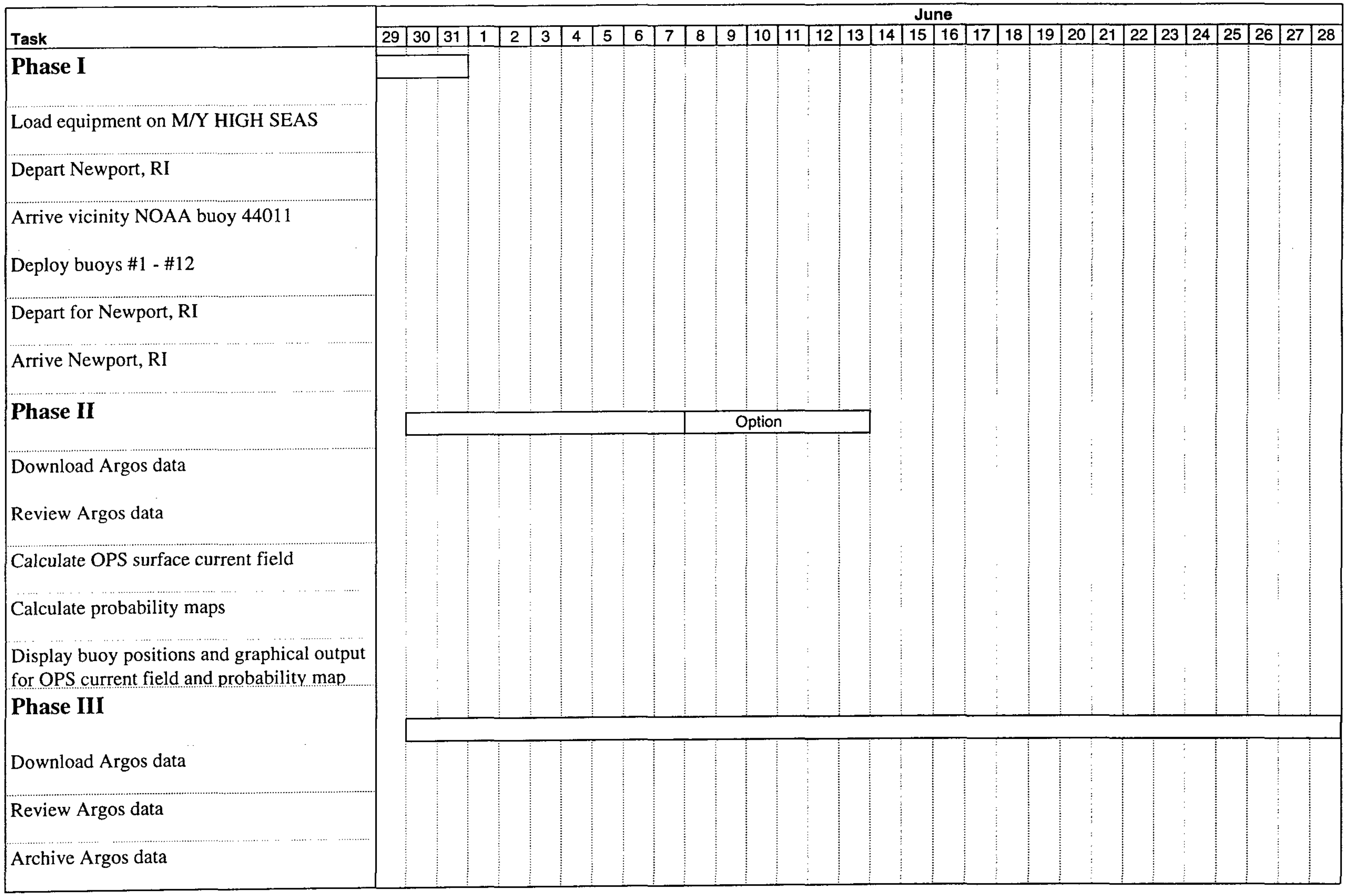

Figure 2. Test Time Line

3.2 Phase I: Buoy Deployment

The Phase I schedule is shown in Table 3.

Table 3. Phase I Schedule

Description	Start
Load equipment on M/Y HIGH SEAS	29 May 1200Z
Depart Newport, RI	29 May 1300Z
Arrive vicinity NOAA buoy 44011	30 May 1000Z
Deploy buoys #1 - #11	30 May 1000Z
Depart for Newport, RI	30 May 2000Z
Arrive Newport, RI	31 May 1400Z

Eleven buoys will be deployed in a lattice pattern, centered on NOAA buoy # 44011 (41 05.00N, 66 35.00W), with 5nm spacing. The buoys will not be recovered.

A chart illustrating the initial buoy pattern is shown in Figure 3, where the positions are as in Table 4. Initial buoy pattern is shown in Figure 4.

Table 4. Buoy Initial Placement Location

Buoy	Latitude DD MM.MMM	Longitude DDD MM.MMM
1	41 05.000 N	066 35.000 W
2	41 05.000 N	066 44.941 W
3	41 09.995 N	066 44.941 W
4	41 09.995 N	066 38.314 W
5	41 09.995 N	066 31.686 W
6	41 09.995 N	066 25.059 W
7	41 05.000 N	066 25.059 W
8	41 00.005 N	066 25.059 W
9	41 00.005 N	066 31.686 W
10	41 00.005 N	066 38.314 W
11	41 00.005 N	066 44.941 W

Phase I checklist is provided in Appendix C.

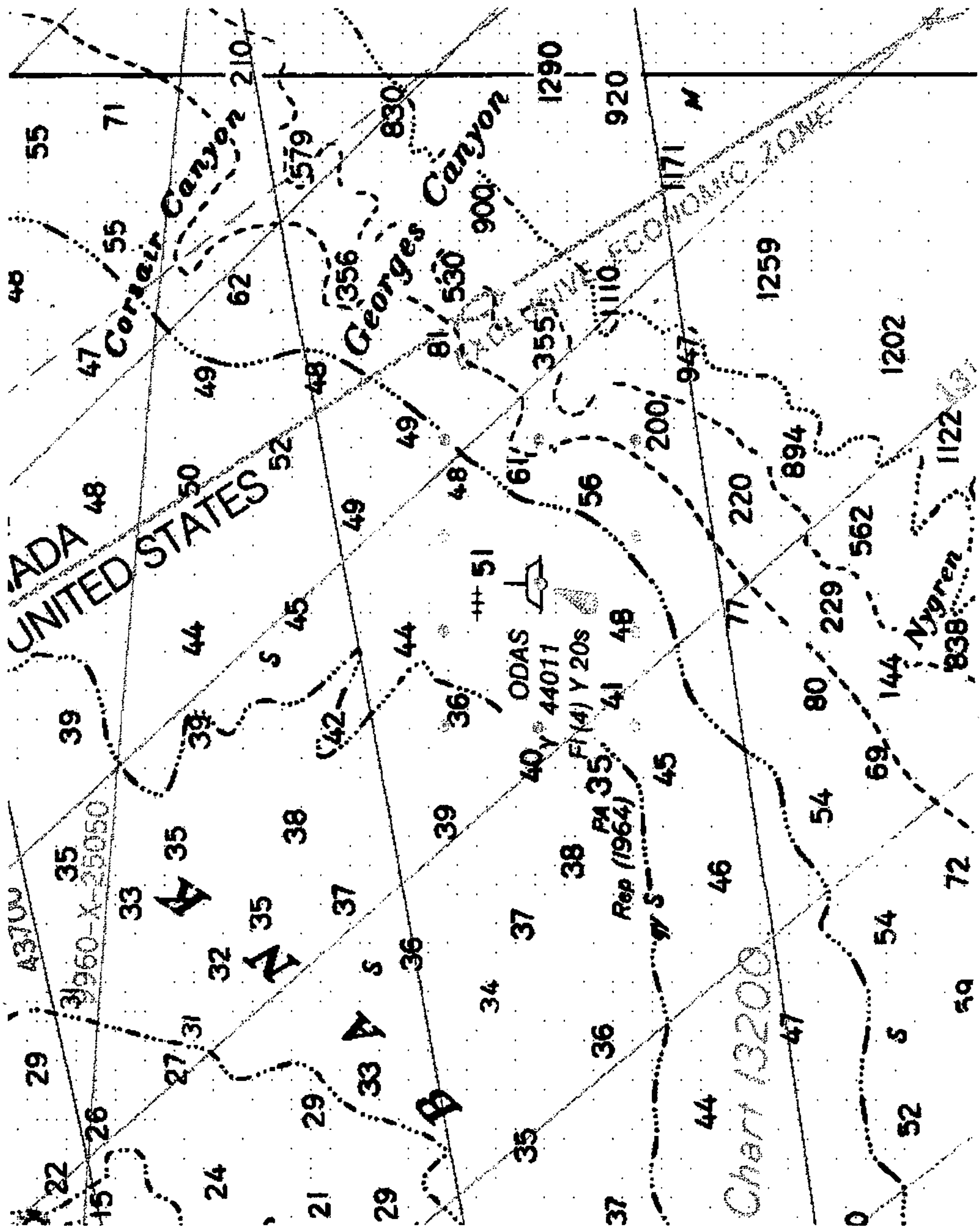

Figure 3. Geographic Chart of Initial Buoy Placement

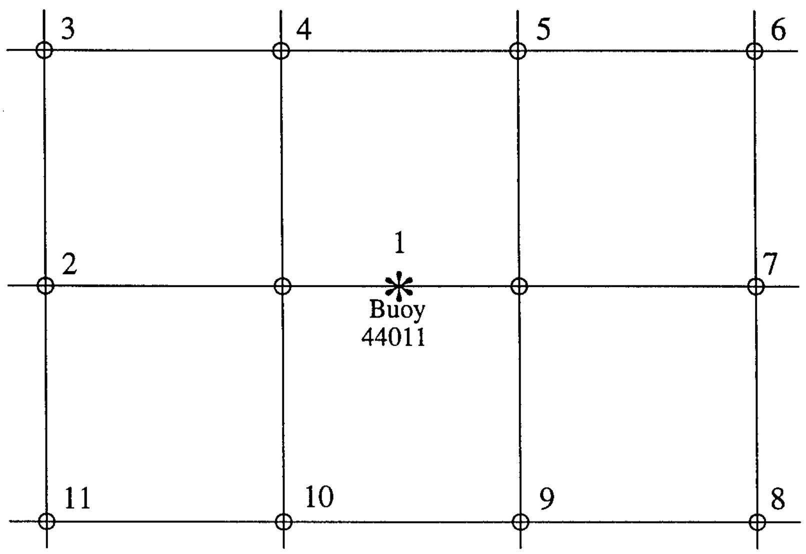

Figure 4. Initial Buoy Pattern

3.3 Phase II: Real Time Estimation

In Phase II, estimates of the surface current field will be made. On 7 June, test results will be reviewed and a decision made to continue Phase II or to begin Phase III.

Phase II consists of five tasks. In Task 1, buoy data will be automatically downloaded four times daily from Service Argos using Internet access (TYMNET local dialup is a backup option). In Task 2, downloaded data will be reviewed and edited. In Task 3, surface current field and uncertainty will be estimated. In Task 4, probability maps for area of uncertainty drift will be calculated. Two models will be used: OPS and CASP 2.0. In Task 5, displays of buoy positions and probability maps will be prepared.

Table 5. Phase II Daily Schedule, 30 May - 7 June

Task	Description	Start Time (Local)
1	Download Argos data	0200 0800 1400 2000
2	Review Argos data	0900 1500
3	Calculate OPS surface current field	1000
4	Calculate probability maps	1000
5	Display buoy positions and graphical output for OPS current field and probability map	1400

A Phase II checklist is given in Appendix C.

3.4 Phase III: Data Collection

In Phase III, the buoy data will be downloaded, reviewed and archived. Phase III will continue until 28 June 2100Z or until the buoys cease transmitting, whichever time is earlier. Buoy battery endurance is shown in Table 1.

Phase III schedule is shown in Table 6.

Table 6. Phase III Daily Schedule, 30 May - 28 June

Description	Start Time (Local)
Download Argos data	0200 0800 1400 2000
Review Argos data	0900 1500

A Phase III checklist is given in Appendix C.

4.0 TEST STATUS REPORTS

A test status report will be posted daily on a password protected Web site beginning 3 June. Graphics of buoy positions, OPS output and probability maps will be included. Sample output is shown in Figures 5, 6, 7 and 8.

Access to the Web site will be provided by the Test Director.

At the end of the first week of the test, a review meeting will be held with the Project Officer.

A summary briefing will be presented one week after test completion.

Test results and archived data will be included in project final report.

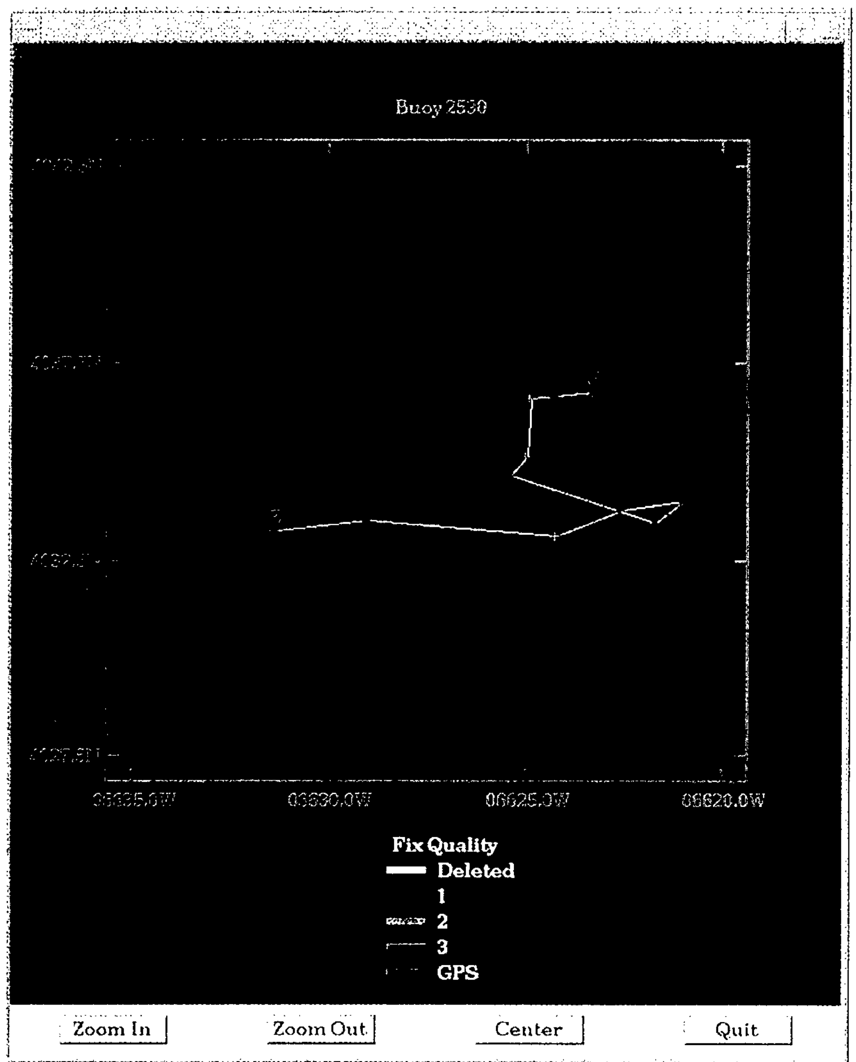

Figure 5. Sample Individual Buoy Track

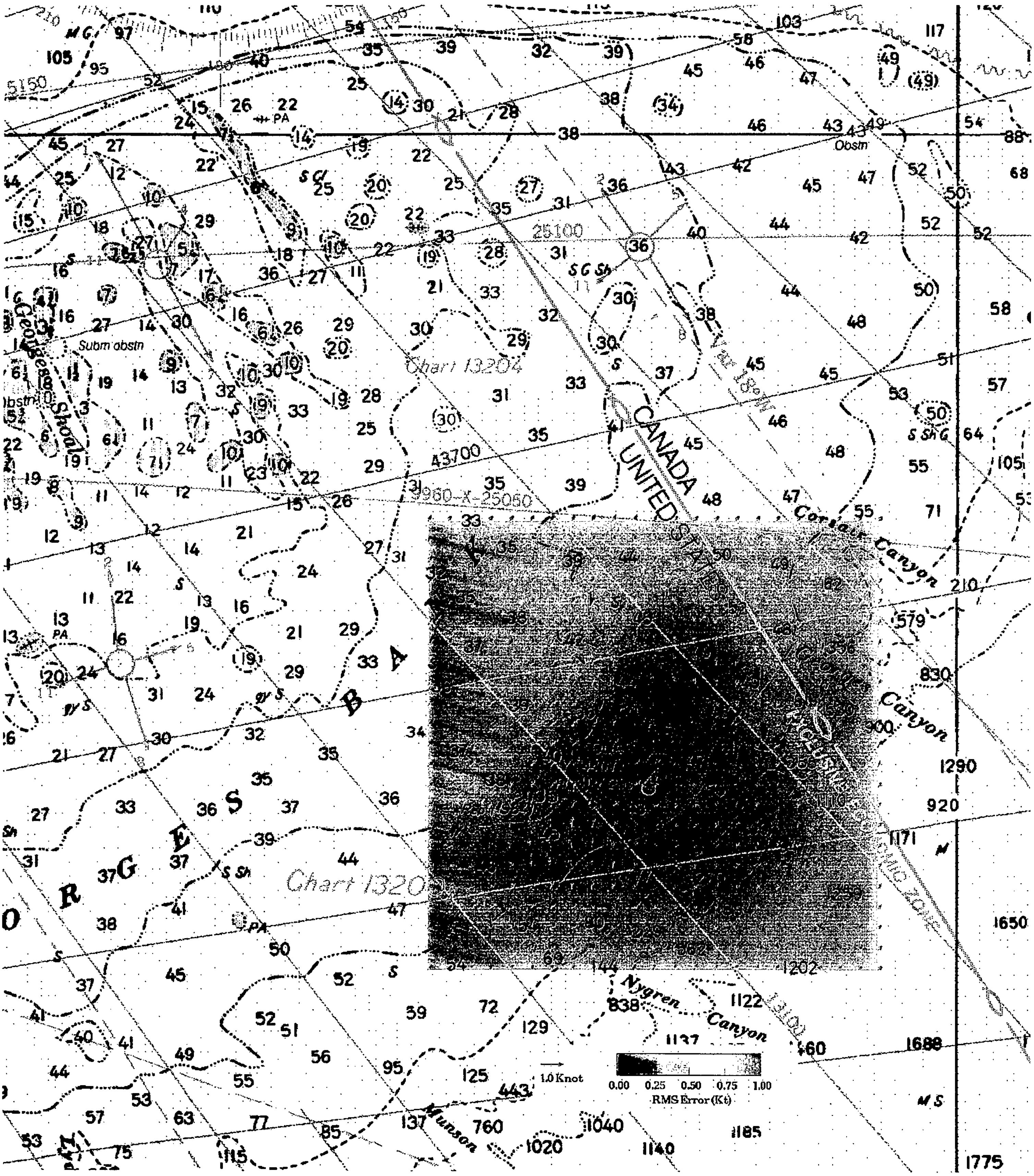

Figure 6. Sample OPS Current Field

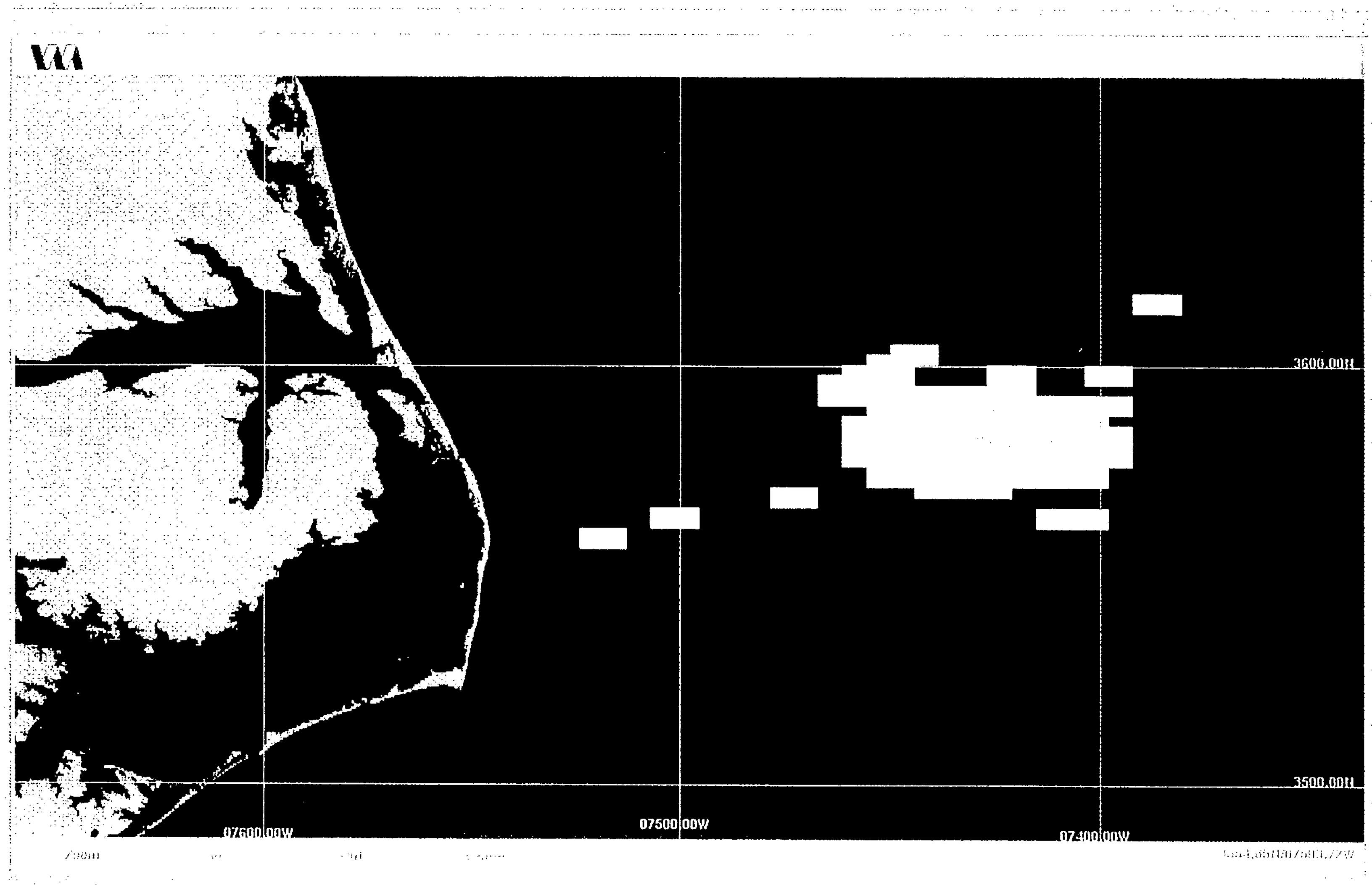

Figure 7. Sample CASP 2.0 Probability Map

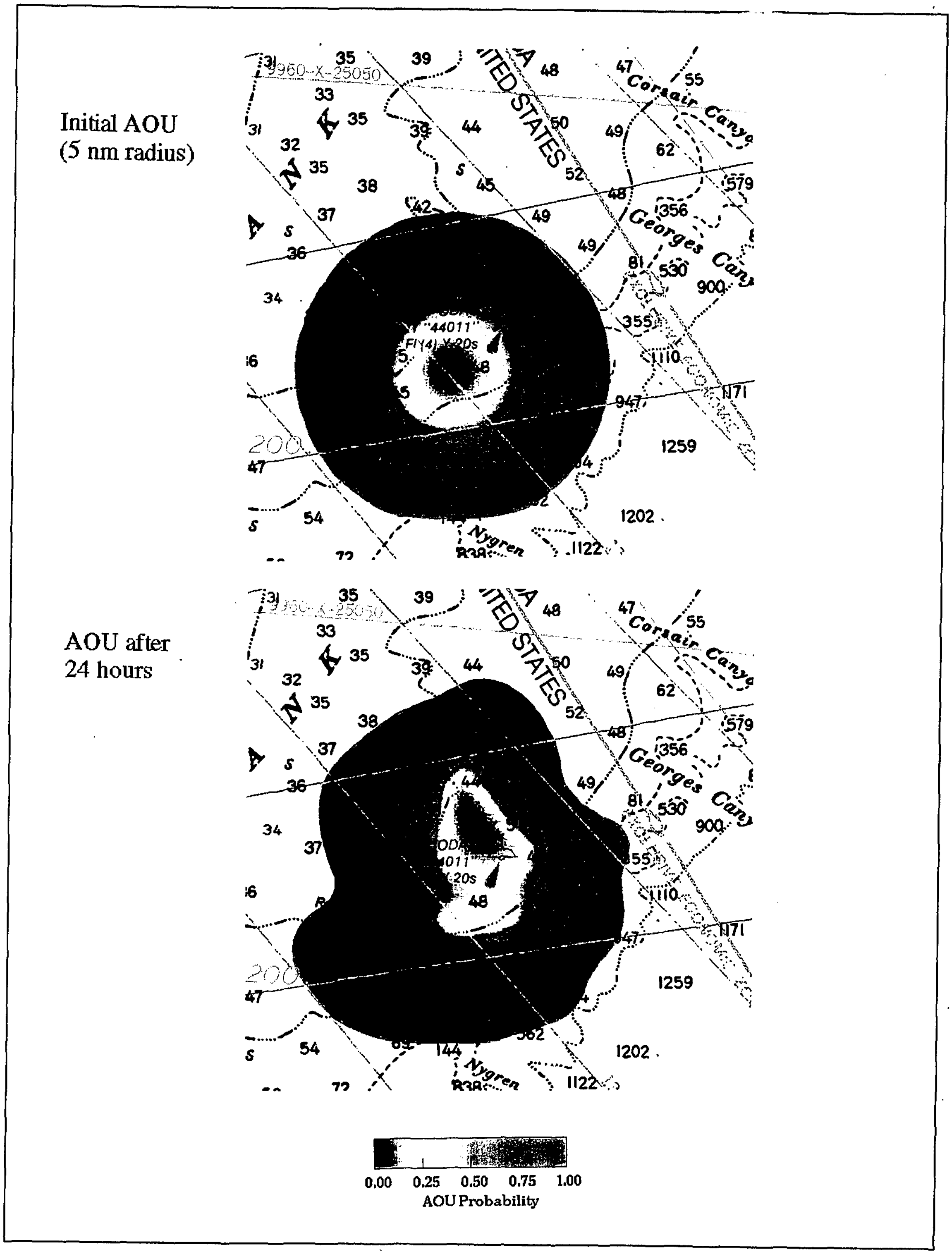

Figure 8. Sample OPS Probability Map

5.0 DATA COLLECTION

Data shown in Table 7 will be collected throughout the test.

Table 7. Data Collected during All Test Phases

Data	Source	Frequency
SLDMB Clearwater datastream(1)	Service Argos	Half hour
SLDMB METOCEAN datastream(2)	Service Argos	Half hour
Wind speed, direction, gust, pressure, sea temperature, wave length, wave period	NOAA buoy 44011	Hourly
Marine weather forecast	NODES	12 hour

Note 1. The Clearwater datastream contains the following information:

- Page 0 (transmitted before the buoy acquires a GPS fix): GPS location rate, Battery voltage, Error Flags, SST (if equipped with SST sensor), GPS Geometric Dilution of Precision (GDOP), GPS status word, Channel 1-4 measurement status and SNR,
- Pages 1-4 (transmitted after the first GPS fix is acquired): date, time, latitude, longitude, temperature (if equipped with sensor, page 1 only), GPS FOM (page 1 only).

This information may be downloaded from Argos or read and decoded from the Gonio RDF. Some information may not be valid on page 0 depending upon the status of the GPS receiver. The buoy cycles between pages 1-4 after the GPS fix is acquired.

Note 2. The METOCEAN datastream contains the information shown in Table 8.

5.1 Phase I

Actual buoy deployment location and time will be recorded on Data Sheet 1 (Appendix B) at time of deployment. Position will be determined using GPS. Buoy transmitter status will be annotated on Data Sheet 1. Buoy transmissions will be computer recorded at time of deployment using the Gonio RDF and a laptop computer. Buoy launch will also be video recorded. A narrative log will be maintained by test personnel.

5.2 Phase II

All downloaded SLDMB buoy data will be computer recorded. NOAA buoy data will also be computer recorded. All input data used to calculate current field and probability maps will be computer recorded. All model output data will be computer recorded.

A narrative log containing observations and lessons learned will be maintained by test personnel.

5.3 Phase III

All downloaded SLDMB buoy data will be computer recorded. NOAA buoy data will also be computer recorded.

Table 8. METOCEAN GPS Davis Drifter Format

Byte #	Data Description	
1	Checksum0(8)	
2	MsgID(2)	Message ID = 1, 2 or 3
	VBAT(6)	Battery Volts
3	SST(8)	Sea Surface Temperature
Current Data:		
4	TTFF(8),	Time to first Fix
5	GPSTIME(6),	Time of GPS fix
	FOM(2)	Figure of Merit
6	Lat(8)...	Latitude...
7	...Lat(8)...	
8	...Lat(3), Lon(5)	
9	Lon(8)...	Not Used, Longitude...
10	...Lon(7), dB0(1)...	Max GPS Signal Level
11	...dB0(2), Sats(6)	Satellite Sum
12	Checksum1(8)	for bytes 13-32
Data for GPSTIME - 0.5 hr.:		
13	Rlat(8)...	Relative Latitude
14	...Rlat(4),	
	Rlon(4)...	Relative Longitude
15	...Rlon(8)	
16	FOM(2), Sats(6)	Figure of Merit, Satellites
Data for GPSTIME - 1.0 hr.:		
17	Rlat(8)...	Relative Latitude
18	...Rlat(4),	
	Rlon(4)...	Relative Longitude
19	...Rlon(8)	
20	FOM(2), Sats(6)	Figure of Merit, Satellites
Data for GPSTIME - 1.5 hr.:		
21	Rlat(8)...	Relative Latitude
22	...Rlat(4),	
	Rlon(4)...	Relative Longitude
23	...Rlon(8)	
24	FOM(2), Sats(6)	Figure of Merit, Satellites
Data for GPSTIME - 2.0 hr.:		
25	Rlat(8)...	Relative Latitude
26	...Rlat(4),	
	Rlon(4)...	Relative Longitude
27	...Rlon(8)	
28	FOM(2), Sats(6)	Figure of Merit, Satellites
Data for GPSTIME - 2.5 hr.:		
29	Rlat(8)...	Relative Latitude
30	...Rlat(4),	
	Rlon(4)...	Relative Longitude
31	...Rlon(8)	
32	FOM(2), Sats(6)	Figure of Merit, Satellites

Notes: (1) Numbers in () indicate the number of bits used.
(2) "..." indicates a data word continuing between bytes in the message

6.0 TEST EQUIPMENT

6.1 Self Locating Data Marker Buoy (SLDMB)

Eleven (11) SLDMB will be deployed for the test. ClearSat-1 Surface Layer Drifter (GPS option) buoys, manufactured by Clearwater Instrumentation, Inc., Watertown, MA, and Argos GPS CODE (DAVIS) drifters manufactured by METOCEAN Data Systems, Ltd., Dartmouth, Nova Scotia, will be used. Technical specifications for the buoys are shown in Figures 9 and 10.

The test buoy ID numbers (also known as Argos Platform Transmittal Terminal (PTT) numbers) are shown in Table 9. Buoys #1 - 7 are provided as GFE; and buoys #8 - 11 were purchased for this test.

Table 9. SLDMB ID #

Buoy	ID
1	9176
2	4574
3	9178
4	4575
5	9177
6	4552
7	4546
8	9881
9	9882
10	9883
11	9884

6.2 NOAA Moored Buoy # 44011

NOAA buoy # 44011 is moored at 41 05.00 N, 66 35.0 W in 88.4 meters of water. A photograph of this type of buoy is shown in Figure 11. The buoy transmits the following data: Day/hour, wind speed (kt), direction, gust (kt), pressure (mbar), sea temperature (F), wave height (ft), and wave period (s).

Near real time data is accessible via the WWW at URL http://www.ems.psu.edu/cgi-bin/wx/off-shore.cgi.

ClearWater Instrumentation, Inc.

ClearSat -1 Surface Layer Drifter

LOCATION BY ARGOS OR GPS*
RELIABLE ARGOS DATA COLLECTION

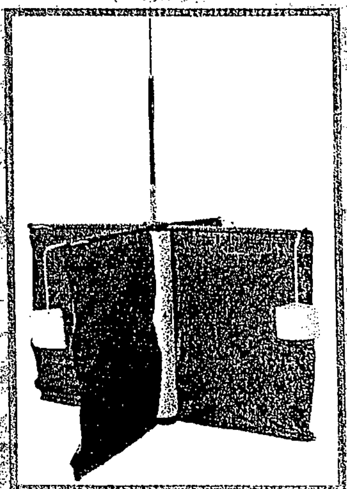

Description

The ClearSat-1 surface drifter accurately tracks the top 1 meter of the surface mixed layer and provides a platform for oceanographic and meteorological measurements at the sea surface. The drifter is configured according to CODE (California Ocean Dynamic Experiment) design considerations. Sail arms can be quickly pulled out from the hull and folded against it along with the antenna for efficient storage. Data from anywhere in the world are reported to the user by satellite telemetry though the Argos system which also makes accurate locations of the drifter's position[1]. Standard instrument suite reports sea surface temperature, and battery condition. The microprocessor controller and transmitter are contained completely within the rugged hull of PVC plastic. Options include salinity (conductivity/temperature), air deployment packaging and GPS positioning (accurate to 20 meters).

Technical Specifications:

Physical:	Hull 8.9 cm. (3.5 in) diameter by 100 cm (39.4 in.) length PVC, total weight 8 kg (17lbs).
Drogue:	1 meter x 1 meter cross section. Center at 80 cm.
Power supply:	12 VDC, 43 AH, sufficient for .75 year at continuous transmission.
Transmit cycle:	Continuous, 8/16, 12/12, 12/24, 24/48 (hours on/hours off).
Sea temperature:	SST, linearized thermistor sensor imbedded in 316-ss through-hull fitting at base of surface float, fast time-constant design. Calibration to 0.1°C provided. Temperature range is -5 to 45 +/- 0.05°C.
Sea surface salinity:	C/T measurement, 0 - 64 +/- 0.026 mmho/cm., -5 - 35 +/- 0.05 C, 12 hourly samples.
*GPS (optional):	Year, month, day, hh:mm:ss +/- 1 sec, latitude and longitude +/- 0.0001 deg., 4 to 13 positions. Single, multi-band antenna for GPS and Argos.
RF output:	1± .3 watt into 50 ohms.
Environmental:	-50 to 30°C, storage, -5 to 45°C, operation.

SLDMB : USCG R+D specification.

For sales and information contact Gary Williams, Voice: (617) 924-2708 Fax: (617) 924-2724 Email: wgwill@world.std.com
CLS/Argos certified.
[1]For further information about Argos data collection services:
U.S.: North American CLS, Inc., 9200 Basil Court, Suite 306, Landover, MD 20785, U.S.A.
Europe: CLS/Service Argos, 18 avenue Edouard Belin, 31055 TOULOUSE Cédex, FRANCE Voice: 61 39 47 74 Telex: 531 752F Fax: 61 75 10 14

Figure 9. Clearwater SLDMB Technical Specification

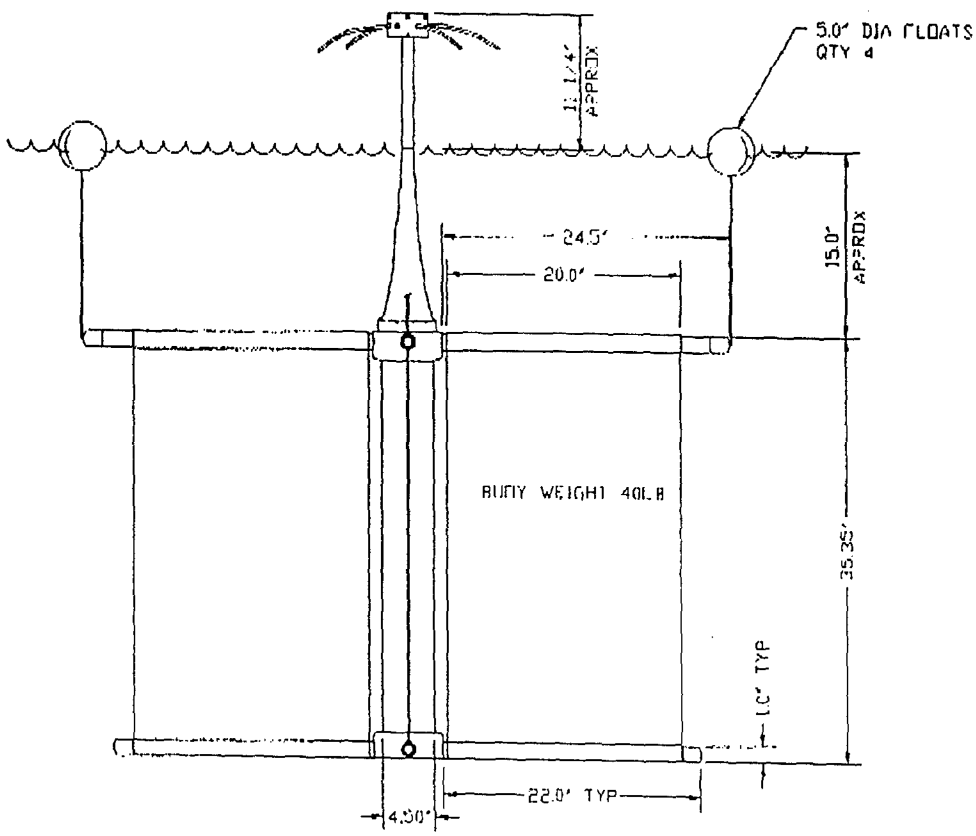

Figure 10. METOCEAN CODE (DAVIS) Drifter Profile Diagram

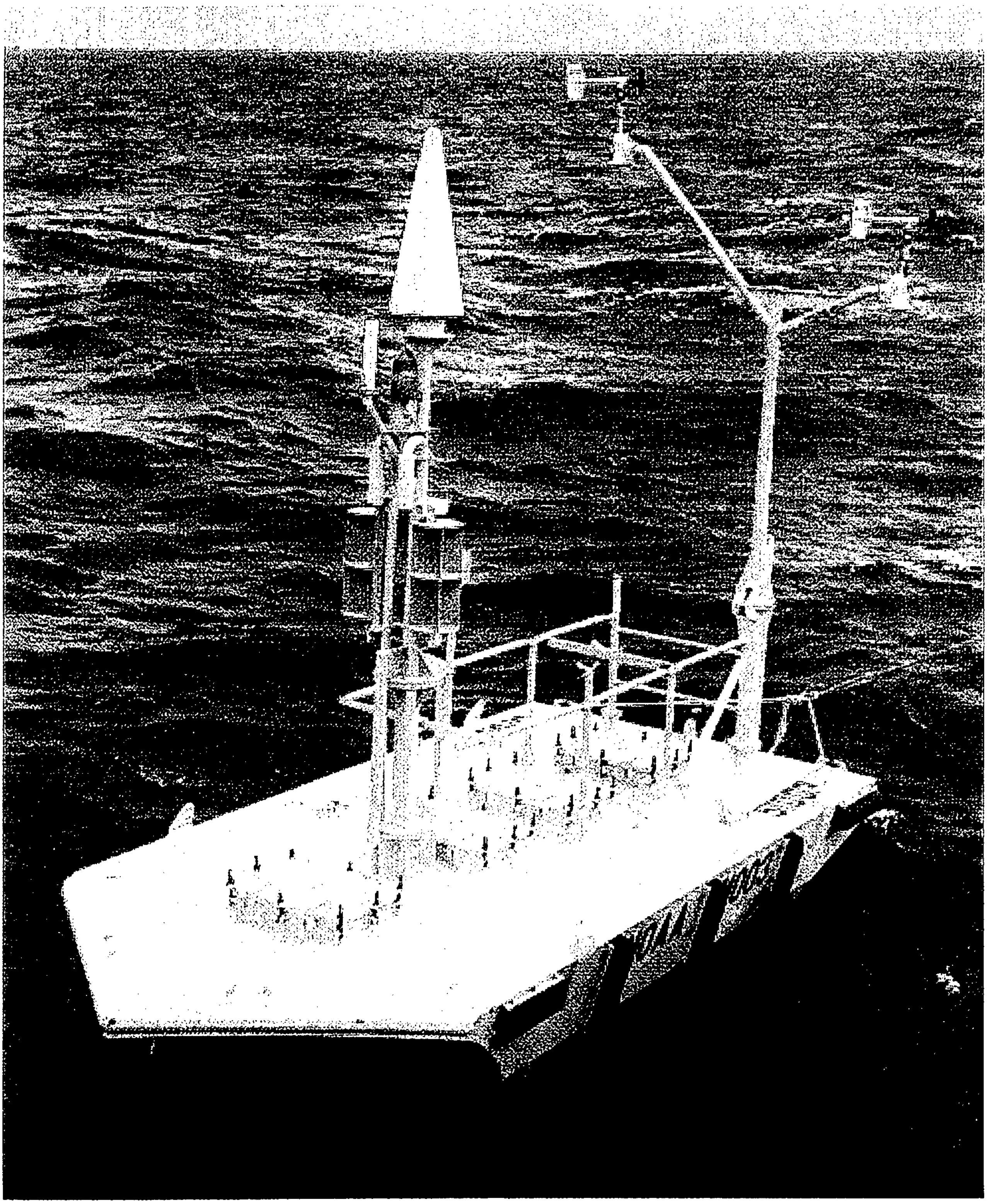

Figure 11. NDBC 6-meter NOMAD Buoy

6.3 M/Y HIGH SEAS

M/Y HIGH SEAS, owned by Bushido Enterprises, Dover, Delaware will be used to deploy the test buoys.

Description of the M/Y HIGH SEAS is shown in Table 10.

Table 10. M/Y HIGH SEAS Description

Burger Motor Yacht
Documentation Number: 523240
Homeport: Richmond, VA
Call sign: WCE 7667
LOA: 67'
Beam: 17'1"
Draft min/max: 4'6"/5'6"
Fuel: 1300 g
Max speed: 17 kt
Engines: 2 x 550 HP

6.4 Gonio 400 UHF Direction Finder

The "Gonio 400" UHF Direction Finder is a portable receiver designed to receive and decode messages emitted by Argos beacons in order to determine the location of the emitter.

Data transmitted by the SLDMB will be recorded using the Gonio RDF and a laptop computer.

Sketches of the receiver and front panel are shown in Figure 12.

6.5 Argos

Argos is a satellite-based system which collects, processes and disseminates environmental data from fixed and mobile platforms worldwide.

Argos was developed under a Memorandum of Understanding (MOU) between the Centre National d'Etudes Spatiales (CNES, the French space agency), the National Aeronautics and Space Administration (NASA, USA) and the National Oceanic and Atmospheric Administration (NOAA, USA).

The system utilizes both ground and satellite-based resources. This includes instruments carried aboard the NOAA polar orbiting environmental satellites (POES), receiving stations around the world and processing facilities in France and the United States.

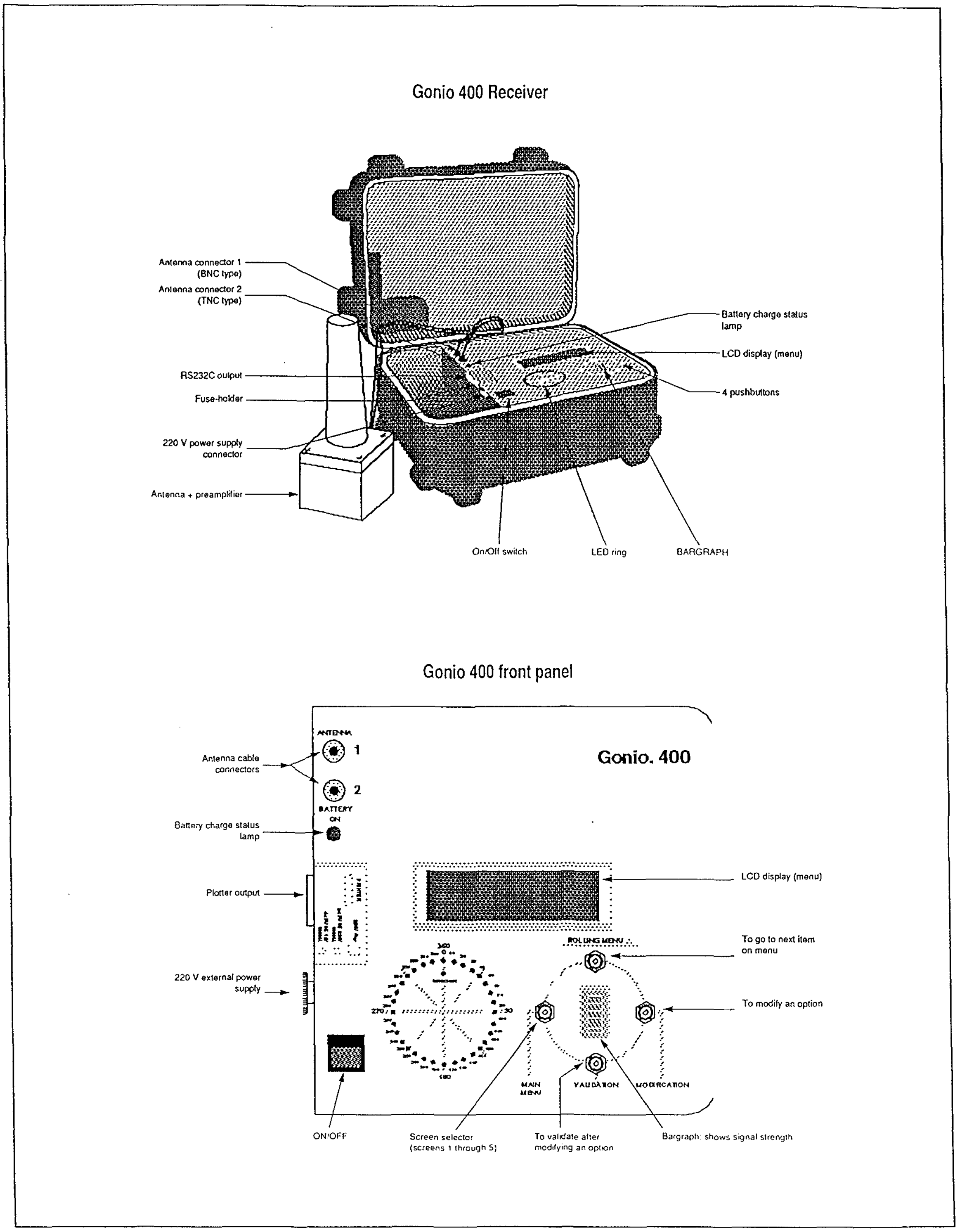

Figure 12. Gonio 400 UHF Direction Finder

The OPS test area is covered by the Wallop's Island ground station. According to Service Argos, 50% of SLDMB transmitted data during the OPS test will be available within 30 minutes and 75% within 1 hour of SLDMB transmission.

Data will be retrieved via Telnet at datadist.argosinc.com. An alternate retrieval path is via local TYMNET dialup access (telephone: (860) 444-1846 (14.4 kbps) or (860) 444-7030 (2400 bps)).

Internet access cost is $0.10/minute; TYMNET is $0.50/minute.

7.0 CONTINGENCY PLANS

7.1 Weather

Low sea state conditions are required during Phase I. No buoys will be deployed unless weather conditions permit the deployment of all buoys within a twelve (12) hour time period.

In general, weather conditions are expected to be favorable for buoy deployment during June in the test area. Marine weather forecasts will be monitored prior to and during Phase I.

If poor weather is forecast for several days on or about 29 May, Phase I will start when the weather improves. Option to extend charter until 3 June is included.

In the event that weather conditions prevent the scheduled departure of M/Y HIGH SEAS, the test participants will remain in Newport, RI for up to 24 hours.

In the event that weather conditions require that M/Y HIGH SEAS seek safe harbor prior to arrival at the test site, M/Y HIGH SEAS will lay over for up to 24 hours at Nantucket Island.

APPENDIX A
Points of Contact

Person	Organization	Address	Telephone/ FAX	Email
LCDR Brian Perkins	U.S. Coast Guard R&D Center	1082 Shennecossett Road Groton, CT 06340	(860) 441-2618 (860) 441-2792	perk81@aol.com
LT Thomas McClay	U.S. Coast Guard R&D Center	1082 Shennecossett Road Groton, CT 06340	(860) 441-2750 (860) 441-2792	LT_T_MCCLAY_RDC01 @cgsmtp.uscg.mil
Arthur Allen	U.S. Coast Guard R&D Center	1082 Shennecossett Road Groton, CT 06340	(860) 441-2747 (860) 441-2792	aallen@gamma.rdc.uscg. mil
Dr. William J. Browning	Applied Mathematics, Inc.	1622 Route 12 P.O. Box 637 Gales Ferry, CT 06335	(860) 464-7259 (860) 464-6036	wjb@applmath.com
Dr. Joseph Discenza	Daniel H. Wagner, Associates	2 Eaton Street Suite 500 Hampton, VA 23669	(804) 727-7700 (804) 722-0249	joe@dhwa.com
W. Gary Williams	Clearwater Instrumentation, Inc.	304 Pleasant Street Watertown, MA 02172	(617) 924-2708 (617) 924-2724	wgwill@world.std.com
Bernard Petolas Lorne Vaasjo	Metocean Data Systems, Ltd.	P.O. Box 2427 D.E.P.S. 40 Fielding Avenue Dartmouth, Nova Scotia	(902) 468-2505 (902) 468-4442	bpetolas@metocean.ns.ca lvaasjo@metocean.ns.ca
Ray Mahr	Metocean Data Systems, Inc.	Building 1103, Suite 149 Stennis Space Center, MS 39529	(601) 688-1819 (601) 688-2839	rmahrjr@ metocean.win.net
User Office	Service Argos, Inc.	1801 McCormick Drive Suite 10 Landover, MD 20785	(301) 925-4411 (301) 925-8995	USEROFFICE@ argosinc.com
Peggy Staubs	U.S. Coast Guard Operations System Center	175 Murall Drive Martinsburg, WV 25401	(304) 264-2583 (304) 264-2554	OSCB@cgsmtp.wcg.mil
Rocky Tomlinson	M/Y HIGH SEAS	c/o Northrop and Johnson	(800) 618-5408 (pager)	
Missy Johnston	Northrop and Johnson	19 Brown and Howard Wharf Newport, RI 02840	(800) 868-5913 (401) 848-0120	

APPENDIX B
Data Sheet

Buoy	ID #	Time (Z)	Location		Activate/Verify Transmitter
			Latitude	Longitude	
1					
2					
3					
4					
5					
6					
7					
8					
9					
10					
11					

APPENDIX C

Phase I Checklist

		Buoy ID #										
	Task	**9176**	**4574**	**9178**	**4575**	**9177**	**4552**	**4546**	**9881**	**9882**	**9883**	**9884**
1.	Verify buoy transmitter											
	after receipt by AMI											
2.	Prepare buoys for launch											
	activate Clearwater transmitter on the half hour (0000 or 0030) at least one hour before launch											
	activate Metocean transmitter one hour before launch											
3.	Record each buoy using Gonio RDF											
4.	Deploy buoy IAW Table 2											
5.	Complete Data Sheet 1											

Phase II Daily Checklist

		Day												
	Task													
1.	Download Argos data													
2.	Review Argos data													
3.	Calculate OPS surface current field													
4.	Calculate probability maps													
5.	Display buoy positions and OPS current field and probability maps													

Phase III Daily Checklist

		Day											
	Task												
1.	Download Argos data												
2.	Review Argos data												
3.	Archive data												

Narrative Log

Time	Narrative

APPENDIX B
OPS USER'S GUIDE

B.1 INTRODUCTION

The Ocean Prediction System (OPS) is designed to generate statistical estimates in real time of ocean current based upon real time Self Locating Data Marker Buoy (SLDMB) data inputs. The OPS program is an X Windows/Motif application designed to be run under HP-UX 9.X.

The OPS program consists of three subprograms. The three programs are buoy data retrieval, buoy data processing, and current field generation and display.

Buoy Data Retrieval. The buoy data retrieval program contacts the Argos data center using either the Internet or Tymnet dialup, downloads the GPS and Argos fix data for the requested buoy IDs, removes redundant data, translates the downloaded data into buoy fix times, positions, and fix type/quality. The downloaded data is then merged with existing fix data for the requested buoys and saved for use as input to the current field calculation.

Buoy Data Processing. The buoy data processing program allows the operator to examine downloaded buoy fix data graphically and numerically, view calculated buoy velocities, delete bad data points from the data set, and re-save the buoy data for later use as current field calculation input.

Current Field Generation and Display. The current field generation program allows the operator to specify Objective Analysis (OA) parameters, calculate and save a current field, and display the current field graphically and numerically.

The operator can display a newly calculated or previously saved current vector field, RMS error, contoured speed values, buoy tracks, and buoy velocities. Overlay options include display of Coast Guard First District boundaries and digital charts. Numerical displays include input parameters, and calculated current values with RMS error. The user may also write an output file containing the current information which may be used as input to an appropriately modified version of CASP.

The operator may also generate, save, and replay slide shows containing current field images at different times in order to observe the time-evolution of the current field. The slide show generation can only be run from the current estimate display.

Program structure is shown in Figure B-1.

NOTE

The OPS program is a prototype system. Calculations and displays are available for the Coast Guard First District. The OA algorithm is designed to process current measurements and associated uncertainty estimates from any source. The OA preprocessing options are restricted to SLDMB data.

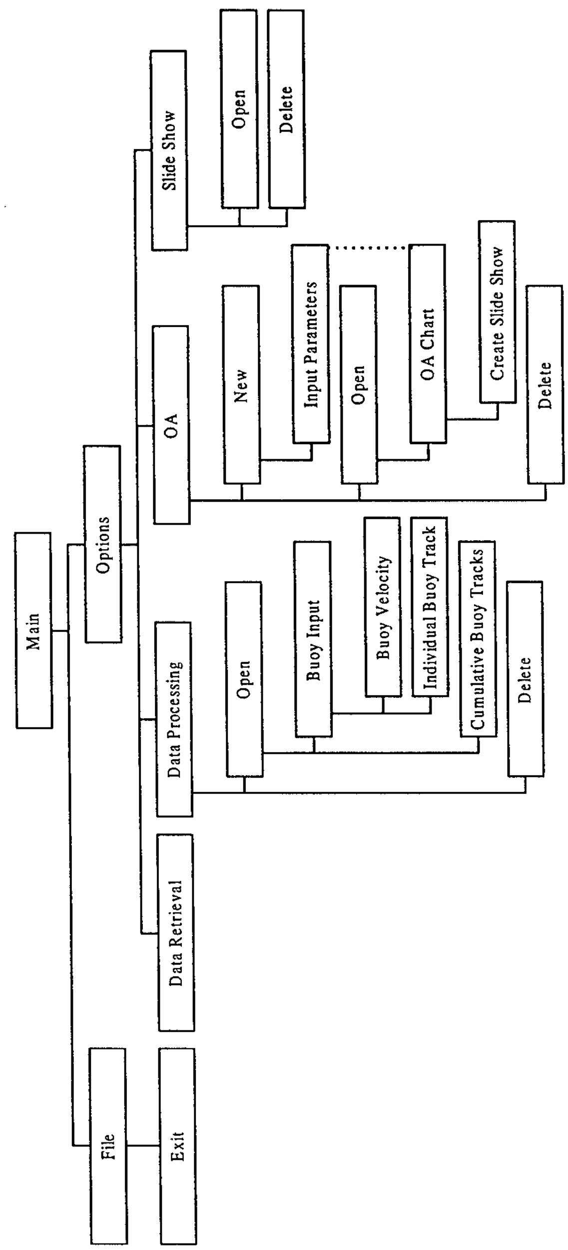

Figure B-1. Program Structure

B.2 OPS MAIN WINDOW OPTIONS

The OPS main window consists of FILE and OPTIONS menus. The main window is shown in Figure B-2.

B.2.1 FILE MENU

The OPS main window FILE menu allows the operator to exit the OPS program through its EXIT menu item. The FILE menu is shown in Figure B-3.

B.2.2 OPTIONS MENU

The OPS main window OPTIONS menu, shown in Figure B-4, allows the operator to retrieve new buoy data, edit new or existing buoy data, calculate a new OA based on archived data, open or delete existing OA fields, and open or delete existing OA slide shows.

B.3 DATA RETRIEVAL OPTION

To retrieve new buoy information, select the DATA RETRIEVAL button from the main window OPTIONS menu shown in Figure B-4. The Data Retrieval Setup Page, shown in Figure B-5, appears, allowing the operator to specify which buoys to retrieve data for and a description of the data to be retrieved. The Data Description text window allows the operator to give the retrieved buoy data a description to distinguish it from previously retrieved data. The Buoy ID text window allows the operator to enter a buoy ID of up to five characters for retrieval. Select the ADD ID button under the text window to add the entered buoy ID to the ID list. Any IDs that are currently in the list may be deleted from the list by selecting the ID and pressing the DELETE ID button.

Once the data description and the IDs are specified for retrieval, select the OK button to retrieve data. The retrieval process is manually started each time the operator wishes to retrieve data. The maximum number of buoys that may be retrieved at one time is 20. If the data description already exists, the retrieval will merge with the existing data description file. Upon completion of the retrieval, the Data Retrieval window will be closed. The CANCEL button will cancel any changes made to the Data Retrieval window and will exit the window with no buoy data retrieved. Argos records with fix quality zero, A, or B, are not processed by the OPS program.

The OPS program uses the script `getargos.csh` to download and process buoy data from the Argos system. The script performs the following actions:

1. Create a script for C-Kermit 5A which will connect with the Argos system and download the buoy data for the requested buoys. This connection can be made using either the Internet or Tymnet dialup.
2. Execute C-Kermit 5A to process the script commands. This makes the connection to Argos, outputs the commands which request the desired buoy data, and captures the output in a file.

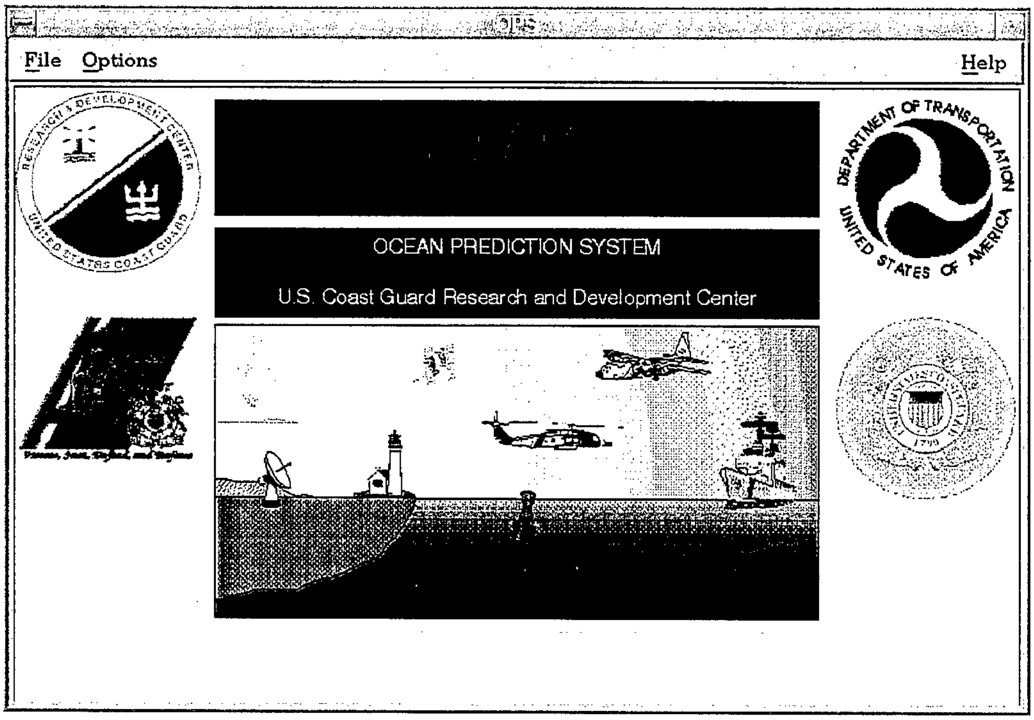

Figure B-2. Main Window Display

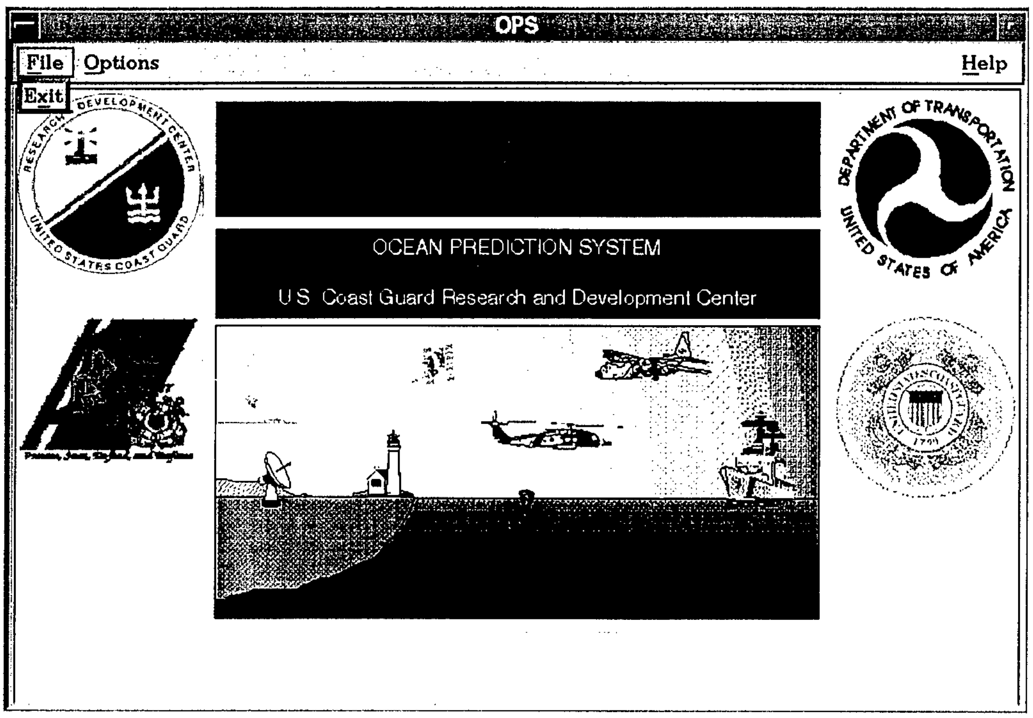

Figure B-3. Main Window FILE Menu

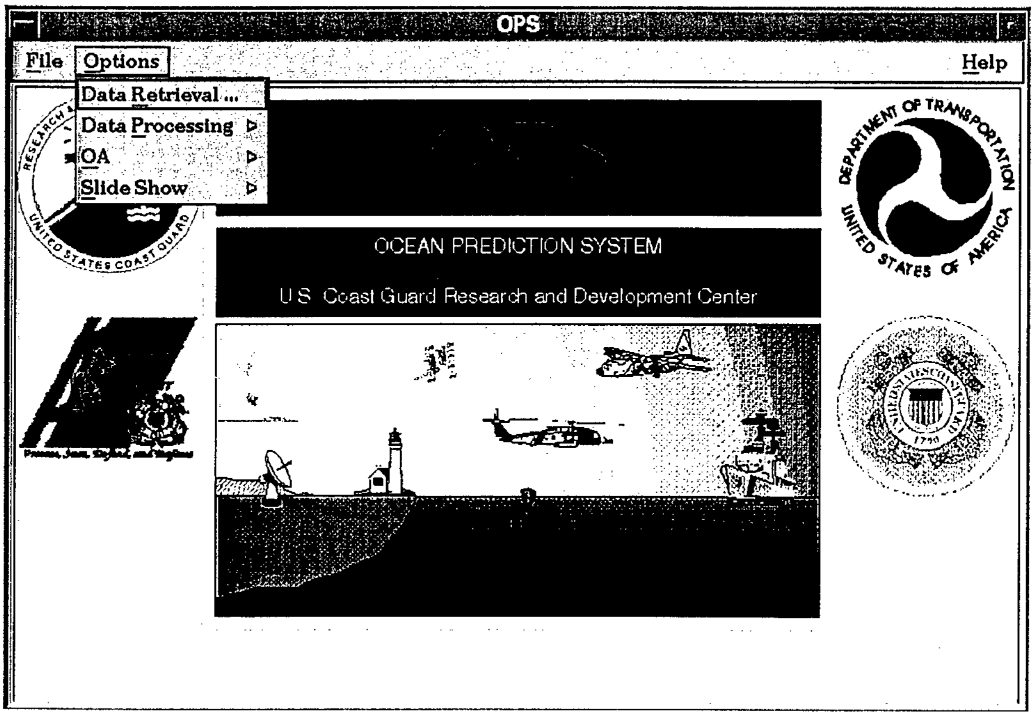

Figure B-4. Main Window OPTIONS Menu

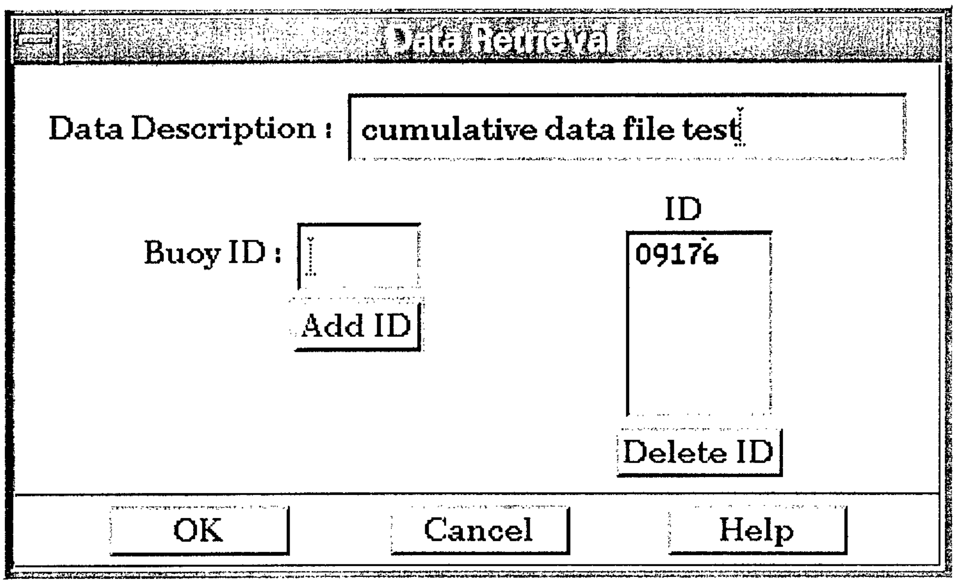

Figure B-5. Data Retrieval Setup Page

3. Run the "argos" program to decode the downloaded data stream.
4. Copy the decoded buoy data file to the main OPS program's data directory.

Downloaded data records contain either Argos fix data or GPS fix data. Argos records include buoy ID, date/time, latitude, and longitude. An example of an Argos data record is:

00046 09176 33 32 D 3 1996-06-12 12:32:38 40.867 293.248 0.000 401650095

Clearwater GPS data format. A GPS record contains data encoded from the GPS receiver. Data records are specified by the buoy manufacturer. A sample GPS data record from the Clearwater buoys used in the OPS Development Test is shown in Table B-1.

Table B-1. Sample GPS Data Record

1996-06-12 12:28:58 1	10	02	00	00
	00	23	CB	00
	1E	2C	00	00
	00	00	00	00
	C5	E9	00	00
	00	C0	00	00
	00	00	A2	D7
	00	00	00	00

The Clearwater buoys transmit four pages (records) with the format given in Table B-1, one every 90 seconds, cycling through the records. The records are received if a satellite is overhead during the transmission. The buoys acquire a GPS fix every 30 minutes, and transmit on each page the latest fix and up to four of the older fixes. With four pages, if all four transmissions are received during a satellite pass, the previous 17 GPS fixes may be downloaded (8.5 hour history). Each page has a 4-bit checksum, the header portion of the record (which contains the latest fix and one fix from the saved history) has a 4-bit checksum, and each of the second, third, and fourth fixes from the history has a 4-bit checksum. If the record header checksum is invalid, the entire record is ignored. If the checksum for the second, third, or fourth fix is invalid, that fix and any following fixes in the same record are ignored. If the checksum for the overall record is invalid, all fixes from that page are marked as questionable in the output data stream, since there is a 1 in 16 chance that bad data has a good checksum when 4-bit checksums are used.

Metocean GPS data format. The Metocean buoys record three pages of data, transmitting one page every 90 seconds. The first page contains the latest GPS fix and the four previous fixes (0 to 2.5 hours old). (GPS fixes are taken on the half-hour.) The second and third pages contain the fixes which are 3 to 5.5 hours old and 6 to 8.5 hours old, respectively. Each page contains a single 8-bit checksum. If this checksum is invalid, the entire page is ignored.

The decoding program prints one line for each valid fix (good or questionable based on the checksum values) with the following format:

04552 1996 153 124842 +41.1655 -066.4167 4 0 999 1

Each line contains the buoy ID, the year, Julian day, HHMMSS, latitude, longitude, fix quality, GPS figure of merit (FOM), sea temperature (SST), and the checksum-OK flag. The FOM and the SST may not be valid if the buoy is not configured to record these values, and the SST is not available on every transmitted data page even if the buoy is configured to record SST. A checksum-OK value of 1 indicates a good fix, and a checksum-OK value of 0 indicates a questionable fix, based on the checksum values.

The data stream contains redundant data to compensate for transmissions lost due to noise or satellite visibility. Duplicate fixes are removed and the data is sorted by time for each buoy ID prior to passing the data to the main OPS program.

B.4 DATA PROCESSING OPTION

B.4.1 OPEN

To view or edit newly retrieved or existing buoy data, select the DATA PROCESSING button from the main window OPTIONS menu shown in Figure B-4. Highlight the data file to be viewed from the Data File Selection window, shown in Figure B-6. Highlighting a data file in the list and pressing the OK button will display two additional graphics: a window containing the buoy information and an animated plot of the cumulative buoy tracks for the selected data file. Figure B-7 shows the Buoy Input window and Figure B-8 shows the plot of the cumulative buoy tracks. Multiple files may be selected for opening. The resulting graphics represent a merging of the selected files. To close the list without opening a file, select the CANCEL button.

B.4.1.1 Buoy Input Window

The Buoy Input window allows the operator to view the time, position, and velocity records for each buoy requested during the data retrieval. These records may be sorted either by time or buoy ID. A buoy record may be removed from use in an OA calculation. Records are only removed from use in the calculation, but are not removed from the archived data file.

The Buoy ID list contains the identification numbers. After highlighting the buoys in the Buoy ID list, the time and position records for each of the buoys will appear in an information list. The information displayed consists of time (DTG), latitude and longitude, buoy fix quality (Argos or GPS), and a "Use" flag that indicates whether the record has been deleted from further use in an OA calculation. To sort the buoy records, specify "Buoy" or "Time" by selecting the button to the immediate left of the appropriate label. A buoy may be deselected from the Buoy ID list by re-highlighting the buoy. Multiple buoys may be selected at one time.

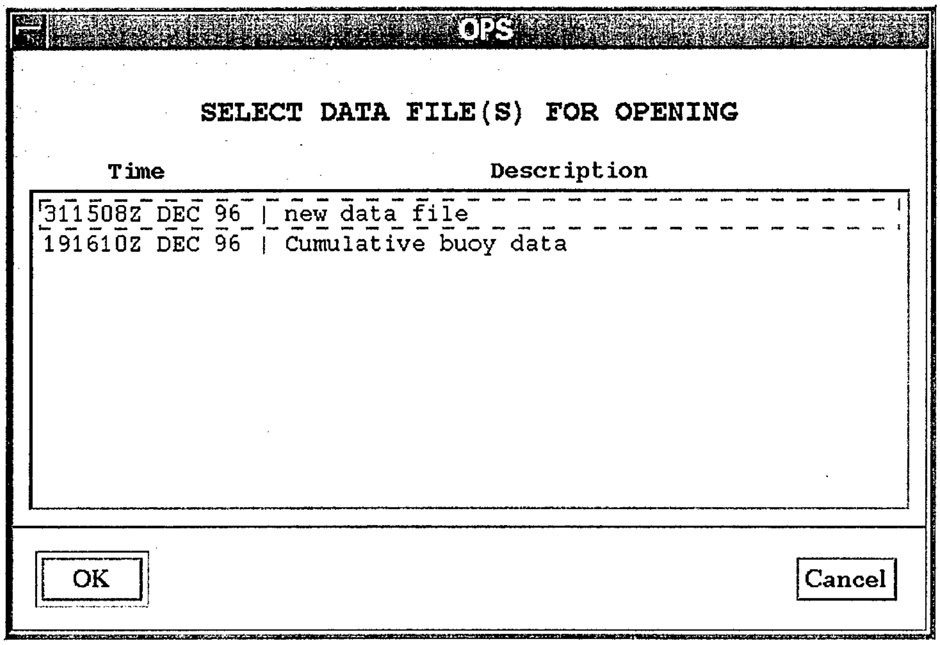

Figure B-6. Data File Selection Window

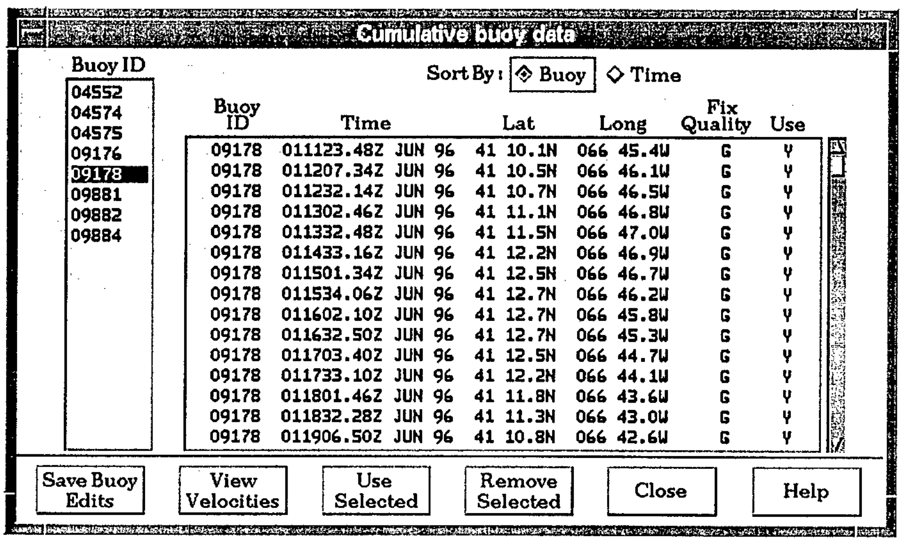

Figure B-7. Buoy Input Window

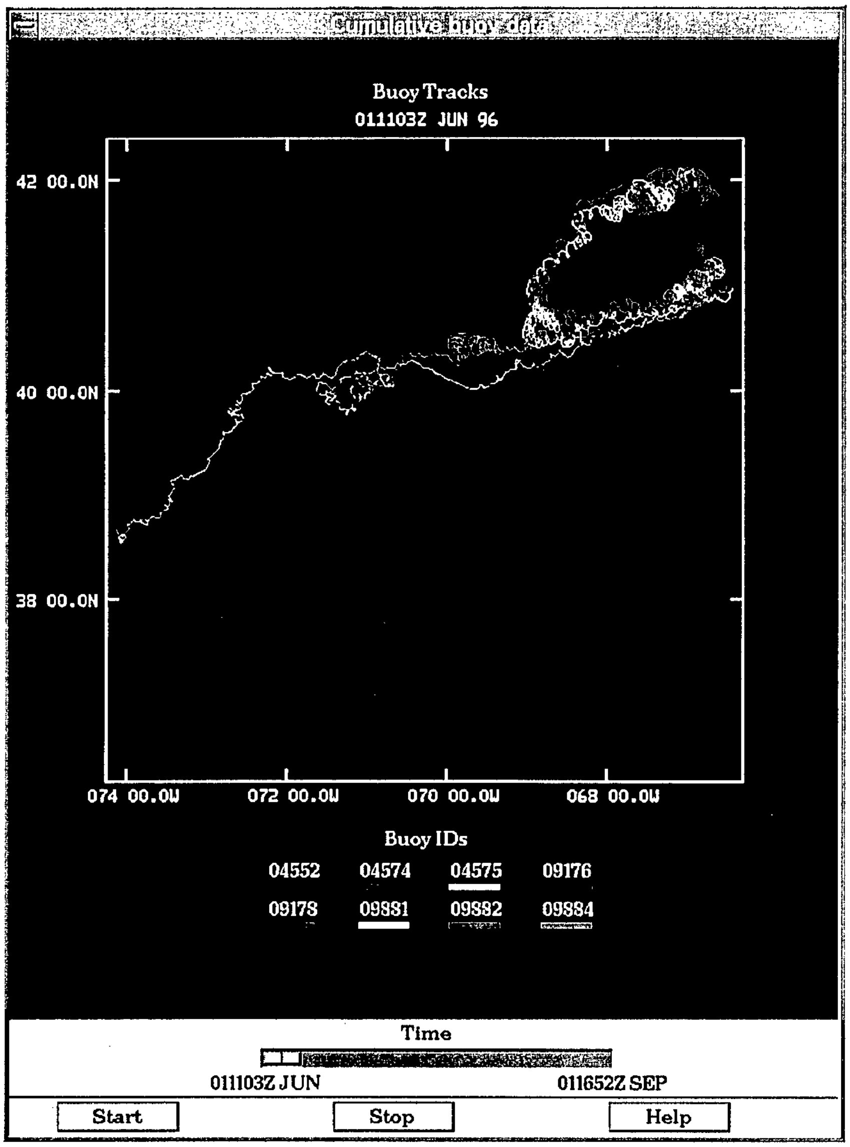

Figure B-8. Cumulative Buoy Track Display

Editing the buoy records consists of adding/removing records from further use in OA calculations. The "Use" flag in the list can be set to either "Y" or "N". A "Y" indicates that the record is currently available for use in OA calculations. An "N" indicates that the record is not to be used in any OA calculation. There are two methods which may be used to add/remove records: highlighting records in the buoy information list (Method 1) or graphically selecting or deselecting the points on a plot of the buoy's track (Method 2).

Method 1: Highlighting a record in the list

To remove a record from future OA calculations, highlight the record in the information list and press the REMOVE SELECTED button at the bottom of the Buoy Input window. The record appears with "N" marked under the "Use" column. To add a record back in for future calculations, highlight the record in the information list and press the USE SELECTED button. The buoy record will now have a "Y" marked under the "Use" column. Multiple records may be added or removed.

There are three ways to select multiple records:

1. Hold the left mouse button down and drag the mouse over the list.
2. Hold the `<Ctrl>` button down and select individual records.
3. To add/delete several records that are between list positions A and B, select position A, then scroll to position B, hold the `<Shift>` button down, and select position B. All items between positions A and B will now be selected.

Method 2: Selecting or deselecting a point on the buoy's track

By double-clicking on a buoy in the Buoy ID list, a window appears with the plot of the selected buoy's track, shown in Figure B-9. A buoy record is represented by a "+" on the track plot. Each record from the list set for use in the OA calculation is represented as part of the connected track. Any record that is removed from the OA calculation is not connected. By selecting a record on the plot with the left mouse button, the selected record becomes highlighted on the Buoy Input window. Selecting a record with the right mouse button will highlight the record in the list and change the "Use" flag of the record. The records are color coded by fix quality.

The buttons on the bottom of the window allow the operator to zoom in on a particular track area, zoom out from the present view, center the view of the track, and close the track window. Press the buttons with the appropriate labels to zoom in or out. The track view will either shrink or expand by a factor of 2. To activate the centering feature, press the CENTER button and the cursor will appear as a "+". Move the cursor to the desired centering location and press the left mouse button. The plot will redisplay with the selected center.

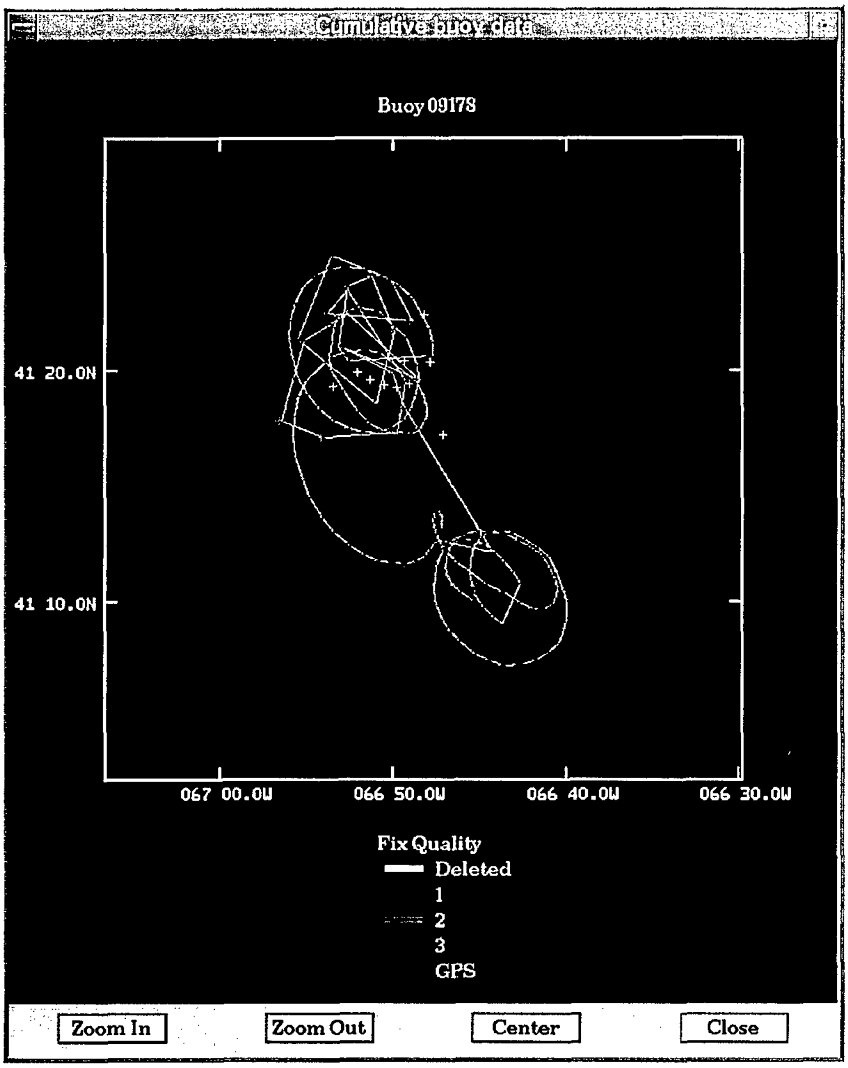

Figure B-9. Individual Buoy Track Display

To view more information on the highlighted buoy IDs, press the VIEW VELOCITIES button on the Buoy Input window. Selecting the VIEW VELOCITIES button will produce a window containing a listing of buoy ID, time (DTG), speed (kt), direction (true bearing), and track quality for each non-deleted buoy record appearing in the Buoy Input information list, shown in Figure B-10. The track quality represents a measure of record validity. A low track quality indicates the need to check the buoy record by comparing its position with the positions of its neighboring records. The REMOVE OUTLIERS button will remove any track quality 0 records from the list and from further use in an OA calculation. The CLOSE button will close the Buoy Velocity window.

The SAVE BUOY EDITS button on the Buoy Input window will archive any changes made to the buoy information list. A window (Figure B-11) appears prompting the operator for a description of the saved data file. Select the OK button to save any changes made to the buoy information list on the Buoy Input window. If not saving any changes to the buoy information list, select the CANCEL button.

The CLOSE button will close the Buoy Input window.

B.4.1.2 Cumulative Buoy Track Window

The cumulative buoy track allows the operator to view all buoy record positions that are to be used for the OA calculation on a single display. Figure B-8 shows a cumulative buoy plot for eight buoys. The display shows the position of each buoy at a given time. These positions are represented by the "+" symbol that moves along each track. The current time for the buoy position can be found just above the plot. To activate the track animation, select the START button at the bottom of the plot window. The "+" symbol for each buoy track will move as the "Time" slider moves ahead in time. The rate at which the slider is moving is 1 second for every 4 hours of data. To deactivate the track animation, select the STOP button. The "Time" slider may be manually moved ahead or back to view a particular time of interest. The buoys shown on the plot are color coded according to their IDs. Any changes made to the record information on the Buoy Input window are automatically updated on the cumulative buoy track display. The cumulative buoy track window is closed when the Buoy Input window is closed.

B.4.2 DELETE OPTION

To delete a data file, select the DELETE button from the DATA PROCESSING menu shown in Figure B-4. A deletion list of existing data files will appear (Figure B-12). By highlighting a data file and pressing the OK button, a window will appear to confirm the file deletion. If the YES button on the confirmation window is selected, the data file will be deleted and the list will close. If the NO button on the confirmation window is selected, no deletion will occur. Pressing the APPLY button will generate the same confirmation window. Selecting the YES button will delete the data file and update the list. Selecting the NO button will not cause any file deletion. Pressing the CANCEL button on the deletion list will close the list with no file deletion. Multiple files may be deleted at one time.

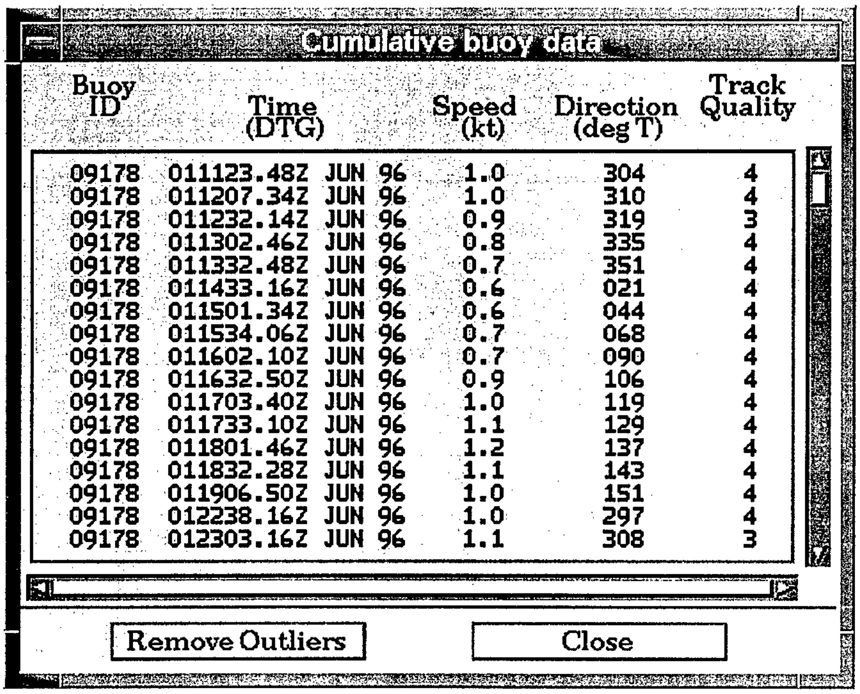

Buoy ID	Time (DTG)	Speed (kt)	Direction (deg T)	Track Quality
09178	011123.48Z JUN 96	1.0	304	4
09178	011207.34Z JUN 96	1.0	310	4
09178	011232.14Z JUN 96	0.9	319	3
09178	011302.46Z JUN 96	0.8	335	4
09178	011332.48Z JUN 96	0.7	351	4
09178	011433.16Z JUN 96	0.6	021	4
09178	011501.34Z JUN 96	0.6	044	4
09178	011534.06Z JUN 96	0.7	068	4
09178	011602.10Z JUN 96	0.7	090	4
09178	011632.50Z JUN 96	0.9	106	4
09178	011703.40Z JUN 96	1.0	119	4
09178	011733.10Z JUN 96	1.1	129	4
09178	011801.46Z JUN 96	1.2	137	4
09178	011832.28Z JUN 96	1.1	143	4
09178	011906.50Z JUN 96	1.0	151	4
09178	012238.16Z JUN 96	1.0	297	4
09178	012303.16Z JUN 96	1.1	308	3

Figure B-10. Buoy Velocity Window

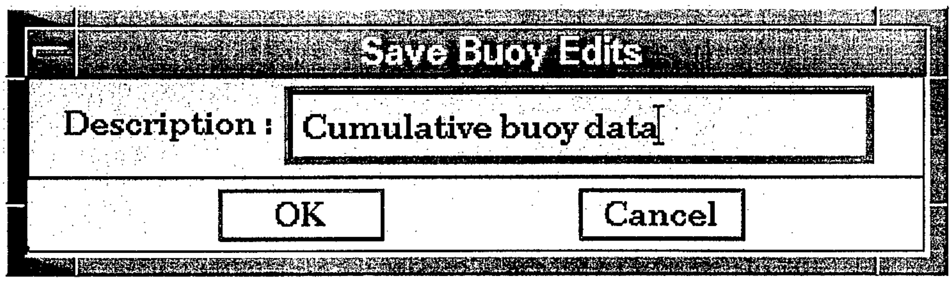

Figure B-11. Save Buoy Edits Window

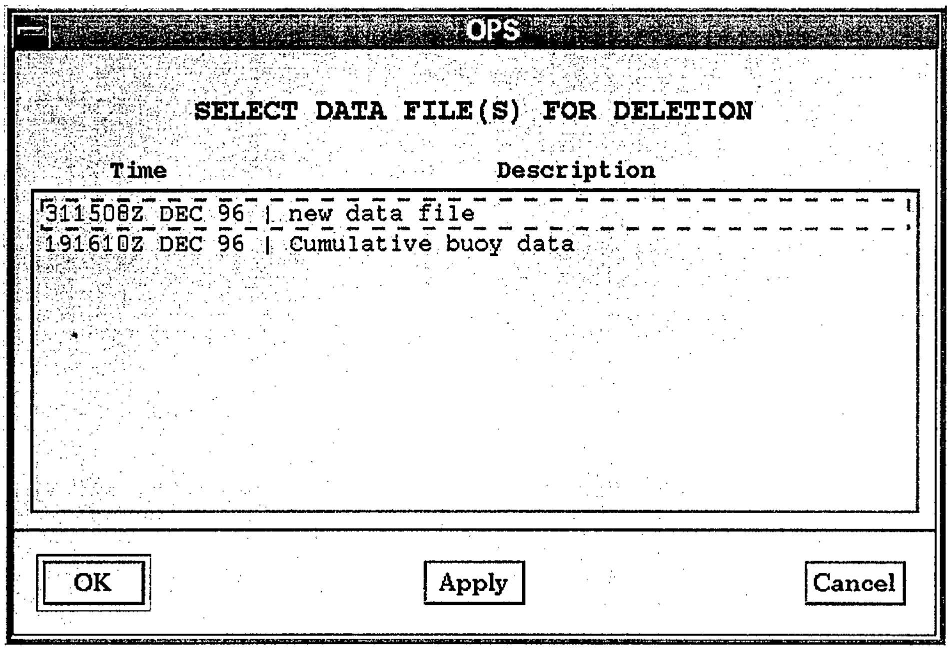

Figure B-12. Data File Deletion Window

B.5 OA OPTION

The main window OPTIONS OA menu item has a submenu with items NEW, OPEN, and DELETE.

B.5.1 NEW

To generate a new OA calculation, select NEW from the main window OPTIONS OA submenu. The OA Input Parameters window shown in Figure B-13 will appear. This window allows the operator to change the OA calculation input parameters listed in Table B-2.

Table B-2. OA Calculation Input Parameters

Parameter	Description
Session Time	Time of session automatically entered by OPS and used as file name for OA solution.
Description	User-entered and used as file name for OA solution.
OA Solution Time	Time in DTG format for OA solution.
Influential Time Window	Time interval, in hours, before and after the OA solution time, in which data is used to calculate OA solution. The maximum influential time window is ± 24 hours. The minimum influential time window is ± 2 hours.
Center Latitude	Latitude, in DD MM.M N/S format, of the center y position of the OA solution area. Latitude values between 36 45.0 N and 45 00.0 N are allowed.
Center Longitude	Longitude, in DDD MM.M E/W format, of the center x position of the OA solution area. Longitude values between 66 30.0 W and 74 00.0 W are allowed.
Area Length	Length (North-South) in nautical miles of the OA area. Maximum area length is 100 nautical miles. Minimum area length is 10 nautical miles.
Area Width	Width (East-West) in nautical miles of the OA area. Maximum area width is 100 nautical miles. Minimum area width is 10 nautical miles.
Grid Spacing	Spacing in nautical miles between grid points. Maximum grid spacing is 10.0 nautical miles. Minimum grid spacing is 0.5 nautical miles.

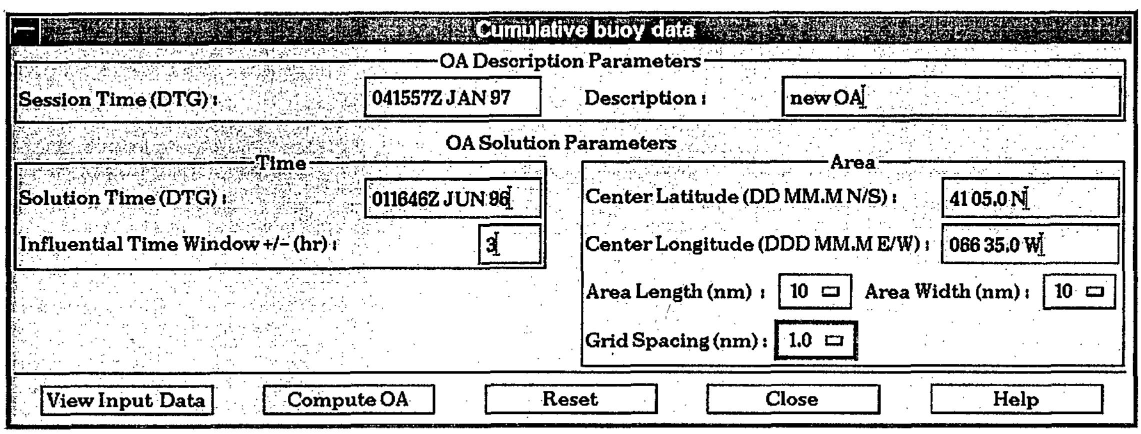

Figure B-13. OA Input Parameters Window

Pressing the VIEW INPUT DATA button displays locations of data points that are within the Influential Time Window about the OA Solution Time. The Solution Time, Influential Time Window, and Area determine the points used in calculating a solution. Solutions are calculated at the specified grid points using only data within the Area selected. Figure B-14 shows an example of the View Input Data display. The data points are color coded according to buoy ID.

To activate the OA calculation, select the COMPUTE OA button on the Cumulative Buoy Data window. A window will appears with the status of the OA calculation. To cancel the calculation, select the CANCEL button on the status window. The OA calculation takes between one and two minutes to calculate 1,000 grid point current estimates. The OA chart options are discussed in Section B.5.4. The OA calculation is automatically saved by the OPS program. To cancel changes made in the OA input parameters, select the RESET button. To close the input parameters window, select the CLOSE button.

B.5.2 OPEN

To open an existing OA, select the OA menu OPEN button. A selection list of OA files will appear as shown in Figure B-15. By highlighting an OA file in the list and pressing the OK button, the OA field will be displayed on a chart. The window for entering the OA input parameters, (Figure B-13), the Cumulative Buoy Track window, (Figure B-8), and the Buoy Input window, (Figure B-7), will also appear. Select the CANCEL button on the selection list to close the list. Only one OA file may be open at a time.

B.5.3 DELETE

To delete an OA file, select the OA menu DELETE button. A deletion list of existing OA files will appear as shown in Figure B-16. Highlighting an OA file and pressing the APPLY button, causes a window to appear confirming the OA file deletion. If the YES button on the confirmation window is selected, the OA file is deleted and the list is updated. If the NO button on the confirmation window is selected, no deletion occurs. The deletion list remains on the screen. By selecting the OK button and pressing YES on the confirmation window, the OA file is deleted and the deletion list is closed. The CANCEL button on the deletion list closes the list without deleting any OA files. Multiple OA files may be deleted at one time.

B.5.4 OA CHART OPTIONS

The chart on which the OA field is displayed consists of the FILE and OPTIONS menus. The chart options are shown in Figure B-17.

B.5.4.1 FILE Menu

The FILE options allow the operator to print the chart contents or to close the chart display. These options are shown in Figure B-18.

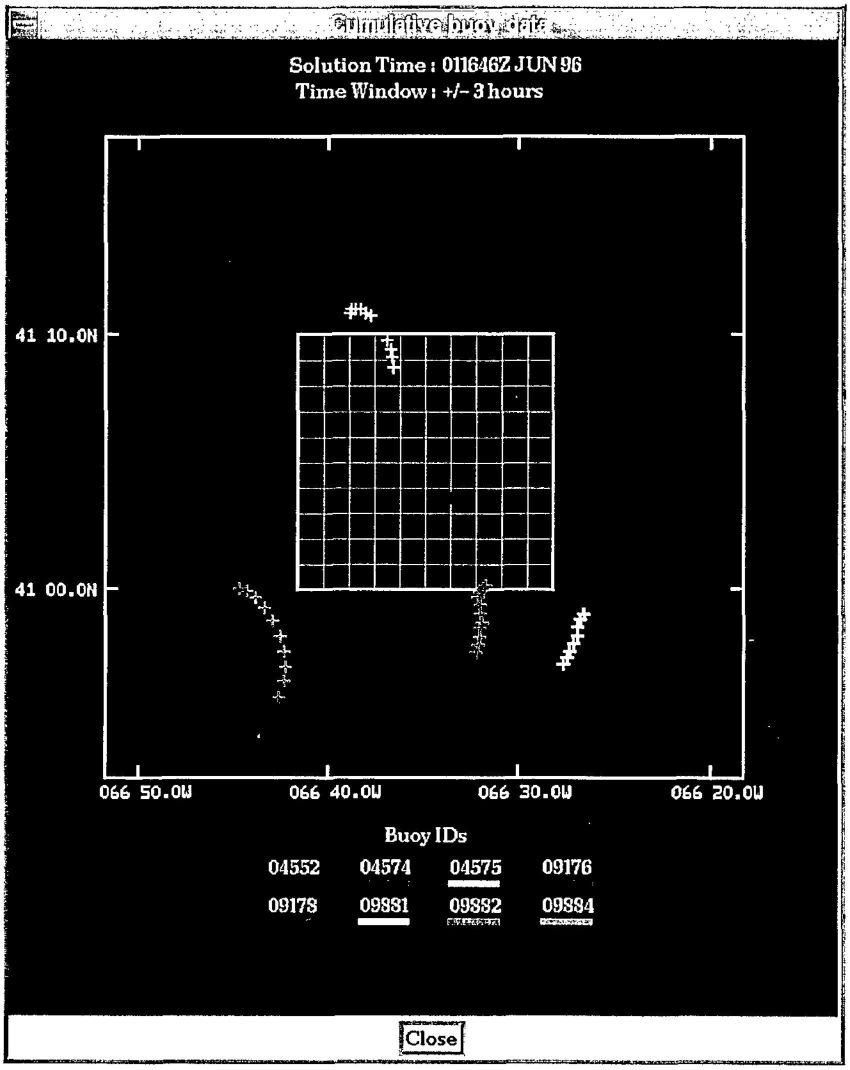

Figure B-14. View Input Data Display

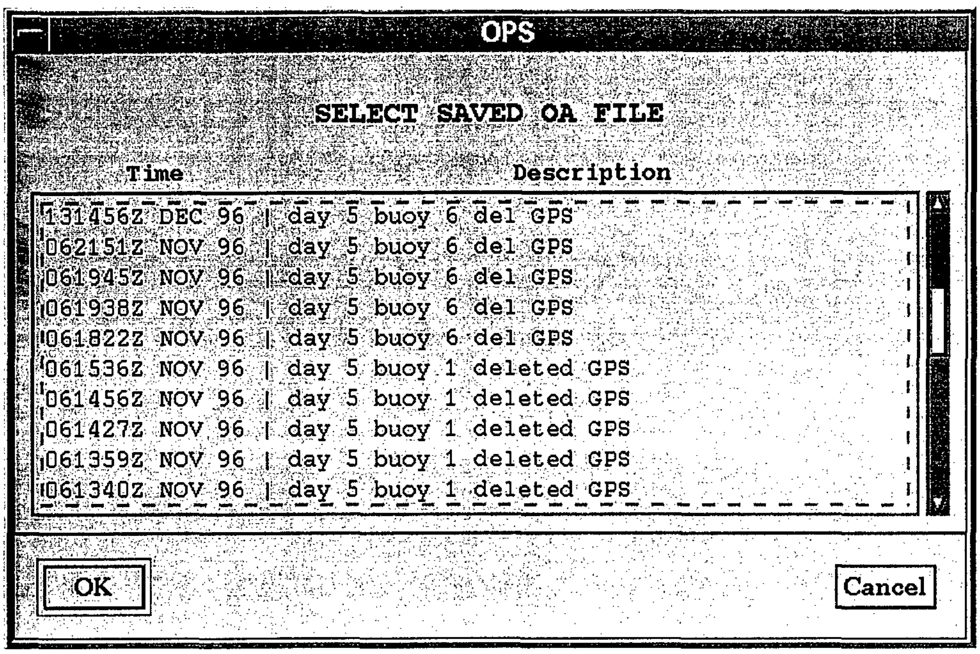

Figure B-15. OA File Selection Window

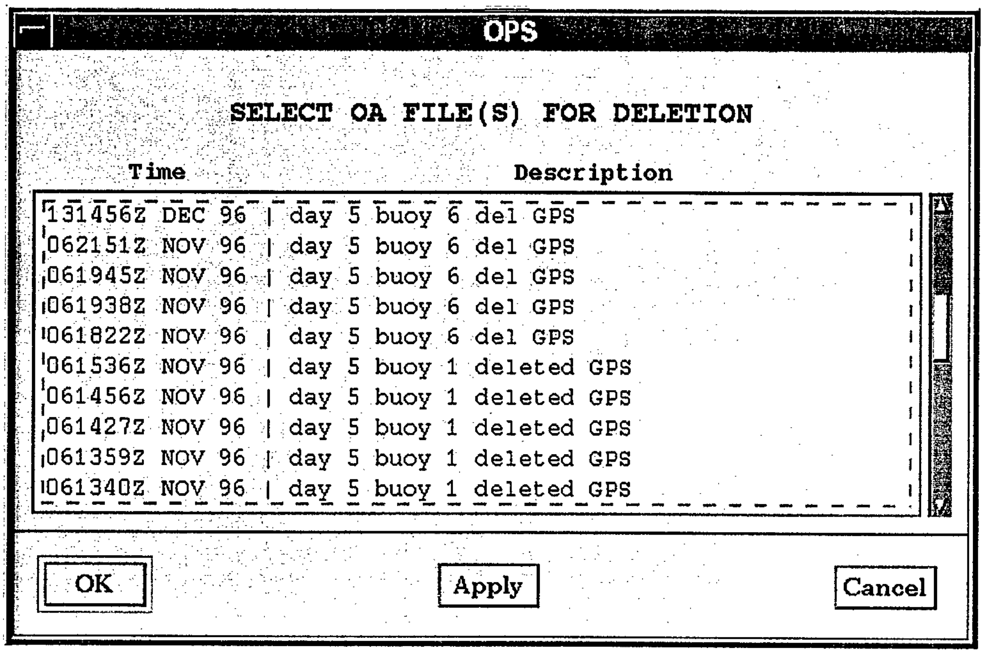

Figure B-16. OA File Deletion Window

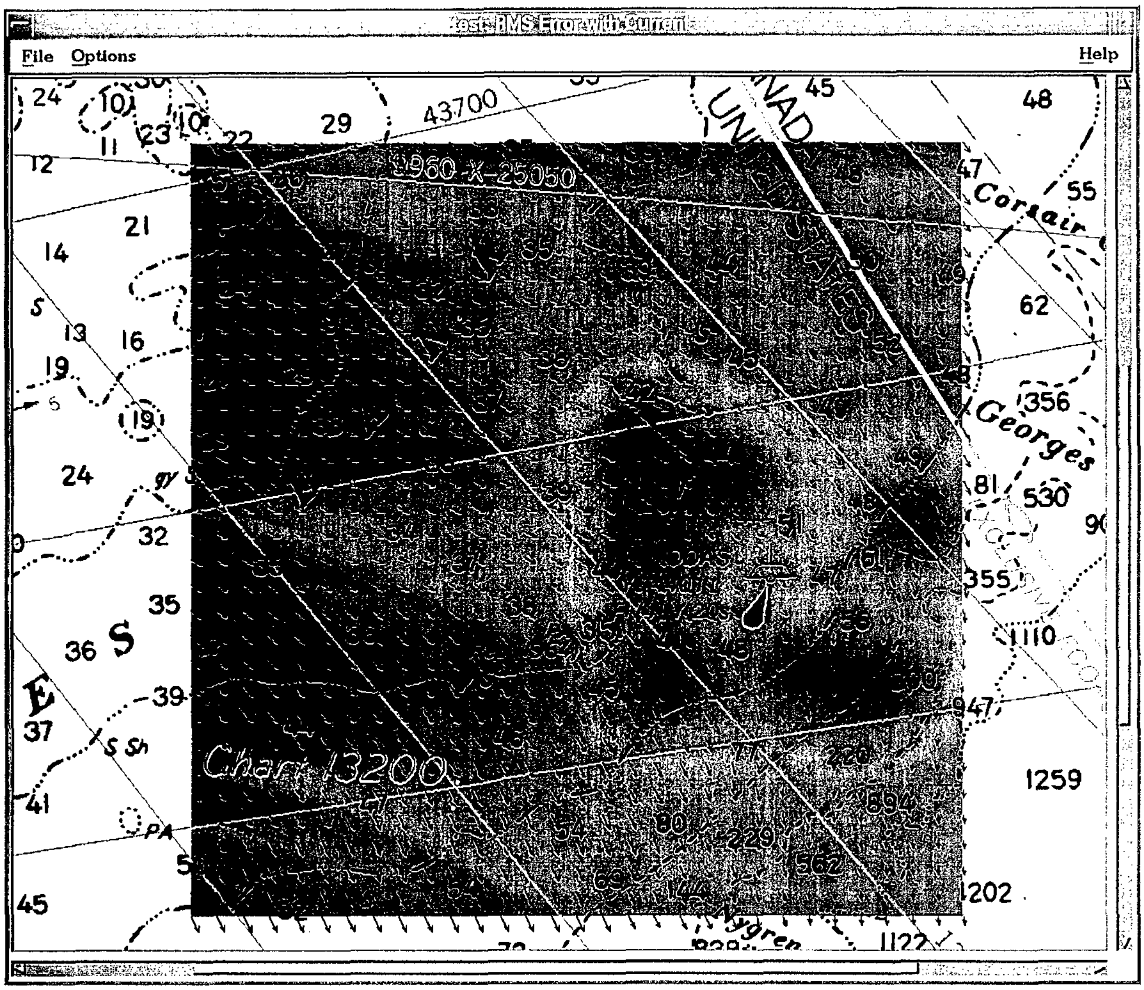

Figure B-17. OA Chart Display

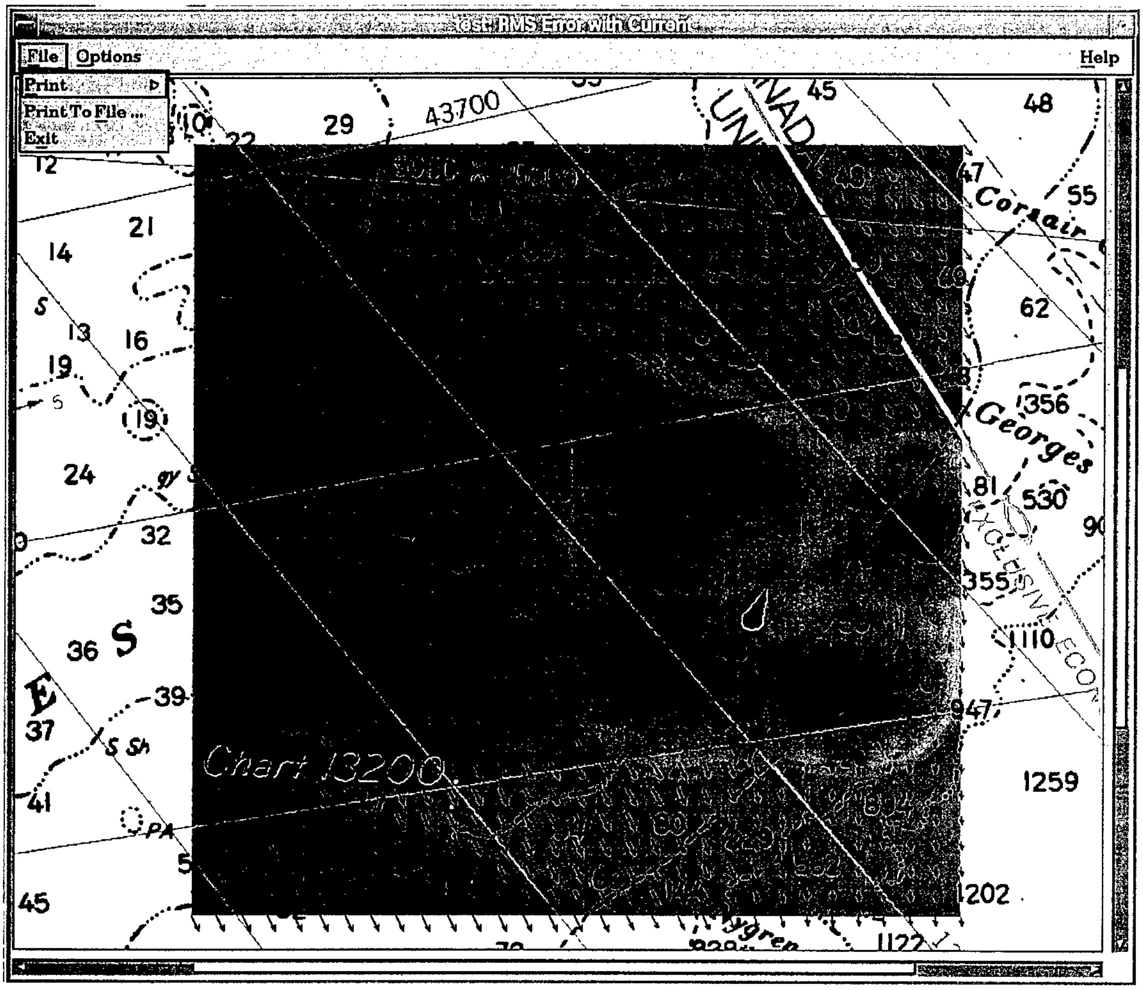

Figure B-18. OA Chart FILE Menu

B.5.4.1.1 PRINT Option

The PRINT option prints the contents of the chart to a selected system printer. Upon installation of the OPS program, a file `ops_printer`, consisting of a list of the system printers, is created. Those system printers are found in a submenu of the chart FILE menu PRINT button. By selecting a submenu item, the chart prints to the corresponding printer.

B.5.4.1.2 PRINT TO FILE Option

The chart FILE menu PRINT TO FILE option writes the contents of the chart to a `.GIF` file. Upon selecting the PRINT TO FILE menu button, the window in Figure B-19 appears prompting for the directory location and name of the `.GIF` file. Enter the full directory pathname into the Selection text area. By pressing the FILTER button at the bottom of the window, the Files list in the window will display any `.GIF` files in the selected directory. To write the chart to a specified `.GIF` file, select the OK button. The CANCEL button will close the window without writing out a `.GIF` file.

B.5.4.1.3 EXIT Option

The chart FILE menu EXIT button closes the chart window along with any OA dependent windows (i.e., Buoy Input, cumulative buoy track, and OA Input Parameters).

B.5.4.2 OPTIONS Menu

The chart OPTIONS menu allows the operator the options of what display he would like on the chart, the view scale of the chart, initializing and sending OA output to CASP, creating a slide show of OA fields, showing a legend for the selected display, showing the solution output for the displayed OA field, showing the parameter information for the OA inputs, and editing the scale settings for maximum current velocity and RMS error. The chart options are shown in Figure B-20.

B.5.4.2.1 DISPLAYS Option

The chart OPTIONS menu DISPLAYS submenu provides various choices as to what can be displayed on the chart. A menu item may be selected or deselected by pressing the ITEM button. An item is selected when a box is found to the immediate left of the menu item label. If an item is selected, pressing the menu item again will deselect the display item and remove the box to its left. The operator has the option to display the features listed in Table B-3.

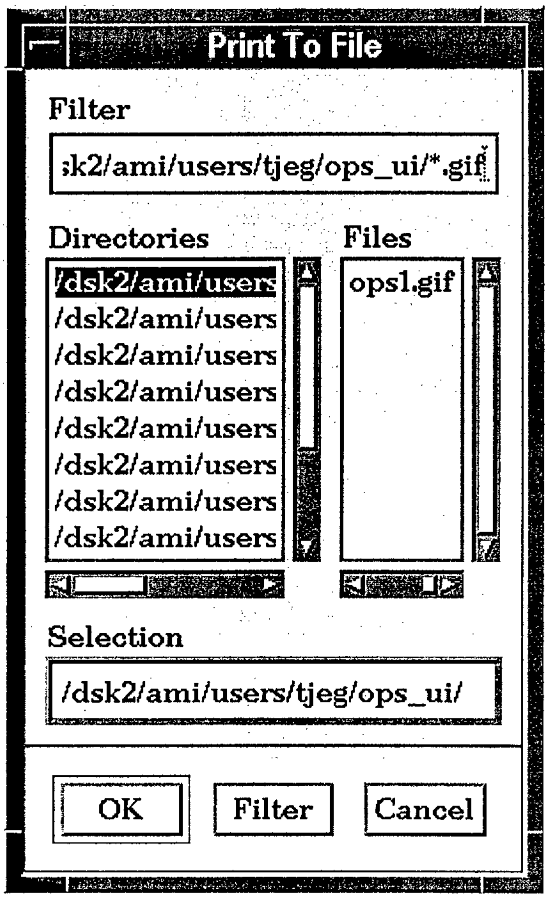

Figure B-19. OA Chart Print to File Window

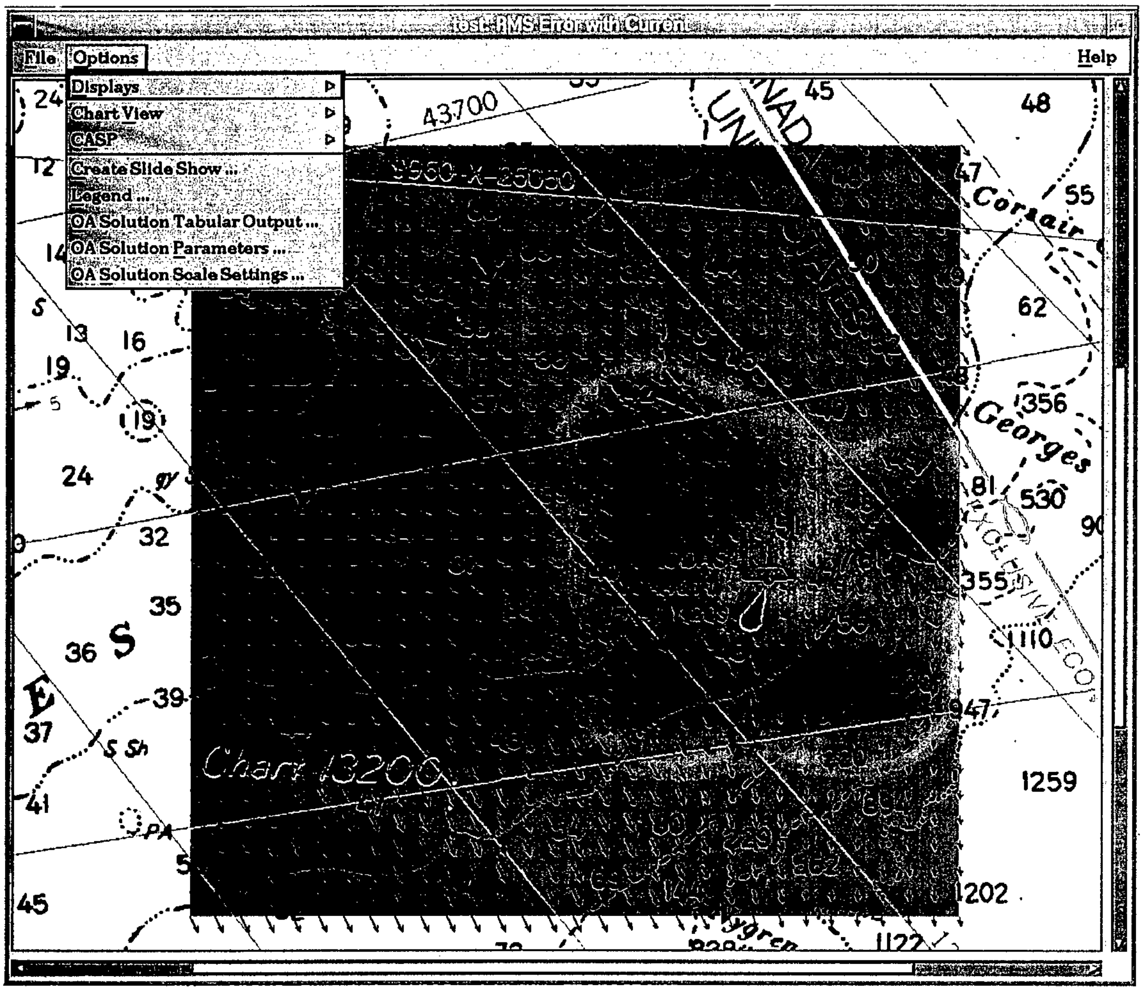

Figure B-20. OA Chart OPTIONS Menu

Table B-3. Display Features

Feature	Description
RMS Error	The display is a color-coded plot of the error values output from the OA calculation. It can only be combined with Current, First District Boundary, and Map Background plots.
Speed Contour	The display is a color-coded plot of the iso-speed contours. It can only be combined with Current, First District Boundary, and Map Background plots.
Current	The display is a plot of the current values output from the OA calculation. It can be combined with any plot.
Buoy Track	The display is a time color-coded plot of the buoy tracks for the specified OA calculation region. It can only be combined with Current, First District Boundary, and Map Background plots.
Buoy Velocity	The display is a time color-coded plot of the calculated buoy velocities for the OA region. It can only be combined with Current, First District Boundary, and Map Background plots.
First District Boundary	The display is a plot of the Coast Guard First District search and rescue boundary. It can be combined with any plot.
Map Background	The display is a plot of the background of the NOAA chart for the specified OA calculation region. It can be combined with any plot.

B.5.4.2.2 CHART VIEW Option

The chart OPTIONS menu CHART VIEW submenu provides zooming capabilities. To get the maximum zoom in on the chart area, select the ZOOM IN X 4 menu item. The ZOOM IN X 2 is half the resolution of the ZOOM IN X 4 zoom. The FULL VIEW zoom is half the resolution of the ZOOM IN X 2. A diamond next to the menu label indicates which menu item is selected.

B.5.4.2.3 CASP Option

The CASP menu has two submenu items, INITIALIZE OUTPUT and SEND OA OUTPUT. The INITIALIZE OUTPUT item will clear the CASP input file, `casp.in`, found in the directory where CASP resides (entered during the installation process). The SEND OA OUTPUT item writes the currently displayed OA field to the `casp.in` file.

B.5.4.2.4 CREATE SLIDE SHOW Option

The chart OPTIONS menu CREATE SLIDE SHOW allows the operator to calculate more than one OA field and stores the OA field displays in a slide show. A window, shown in Figure B-21, appears prompting the operator for the start time, end time, the number of frames, and a description for the OA slide show. The minimum number of frames for the slide show is 2. The maximum number of frames for the slide show is 25. As an example, a slide show starting at 010000Z

JAN 97 and ending at 010400Z JAN 97 with 5 frames will calculate OA fields at 010000Z, 010100Z, 010200Z, 010300Z, and 010400Z. The slide show uses the Influential Time Window and the OA Area Parameters found on the OA Input Parameters window.

To activate the slide show, select the OK button on the window. A window will appear showing the status of the slide show. To cancel the slide show, press the CANCEL button found inside the status window. Once created, the slide show can be opened from the main window SLIDE SHOW Options OPEN button. An OA calculation that contains no data points within the specified Influential Time Window causes the slide show to be cancelled.

B.5.4.2.5 LEGEND Option

To view a legend for the display selected, press the LEGEND item on the chart OPTIONS menu, shown in Figure B-22. A window appears with the key for the chart display. The keys for the chart display types are listed in Table B-4.

Table B-4. Chart Display Types

Display Type	Key
RMS Error	Color spectrum for the OA error magnitude.
Speed Contour	Color spectrum for the OA velocity magnitude.
Current	Arrow to represent the velocity magnitude and direction.
Buoy Track	Color spectrum for the OA calculation time span.
Buoy Velocity	Color spectrum for the OA calculation time span, arrow to represent velocity magnitude and direction.

To close the legend window, select the CLOSE button at the bottom of the window.

B.5.4.2.6 OA SOLUTION TABULAR OUTPUT Option

To view the output values displayed in the OA field, select the OA SOLUTION TABULAR OUTPUT item on the chart OPTIONS menu shown in Figure B-20. A window, shown in Figure B-23, appears displaying the output position, velocity magnitude and direction, and the RMS error for each of the OA region grid points. To close the window, select the CLOSE button at the bottom of the window. An alternative way of viewing the OA output values is to click and drag the right mouse button over the displayed OA region. The values for the selected displays are listed in Table B-5.

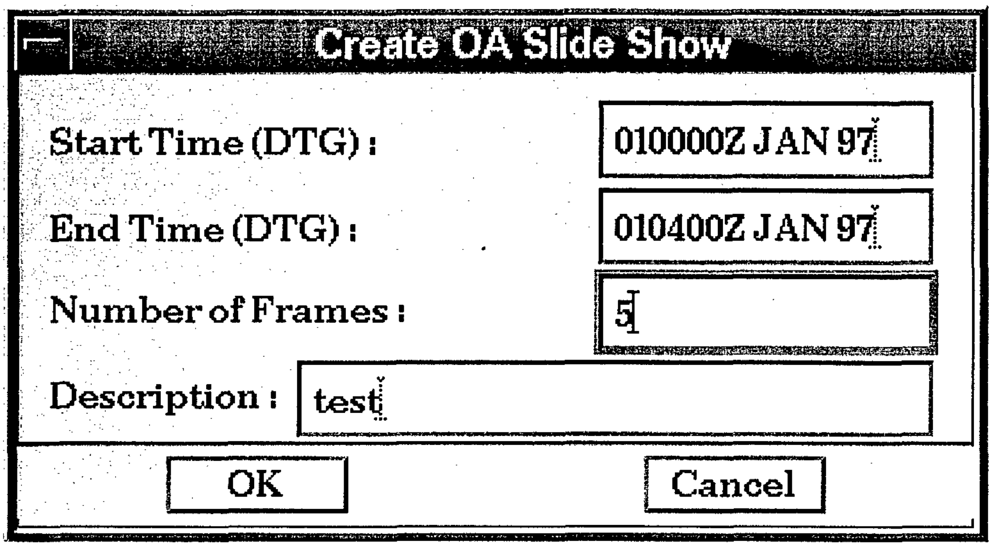

Figure B-21. OA Chart Create OA Slide Show Window

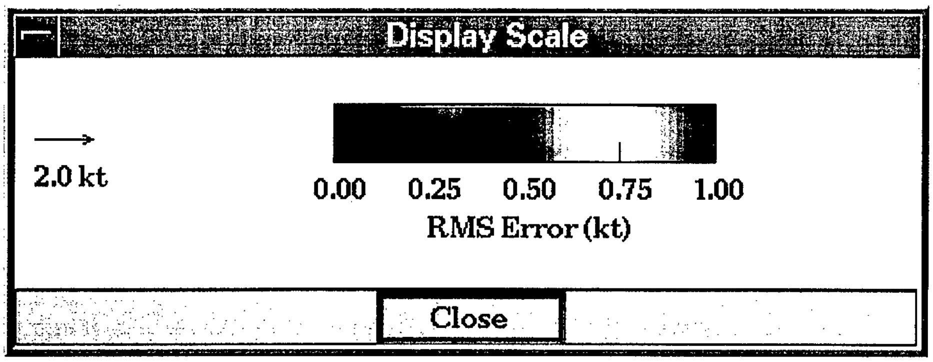

Figure B-22. OA Chart Display Scale Legend Window

OA Solution at 011646Z JUN 96

Lat	Long	Direction (deg T)	Speed (kt)	RMS Error (kt)
41 07.5N	066 52.0W	115	0.8	0.4
41 07.5N	066 50.0W	116	0.9	0.3
41 07.5N	066 48.0W	117	0.9	0.2
41 07.5N	066 46.0W	117	0.9	0.1
41 07.5N	066 44.0W	119	0.9	0.0
41 07.5N	066 42.0W	123	0.8	0.1
41 07.5N	066 40.1W	126	0.8	0.2
41 07.5N	066 38.1W	130	0.7	0.2
41 07.5N	066 36.1W	126	0.5	0.3
41 07.5N	066 34.1W	135	0.5	0.3
41 07.5N	066 32.1W	142	0.6	0.3
41 07.5N	066 30.1W	152	0.7	0.3
41 07.5N	066 28.1W	155	0.8	0.2
41 07.5N	066 26.1W	158	0.9	0.2
41 07.5N	066 24.1W	159	1.0	0.1
41 07.5N	066 22.2W	159	1.0	0.1
41 07.5N	066 20.2W	159	1.0	0.2

Close

Figure B-23. OA Solution Tabular Output Window

Table B-5. Selected Display Types

Display Type	Information Displayed
RMS Error with Current	Latitude, longitude, RMS error, and velocity magnitude and direction.
RMS Error	Latitude, longitude, and RMS error.
Speed Contour	Latitude, longitude, and velocity magnitude and direction.
Current	Latitude, longitude, and velocity magnitude and direction.

For all other display types, click and drag the right mouse button over the OA region to display the chart latitude and longitude values. The same information is displayed for areas outside the OA region.

B.5.4.2.7 OA SOLUTION PARAMETERS Option

To view the parameters that were input into the OA calculation, select the PARAMETER INFORMATION item from the chart OPTIONS menu shown in Figure B-20. A window will appear showing the input parameters given in Table B-6.

Table B-6. Input Parameters

Parameter	Format
Solution Time	DTG
Influential Time Window	Hours
Center Latitude	DD MM.M N/S
Center Longitude	DDD MM.M E/W
Area Length, Width	Nautical miles
Grid Spacing	Nautical miles

An example of the parameter window is shown in Figure B-24. To close the parameter window, select the CLOSE button at the bottom of the window.

B.5.4.2.8 OA SOLUTION SCALE SETTINGS Option

To change the scaled values for maximum RMS error and unit length for current, select the OA SOLUTION SCALE SETTINGS item from the chart OPTIONS menu shown in Figure B-20. The window shown in Figure B-25 appears showing the values for maximum RMS error and unit length for current. To activate changes to the maximum RMS error or unit length for current, press the APPLY or OK button. By pressing the APPLY button, the chart is replotted and the settings window remains on the screen. By pressing the OK button, the chart is redisplayed and the settings window is closed. The CANCEL button will not activate any changes and will close the settings window.

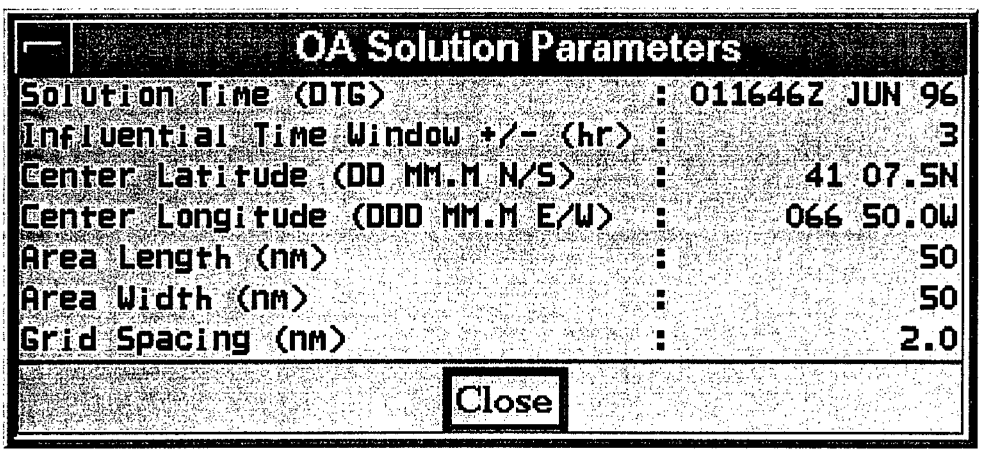

Figure B-24. OA Solution Parameters Window

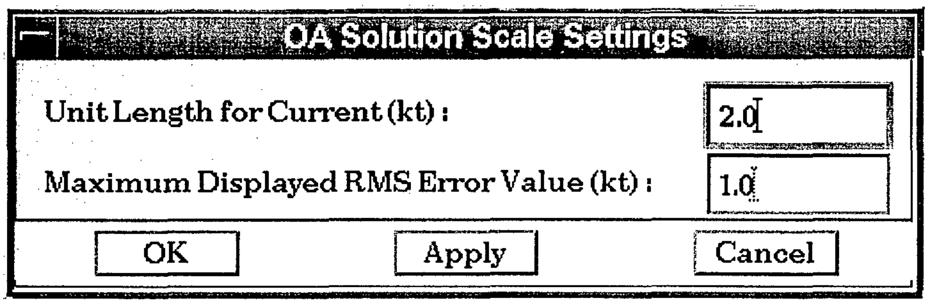

Figure B-25. OA Solution Scale Settings Window

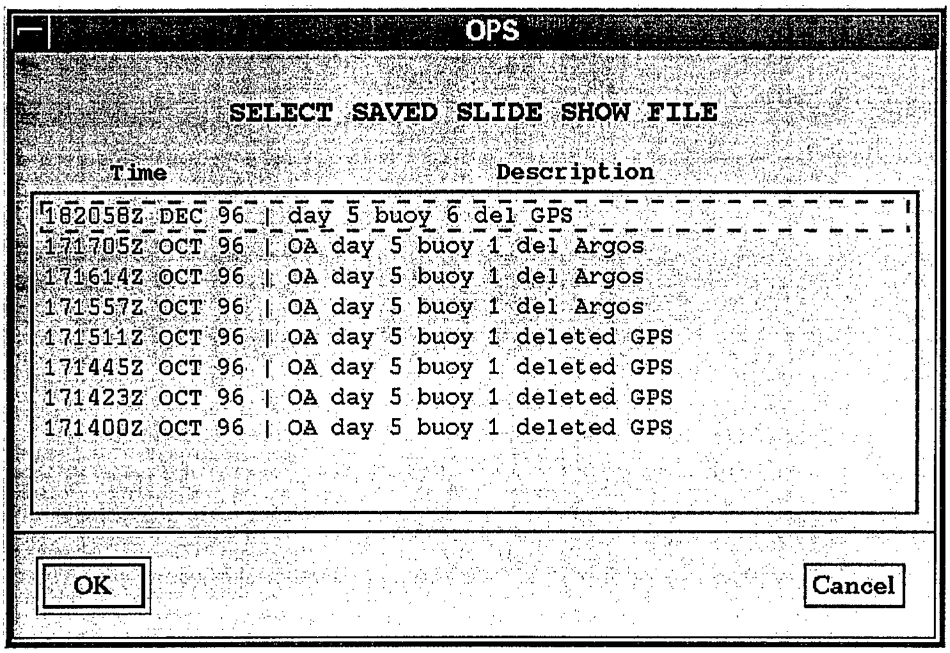

Figure B-26. File Selection for Slide Show Window

B.6 SLIDE SHOW OPTION

The main window Options menu SLIDE SHOW button displays a submenu of options that allows an existing slide show to be opened or deleted.

B.6.1 OPEN

To open a slide show, select option OPEN from the SLIDE SHOW menu shown in Figure B-4. A selection list, shown in Figure B-26, appears from which the operator may select the slide show to be displayed. Highlighting a slide show and pressing the OK button displays the selected slide show, shown in Figure B-27. The slide show window consists of a list of slides, a Speed scale to set the time between displaying the slides, a legend for the OA error and/or velocity, a display area for the slide, and buttons that allow for starting and stopping the slide show, and closing the slide show window. Only one slide show may be open at one time.

The slide show window allows for the slide show to be manually or automatically. To automatically step through the slide show, select the START SHOW button at the bottom of the slide show window. This will display the first slide in the list, wait for a specified time interval, and then display the next slide in the list. The time between displaying slides may be controlled by moving the Speed scale to the desired interval. The time for updating ranges from Slow (5 second interval) to Fast (half-second interval). Each time a slide is displayed, the list will highlight that slide. To stop an automatic slide show, select either the STOP SHOW button or the CLOSE button. If there is one slide of interest, the operator may manually select the slide by highlighting the slide in the list.

To close the slide show selection list, select the CANCEL button.

B.6.2 DELETE

To delete a slide show, select the DELETE button from the SLIDE SHOW menu shown in Figure B-4. A deletion list (Figure B-28) of existing slide shows appears. Highlighting a slide show and pressing the APPLY button causes a window to appear confirming the slide show deletion. If the YES button on the confirmation window is selected, the slide show is deleted and the list is updated. If the NO button on the confirmation window is selected, no deletion occurs. By highlighting a slide show and pressing the OK button, the same confirmation window appears. By pressing the YES button, the slide show is deleted and the list closes. Selecting the CANCEL button on the list selection will close the list. Multiple slide shows may be deleted at one time.

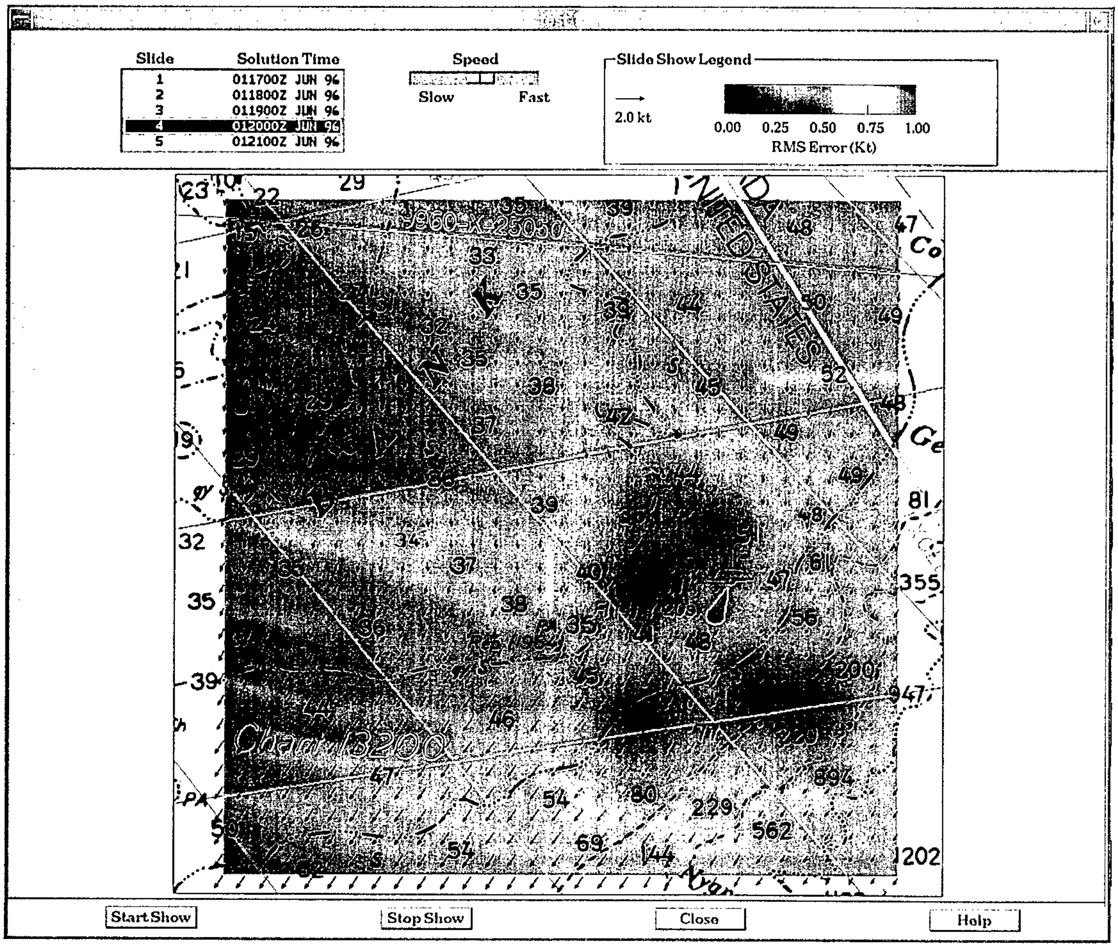

Figure B-27. Slide Show Window

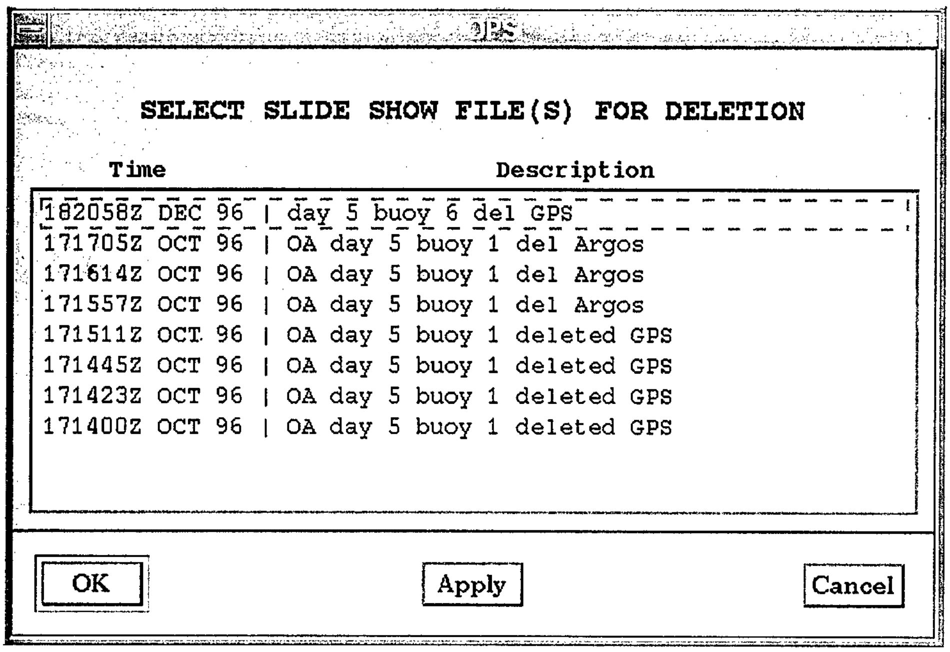

Figure B-28. Slide Show File Deletion Window

B.7 INSTALLATION INSTRUCTIONS

OPS can be installed as a stand-alone program on a system running HP-UX 9.X. These instructions assume that the person installing the program has sufficient familiarity with HP-UX to use an editor, assign a directory for installation, select the ownership of the installed program, and to assign the directory in which CASP currently resides. To install the OPS program as a stand-alone program, complete the following steps using the 4mm DAT OPS installation tape.

1. Login as the program owner.
2. Move to the /tmp directory by entering the command

   ```
   cd /tmp
   ```

   followed by pressing the <Return> key.
3. The installer will need to know the character 4mm DAT tape drive device name in order to transfer files from the installation tape. An example for a character tape drive device name is /dev/rmt/3m.
4. Insert the installation tape into the machine. Transfer the files from the tape into the /tmp directory by entering the command

   ```
   tar -xvf [tape drive]
   ```

   where [tape drive] is the block tape drive device name. This command will transfer the installation files. When the command prompt appears, continue to step 5.
5. To build the installation, enter the command

   ```
   ./ops_install
   ```

   and press the <Return> key. This will start the program installation. The installer will have to specify the full path directory name in which to install the OPS program and the full path directory name in which CASP currently resides.
6. When the message

   ```
   Installation complete
   ```

   is displayed, remove the installation tape by pressing the eject button.
7. The installation creates an empty file ops_printer. This file must be modified by inserting the available printer names. The OPS program can currently only print to Postscript printers. The available printers may be determined by entering the command

   ```
   lpstat -v
   ```

   followed by pressing the <Return> key. The printer names must be inserted in the form

   ```
   [color]-p-[name]
   ```

where [color],[class],and [name] will specify each printer. The value [color] is 'c' for color printer or a 'b' for black and white. The value [class] must be a 'p', which represents a postscript printer. The value [name] represents the printer name. An example for a color Postscript printer, named pj is c-p-pj.

B.7.1 PROGRAM STARTUP

To run the OPS program, login as the OPS program owner and move to the installation directory by entering the command

```
cd [installation directory]
```

and pressing the <Return> key. [installation directory] is the directory that was entered in the installation process.

The display for the UNIX machine must be set before starting the program. This may be completed by entering the command

```
setenv DISPLAY unix:0.0
```

followed by pressing the <Return> key. unix:0.0 refers to display 0, screen 0 on the local host.

After accessing the correct directory and setting the display, enter the command

```
ops
```

followed by pressing the <Return> key. This will start the OPS program.